A Hybrid Frequency Modulated CDMA Communication System

by

Tianshi Li

Thesis submitted to the faculty of the

Virginia Polytechnic Institute and State University

in partial fulfillment of the requirements for the degree of

MASTER OF SCIENCE

in

Electrical Engineering

APPROVED:

Brian D. Woerner

Dr. Brian D.Woerner, Chairman

Jeffrey H. Reed

Dr. Jeffrey H. Reed

Charles W Bostian (BDW)

Dr. Charles W. Bostian

JULY, 1996

Blacksburg, Virginia

Keywords: Wireless Local Loop, Cellular, CDMA, FM, Communication System

A Hybrid Frequency Modulated CDMA Communication System

by

Tianshi Li

Committee Chairman: Dr. Brian D.Woerner

Bradley Department of Electrical Engineering

(ABSTRACT)

The wireless communications industry has experienced tremendous growth worldwide in the past decade. Numerous cellular communication systems have been developed to meet this need. In North America, AMPS, IS-54, IS-95 and GSM are the most popular cellular systems ruling the market. In developing nations, Wireless Local Loop (WLL) services will be in great demand in the coming years. While some service providers may adapt existing cellular standards to this application, WLL does not require the support for mobility which is available in a full cellular system. As a result, substantial cost savings may be obtained through dedicated WLL implementations.

In this thesis, a new wireless communication system is investigated. The system combines the low cost and flexibility of analog frequency modulation with the capacity and multipath advantages of a Code Division Multiple Access (CDMA) system. This system aims to provide WLL telephone services at low cost, with wireline grade voice quality, fast infrastructure deployment and ease of planning.

In this thesis, a theory for FM/CDMA system performance is established. Closed form analytical expressions of signal to multiple access interference ratio are obtained using both upper bounds and lower bounds. The hybrid system is also optimized for the optimum combination of modulation index and processing gain. In addition, a software test-bed is developed to model different FM demodulation schemes, evaluate the tradeoff of FM modulation index versus CDMA processing gain and the system robustness, compare the forward link and the reverse link system performance and investigate the effect of power control schemes.

ACKNOWLEDGEMENTS

I would like to thank Professor Brian D. Woerner for being my advisor who provided me this great opportunity to work on this thesis. I would also like to thank Professors Jeff Reed and Charles Bostian for being my committee members and giving corrections and comments on my thesis. I would also like to thank Jim Shea and Royal Brunce of SigTek, Inc who sponsored and gave valuable suggestions during the entire project.

I am very grateful to all the people who assisted me throughout my thesis. I would like to thank Professor Ivan Howitt who gave me detailed analysis on my early stage simulation results. I would also like to thank George Aliftiras, Mike Buehrer, Rick Cameron, Neiyer Correal, Francis Dominique, George Eapen, Rong He, Kevin Saldanha and Ning Yang for their discussion on my simulation. Special thank goes to my project partner Yash Vasavada who spent so many time together on this project. I really appreciate everyone for their support and friendship over the past two years.

This thesis is dedicated to my parents and sisters for their constant support during my study at Virginia Tech.

TABLE OF CONTENTS

LIST OF FIGURES

Chapter 1
Introduction

Thirteen years after the first commercial deployment of a cellular telephone network in Chicago, wireless communication services are undergoing rapid growth. The number of subscribers is climbing at a rate as high as 50% each year [Mei96]. Recently, 89 PCS providers bid a total of $10.2 billion dollars in the C block Personal Communication Services (PCS) license auction and will spend even more on PCS infrastructure deployment [Mey96]. These astonishing figures give only a glimpse of the growing trends in the wireless industry.

While cellular and PCS service have garnered most of the attention in the U.S. market, Wireless Local Loop (WLL) service will be a key contribution of the wireless industry to developing nations [Cla95][Cox86][Hau94]. WLL will likely provide a low cost means of telephone service to areas without installed copper wire bases. WLL systems share many common features with cellular telephone services. The chief difference is that WLL systems need not support user mobility. This chapter gives an overview of the cellular concept, cellular communication systems and the purpose of the research presented in this thesis.

1.1 Cellular Concept

Unlike wireline telephone or data networks, cellular systems provide service through a wireless link to achieve an end-to-end connection. The signal is carried by an electromagnetic wave which is attenuated by about 40 dB as the distance travelled doubles [Oku68][Hat90]. Because of this attenuated propagation characteristic, the signal will be confined within a desired area, called a cell, if the transmitted power and the processing of the received signal are properly designed. This allows reuse of limited communication resources such as frequency spectrum or code sets throughout a service area by covering it with a number of carefully designed cells [Mac79]. In each cell, a base station communicates with the mobile users through an air interface protocol. When a mobile travels from one cell to another, service is switched and handled by another base station without interruption. The base stations are connected to the Mobile Switching Centers (MSC) via a leased wireline or a microwave link. The MSCs are responsible for roaming, routing, switching and other network management. Different MSCs are connected via the Public Switched Telephone Network (PSTN) by the common channel signaling protocol Signaling System 7 (SS7) [Mod92].

1.2 Cellular Communication Systems

Based on this cellular concept, different air interface protocols have been proposed and implemented throughout the world. In North America, three major cellular standards are used in the growing market.

The Advanced Mobile Phone System (AMPS), the first generation cellular system was developed by Bell Labs in late 1970s [You79]. It uses analog Frequency Modulation (FM) with a channel occupancy of 30 kHz. A total of 50 MHz of spectrum in the 824-894 MHz range is allocated between dual carriers in each geographic area. The basic principles of the AMPS are as follows. The baseband voice is first processed by a 2:1 dB compander. Then it is passed through a pre-emphasis filter with a 6 dB/octave highpass frequency response slope between 300 Hz and 3 kHz. A deviation limiter follows to ensure the maximum frequency deviation will not exceed ± 12 kHz. A post deviation limiter filter is used to attenuate high frequency components to reduce energy bled over to the adjacent channels. Frequency modulation with an IF channel bandwidth of 30 kHz is employed. To ensure voice quality, the SNR should be greater than 18 dB. Because the AMPS system has been optimized for voice transmission, many similar FM standards have been developed, and we will show that the FM portion of our WLL system makes use of a similar set of parameters.

The Electronics Industry Association (EIA) Intermediate Standard 54 (IS-54), also referred to as Digital AMPS (D-AMPS), is a second generation wireless standard coming into use in early 1993. It has been supported and promoted by AT&T Wireless due to its similar channel assignment system. In D-AMPS, analog voice is converted into digital format to incorporate powerful speech coding, channel coding and interleaving to enhance capacity and voice quality. A D-AMPS frequency channel is 30 kHz wide and is shared by 3 users using a Time Division Multiple Access (TDMA) scheme. Therefore, the D-AMPS system achieves three time as much gross system capacity as the AMPS system. The gross bit rate of D-AMPS system is 48.6 Kbps. In order to accommodate it into a 30 kHz channel, $\pi/4$-Differential Quadrature Phase Shift Keying ($\pi/4$-DQPSK) modulation scheme is employed here. Also, a square root raised cosine pulse shaping filter with a rolloff factor of 0.35 is used to reduce the intersymbol interference.

Two months after the acceptance of D-AMPS by the EIA, Qualcomm proposed a new digital air interface based on the spread spectrum communication techniques, now known as IS-95. This system occupies 1.25 MHz, only 10% of the total spectrum allocated to an AMPS service provider. But the system capacity is claimed to be 15-20 times as much as for AMPS [Gil91]. To achieve this goal, a number of sophisticated techniques are used in the IS-95 system design. On the forward link from the base station to the mobile unit, the output of the vocoder is sampled at a variable rate of 1200 bps, 2400 bps, 4800 bps, 9600 bps and 13 kbps. The data are encoded by a convolutional encoder, interleaved by a block interleaver, scrambled by a decimated long code, and multiplexed by a long code and power control bit. The output of the multiplexer is spread by a Walsh code at a rate of 1.2288 Mega chips per second (Mcps) which is assigned to each particular user. Then a base station specified pilot PN sequence is used to modulate the in-phase and quadrature channel. The binary in-phase and quadrature outputs are mapped into the phase of the transmitted signal according to $\pi/4$-Quadrature Phase Shift Keying ($\pi/4$-QPSK) modulation scheme. On the reverse link from the mobile unit to the base station, a Walsh code is used as 64-ary orthogonal data modulation. The data signal is spread by a pseudo noise (PN) like long code, and $\pi/4$-Offset QPSK ($\pi/4$-OQPSK) is used as quadrature modulation. In IS-95, the transmitted signals of different users occupy the same channel bandwidth. A virtual channel is specified by the spreading code assigned to each user. This technique is well known as Code Division Multiple Access (CDMA).

1.3 Wireless Local Loop Systems

WLL systems share a number of common characteristics with cellular systems. A WLL system must employ wireless transmission over distances comparable to those on cellular links. In order to achieve an acceptable capacity, WLL systems must also make use of frequency reuse in a manner similar to cellular systems. The chief difference between cellular and WLL is that WLL systems need not support user mobility [Cox86]. However, the first generation of WLL systems appear to be based largely on the existing cellular standards such as those discussed in Section 1.2 [Haj96]. A number of WLL providers have also investigated the use of cordless telephone system such as DECT [Och89][Mul91][Owe93][Rom94]. However, it should be possible to exploit the fixed nature of the WLL system to develop simpler standards at low cost, which will be a particularly important factor in determining the success of WLL system in developing markets.

1.4 Purpose of the Research

In this research, a new WLL communication system is investigated. This system combines the analog FM modulation component of AMPS system and the CDMA technique of IS-95 to create a new hybrid FM/CDMA WLL system. The purpose of employing analog FM modulation is to avoid the system complexity and high cost of a fully digital CDMA system which requires advanced processing techniques to implement voice and channel coding. In addition, the analog format of FM modulation allows the use of high speed modems originally designed for wireline telephony [Kat91]. This characteristic is particularly important since WLL systems are to be marketed as a direct substitute for wireline service.

At the same time, the hybrid FM/CDMA WLL system discussed here retains many of the inherent advantages of a CDMA system such as increased capacity due to universal frequency reuse and resistance to multipath fading [Gil91]. While such a system will clearly not have the capacity of a fully digital CDMA implementation, it may be possible to obtain a set of tradeoffs of cost, capacity and performance which is uniquely suited to the WLL application.

The first goal of the research is to establish a theory for FM/CDMA system performance by deriving closed form analytical expressions of the Signal to Interference Ratio (SIR) for the input and output signals of a differentiation type FM demodulator. This theory provides very clear guidance in optimization of the system performance. It also provides fundamental insights into the role of FM modulation. By trading bandwidth for performance, FM is seen to be analogous to error correction coding for a fully digital CDMA system.

The second goal of the research is to develop a software test-bed to examine the feasibility of the system and optimize the system through the tradeoff between the FM modulation index and the spread spectrum processing gain. The system capacity is examined by the simulator. The effect of imperfect power control is also a subject of investigation.

This thesis results from a sponsored simulation study performed in the MPRG laboratory. The thesis may be thought of as a companion document to the thesis of Yash Vasavada [Vas96]. While both theses present simulation models for the same basic FM/CDMA system, both make unique contributions. [Vas96] investigates a number of important cases such as the performance in multipath and the power control algorithm. This thesis undertakes a rigorous development of analytic bounds for SIR, and a thorough study of the system operating point.

1.5 Outline of the Thesis

The remainder of this thesis is organized as follows: In Chapter 2, a detailed description of four types of FM demodulation techniques is presented. The models for differentiation, quadrature, arctangent and phase locked loop FM demodulation help establish the system model used later in simulation. The FM threshold phenomenon which gives rise to the tradeoff in operating point selection is discussed. In Chapter 3, an overview of different multiple access schemes and CDMA system principles are presented. Chapter 4 establishes a theory and judges the system performance through the derivation of input and output SIR of a differentiation demodulator. Upper and lower bounds on system performance are obtained. Chapter 5 describes the model for the WLL system studied here. Based on the tentative operation parameters, the system performance is evaluated using the theory developed in Chapter 4. A set of new parameters is proposed to optimize the system performance. Chapter 6 describes the simulation approach and shows the simulation results in a variety of cases, including different demodulation schemes, the system performance under different IF channel occupancy, the system capacity, the forward link and reverse link system performance, and the effect of power control schemes. Finally, the thesis concludes with a summary and suggestions for future work in Chapter 7.

Chapter 2
Frequency Modulation

In this chapter, we review the basic principles of frequency modulation which will be applied throughout this thesis.

In Continuous Wave (CW) modulation systems, a radio frequency sinusoid is used as the carrier in which the amplitude, phase or frequency is modulated by the information signal. In the application of WLL communications, the information is typically baseband human speech. Depending on the method in which the information signal is applied to the system, the modulation scheme can be categorized as linear modulation or nonlinear modulation. The direct implementation of linear modulation techniques is Amplitude Modulation (AM). Fig. 2.1 shows the block diagram of a Double Sideband Suppressed Carrier (DSB-SC) AM transmission system [Cou93].

The general property of Amplitude Modulation can be illustrated by DSB-SC AM:

$$v(t) = m(t)cos(\omega_c t), \tag{2.1}$$

where ω_c is the carrier angular frequency, $m(t)$ is the modulating signal, and $v(t)$ is the mod-

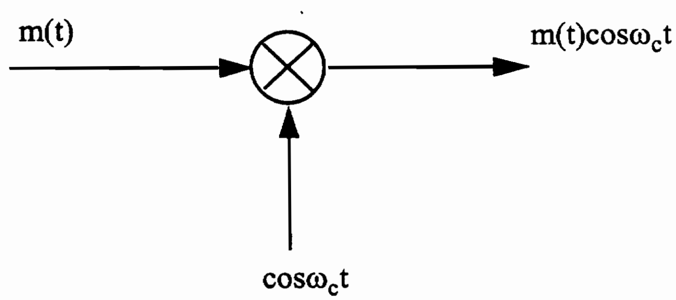

Figure 2.1: Amplitude Modulation

ulated signal. Therefore, the amplitude of the transmitted signal varies with time. However, in wireless communications, due to the multipath propagation in an unconstrained transmission medium, the typical environment is a fading channel where the amplitude of the transmitted signal suffers as much as 30 dB attenuation in fading nulls [Fun93]. Information contained on the amplitude is subject to severe corruption. Therefore, AM shows poor performance in wireless communications environment. However, nonlinear modulation techniques which preserve a constant envelope property exhibit much better performance in fading environments and therefore are used in the AMPS system and other wireless FM systems.

2.1 Frequency Modulation

Linear modulation is, however, not the only means of modulating a sinusoidal carrier [Cou93]. The frequency and phase of a sinusoid can also be modulated by information signal. Angle Modulation, a general category of frequency modulation and phase modulation is a type of nonlinear modulation. One of the most striking characteristics of frequency modulation is that the Signal to Noise Ratio (SNR) of the output can be significantly improved by increasing the frequency deviation of the modulation, or the Intermediate Frequency (IF) bandwidth, while keeping the transmission power fixed. The larger the IF bandwidth, the greater the output SNR, therefore the better the output voice quality. The penalty for SNR improvement is two-fold. First, the transmitted signal occupies a wider IF bandwidth, a precious asset in wireless communications. Second, the received signal power moves closer to the FM threshold as the IF bandwidth increases. When the received signal power falls below the FM threshold, the output noise power increases significantly. The received signal loses the advantage of immunity to noise corruption inherent in FM techniques.

Exponential transformation is the most easily implemented nonlinear modulation representation in a practical system. A frequency modulated signal can be expressed as

$$s(t) = A_c cos[\omega_c t + \theta(t)], \tag{2.2}$$

where A_c is the constant carrier amplitude, ω_c is the carrier angular frequency, and the phase $\theta(t)$ is a function of the information signal:

$$\theta(t) = D_f \int_{-\infty}^{t} m(x)\, dx, \tag{2.3}$$

where D_f is the frequency deviation constant and $m(t)$ is the information signal.

For a fixed information signal $m(t)$, the frequency deviation constant D_f determines the IF bandwidth a modulated signal occupies. The larger the frequency deviation constant, the wider the IF bandwidth required for distortionless transmission. Another measure of bandwidth occupancy is given by the modulation index β, which is defined as the peak frequency deviation ΔF, normalized by the bandwidth of the information signal B:

$$\beta = \frac{\Delta F}{B}, \tag{2.4}$$

where

$$\Delta F = max\{\frac{1}{2\pi}[\frac{d\theta(t)}{dt}]\}. \tag{2.5}$$

Substituting Eqn. (2.3) into Eqn. (2.5), we have

$$\Delta F = \frac{1}{2\pi} D_f V_p, \tag{2.6}$$

where $V_p = max[m(t)]$. Note that the modulation index is directly proportional to the IF bandwidth.

Fig. 2.2 illustrates an FM signal modulated by a sinusoid. The constant envelope property of the FM signal is very attractive for wireless communications where fading caused by multipath propagation deteriorates the system performance. For FM, the information signal is contained in the phase term, rather than the amplitude. Therefore, FM has much better fading resistance than AM. Furthermore, hardlimiting the FM signal improves the system performance by eliminating the amplitude fluctuations caused either by white Gaussian noise or channel fading.

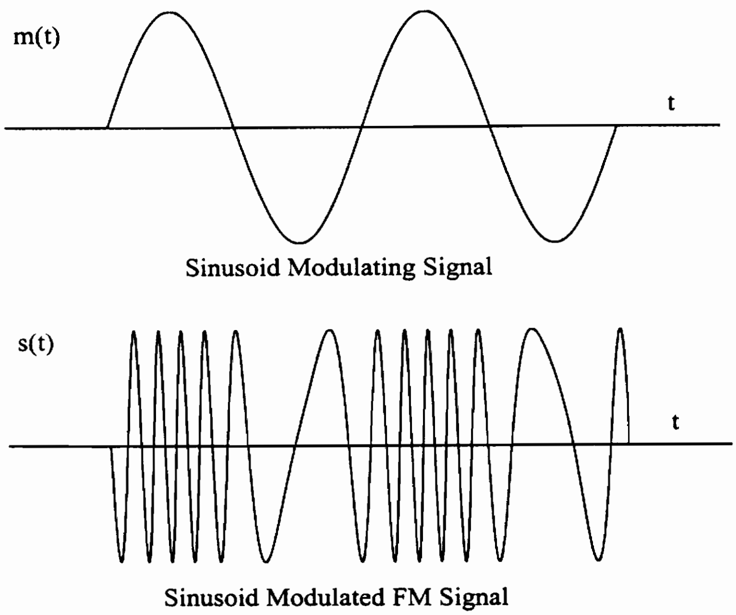

Figure 2.2: FM Signal Modulated by a Sinusoid

2.2 Wideband FM (WBFM)

Since larger modulation indices yield better system performance in FM, it is tempting to utilize larger bandwidth to achieve this goal. For modulation index $\beta > 1$, the Power Spectral Density (PSD) of WBFM signal is approximated by the Probability Distribution Function (PDF) of the modulating signal [Row65]. The reason behind this quasi-static approximation lies in the fact that the for FM, the instantaneous frequency varies in proportion to the modulating signal voltage according to Eqn. (2.3). The wideband FM spectrum can be approximated as

$$S_{fm}(f) = \frac{\pi A_c^2}{2D_f}\{f_m[\frac{2\pi}{D_f}(f - f_c)] + f_m[\frac{2\pi}{D_f}(-f - f_c)]\}, \tag{2.7}$$

where A_c is the amplitude of the carrier, D_f is the FM frequency deviation constant, f_m is the probability distribution function of the modulating signal.

We will see later in this thesis that there is a tradeoff between increasing the IF bandwidth of the FM signal and increasing the spread spectrum processing gain.

2.3 FM Demodulation Schemes

As mentioned earlier, the received signal is subject to multipath propagation which causes fading in a wireless communication environment. The received signal is further corrupted by Additive White Gaussian Noise (AWGN). To understand the basic performance of frequency modulation, we assume the channel characteristic is limited to AWGN. The FM signal is passed through a network whose amplitude and phase-shift preserves a linear relationship so that the original baseband signal can be recovered from the FM demodulator without distortion introduced by the frequency dependent nonlinearity of the network. This section investigates four types of FM demodulation schemes: Differentiator, Quadrature, Arctangent and Phase-Locked Loop (PLL).

2.3.1 Differentiator

The FM demodulator which is the easiest to conceptualize is a differentiator which converts the frequency variation to an amplitude variation [Cou93][Pan65]. The baseband signal is recovered by passing this amplitude modulated signal through an envelope detector. A block diagram of a differentiator used for FM demodulation is shown in Fig. 2.3.

The received signal, a combination of the desired FM signal and AWGN, is passed through a bandpass filter to bandlimit the white Gaussian noise. Then the filtered signal is downconverted from the radio frequency (RF) to the intermediate frequency (IF). The output of the differentiator $v_3(t)$ is related to the input of the differentiator $v_2(t)$ by

$$v_3(t) = K\frac{d}{dt}v_2(t), \tag{2.8}$$

where K is the differentiator gain.

In the frequency domain, a differentiator is represented by a transfer function described

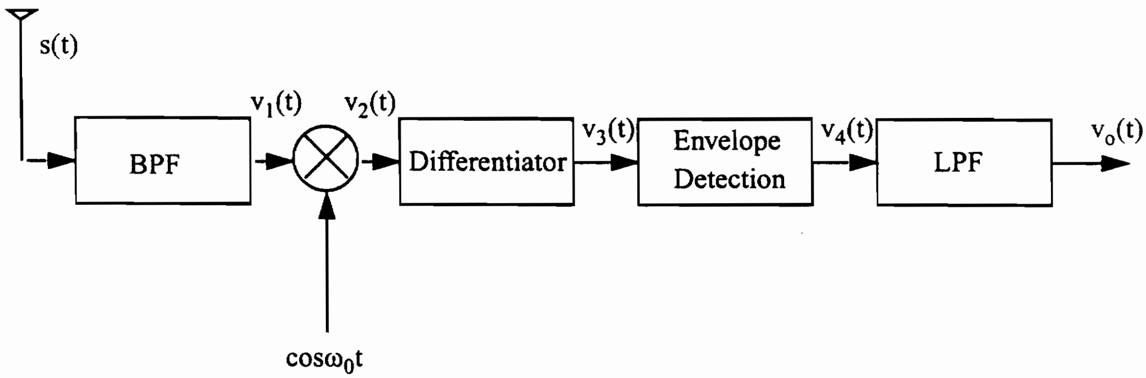

Figure 2.3: Block Diagram of a Differentiation FM Demodulator

by

$$H(\omega) = Kj\omega. \tag{2.9}$$

The input of the differentiator is

$$v_2(t) = A_c cos[\omega_c t + \theta(t)], \tag{2.10}$$

where $\theta(t)$ is given by Eqn. (2.3).

Then the output of the differentiator is

$$v_3(t) = K\frac{d}{dt}v_2(t) = -KA_c[\omega_c + \frac{d}{dt}\theta(t)]sin[\omega_c t + \theta(t)]. \tag{2.11}$$

The output of the envelope detector is the amplitude of the sinusoidal waveform, with a sign reversal:

$$v_4(t) = KA_c[\omega_c + \frac{d}{dt}\theta(t)]. \tag{2.12}$$

With a capacitor or balanced demodulation technique, the DC term of above expression can be eliminated:

$$v_o(t) = KA_c\frac{d}{dt}\theta(t) = KA_c D_f m(t). \tag{2.13}$$

The baseband signal $m(t)$ is thus recovered.

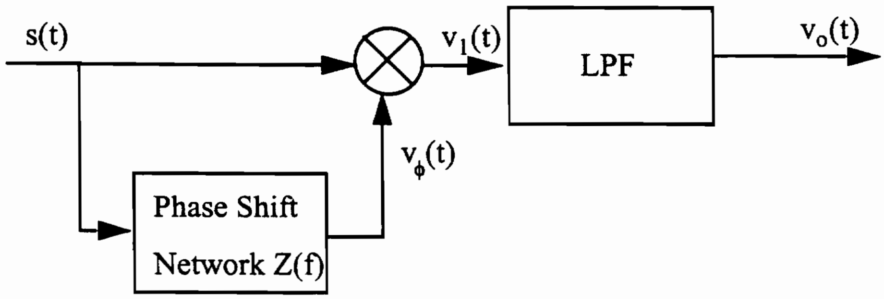

Figure 2.4: Block Diagram of the Quadrature FM Demodulator

2.3.2 Quadrature Demodulation

Quadrature demodulation is another popular detection technique which is easily implemented in an integrated circuit [Rap96]. Fig. 2.4 shows the block diagram of the quadrature demodulator.

Suppose $s(t)$ is the received FM signal which has already been downconverted to IF. The quadrature signal is obtained from the FM signal by passing it through a phase shift network $Z(f)$. The phase response function of the network should satisfy

$$\phi(f) = -\frac{\pi}{2} + 2\pi K(f - f_c), \tag{2.14}$$

where K is a constant, f_c is the intermediate carrier frequency, and $f(t)$ is the instantaneous frequency of the input FM signal, which is defined as

$$f(t) \equiv f_c + \frac{1}{2\pi}\frac{d}{dt}\theta(t) = f_c + \frac{D_f}{2\pi}m(t). \tag{2.15}$$

After the FM signal passes through the phase shift network, the output can be expressed as

$$v_\phi(t) = A_c cos[\omega_c t + \theta(t) + \phi(t)]. \tag{2.16}$$

The quadrature signal is multiplied by the FM signal to generate the demodulated signal by using a product detector so that

$$v_1(t) \quad = \quad v_\phi(t)s(t) = A_c^2 cos[\omega_c t + \theta(t) + \phi(t)]cos[\omega_c t + \theta(t)]$$

$$= \frac{A_c^2}{2}\{cos[2\omega_c t + 2\theta(t) + \phi(t)] + cos[\phi(t)]\}. \quad (2.17)$$

The double carrier frequency term is removed by the low pass filter. The recovered baseband signal $v_o(t)$ is

$$\begin{aligned} v_o(t) &= LPF\{v_1(t)\} = \frac{A_c^2}{2}cos\{\phi[f(t)]\} \\ &= \frac{A_c^2}{2}cos[-\frac{\pi}{2} + 2\pi K(f - f_c)] \\ &= \frac{A_c^2}{2}cos[-\frac{\pi}{2} + 2\pi K\frac{D_f}{2\pi}m(t)] \\ &= \frac{A_c^2}{2}sin[KD_f m(t)]. \end{aligned} \quad (2.18)$$

If the phase variation is small, $KD_f m(t) \ll 1$, then

$$v_o(t) = \frac{A_c^2}{2}KD_f m(t) \propto m(t). \quad (2.19)$$

Therefore, the output of a quadrature detector is proportional to the baseband signal $m(t)$ and the original speech signal is recovered.

2.3.3 Arctangent Demodulation

For the arctangent demodulator, the received FM signal can be expressed in the quadrature representation:

$$\begin{aligned} s_{FM}(t) &= A_c cos[\omega_c(t) + \theta(t)] \\ &= A_c cos[\theta(t)]cos\omega_c t - A_c sin[\theta(t)]sin\omega_c(t) \\ &= x(t)cos\omega_c t - y(t)sin\omega_c(t), \end{aligned} \quad (2.20)$$

where $x(t) = A_c cos[\theta(t)]$, and $y(t) = A_c sin[\theta(t)]$.

The phase is related to the in-phase and quadrature terms by

$$tan[\theta(t)] = \frac{y(t)}{x(t)}, \quad (2.21)$$

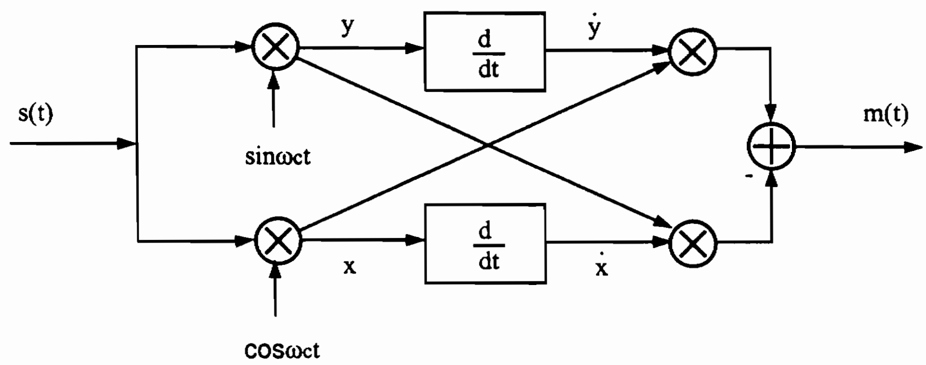

Figure 2.5: Block Diagram of Arctangent Demodulation

or

$$\theta(t) = tan^{-1}[\frac{y(t)}{x(t)}]. \tag{2.22}$$

Differentiating the phase yields

$$\frac{d\theta}{dt} = \frac{\frac{\dot{y}(t)x(t) - \dot{x}(t)y(t)}{x^2(t)}}{1 + [\frac{y(t)}{x(t)}]^2} = \frac{\dot{y}(t)x(t) - \dot{x}(t)y(t)}{x^2(t) + y^2(t)}. \tag{2.23}$$

The left hand side of above equation is $D_f m(t)$ according to Eqn. (2.3). Therefore,

$$m(t) = \frac{\dot{y}(t)x(t) - \dot{x}(t)y(t)}{D_f[x^2(t) + y^2(t)]}. \tag{2.24}$$

Based on this algorithm, the arctangent FM demodulation can be implemented as shown in Fig. 2.5. Notice that since $x^2(t) + y^2(t) = A_c^2$, the square and division operations do not need to be implemented.

2.3.4 Phase Locked Loop (PLL)

A PLL is a closed loop feedback system which can be used to track either the phase or frequency information of a received signal [Gar79]. A basic PLL consists of three components: a phase detector, a low pass filter and a voltage-controllable oscillator (VCO). Fig. 2.6 shows the block diagram of a basic PLL.

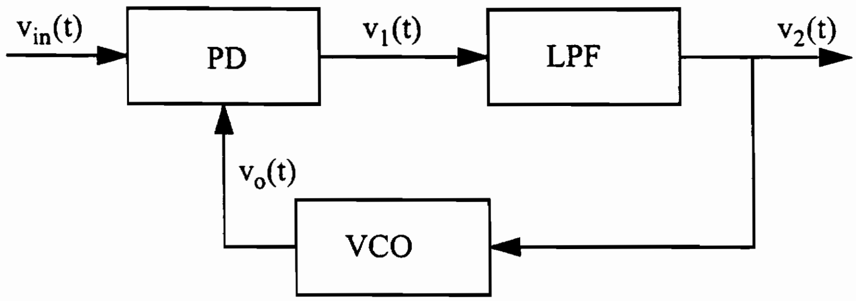

Figure 2.6: Block Diagram of Basic PLL

A phase detector is a device which converts the phase difference between the two input signals into a voltage difference. It may be implemented by a double balanced mixer or simply a multiplier. The phase error versus error voltage of a phase detector with a sinusoidal characteristic is shown in Fig. 2.7.

A VCO is a device which generates a periodic waveform whose frequency is determined by the applied voltage. The free running frequency f_0 is the frequency when no external voltage is applied. Assume K_v is the frequency sensitivity of the VCO, where

$$K_v = \frac{d\omega}{dv}. \tag{2.25}$$

The output of a VCO $v_0(t)$ is related to the input of the VCO $v(t)$ by

$$v_0(t) = A_0 cos[\omega_0 t + \theta_0(t)], \tag{2.26}$$

where

$$\theta_0(t) = K_v \int_{-\infty}^{t} v(\tau)\, d\tau. \tag{2.27}$$

The basic principle of a PLL used as an FM demodulator is based on the feedback nature of the closed servo loop. The closed loop is trying to operate at a zero error voltage state which forces the output of a VCO to follow the change of the input FM signal. Due to the differentiation relationship between the input and output of a VCO, if the output of the VCO is to follow the received FM signal, the input of the VCO is the differentiation of the

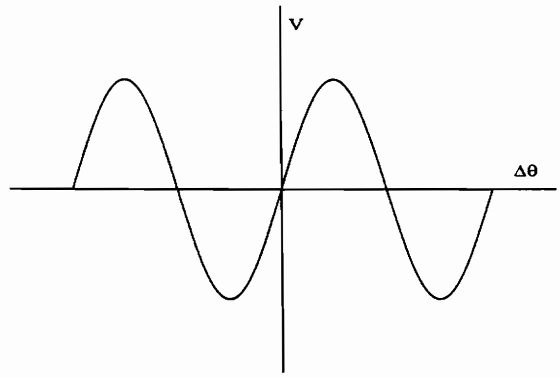

Figure 2.7: Phase-Voltage Response of a Sinusoidal Phase Detector

FM signal in the absence of the carrier, which is the baseband voice signal. The operating principle of a PLL as an FM demodulator is best illustrated in the frequency domain.

Suppose the input signal of a PLL is

$$v_{in}(t) = A_i sin[\omega_c t + \theta_i(t)], \tag{2.28}$$

where, $\theta_i(t) = D_f \int_{-\infty}^{t} m(x)\, dx$, $m(x)$ is the baseband modulating signal. In the frequency domain

$$\Theta_i(f) = \frac{D_f}{j2\pi f} M(f), \tag{2.29}$$

where $\Theta_i(f)$ is the Fourier transform of $\theta_i(t)$, and $M(f)$ is the Fourier transform of $m(t)$. Assume the frequency response of the low pass filter is $F_1(f) = F(f)$, and the frequency response of the VCO is $F_2(f) = \dfrac{K_v}{j2\pi f}$. The phase representation of a PLL is shown in Fig. 2.8.

For a locked PLL, $\theta_i(t) \approx \theta_o(t)$, the phase error $\theta_e(t)$ is very small. Therefore, $sin[\theta_e(t)] \approx \theta_e(t)$. The PLL equation is reduced to a linear equation. Hence

$$V_2(f) = \frac{(j\frac{2\pi f}{K_v})F_1(f)}{F_1(f) + j(\frac{2\pi f}{K_v K_d})} \Theta_i(f), \tag{2.30}$$

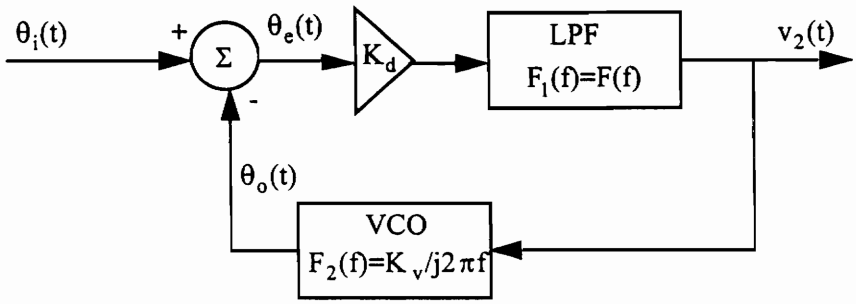

Figure 2.8: Phase Representation of PLL

where $V_2(f)$ is the Fourier transform of $v_2(t)$.

Suppose the baseband bandwidth of $m(t)$ is B, and $F_1(f)$ is an ideal low-pass filter.

$$F_1(f) = \begin{cases} 1 & |f| \leq B \\ 0 & \text{otherwise.} \end{cases}$$

If $\frac{K_d K_v}{2\pi} \gg B$, then

$$V_2(f) = \frac{D_f}{K_v} M(f). \tag{2.31}$$

In the time domain

$$v_2(t) = \frac{D_f}{K_v} m(t), \tag{2.32}$$

which is the desired output characteristic.

Although a PLL offers no improvement over the conventional differentiator for input SNR above threshold, it does provide threshold extension, which allows the system to operate at a lower input SNR. This is very attractive for a system which operates over a wide dynamic range of input SNR.

2.4 FM System Performance with Differentiation Demodulation

2.4.1 Input and Output Signal to Noise Ratio

The output SNR of an FM system with differentiation demodulation has been derived in many textbooks [Cou93][Tau86][Pan65]. The FM system is modeled using the following assumptions.

1. The system is operating at a sufficiently high input SNR, in a region above the threshold of the FM demodulator.
2. The channel noise is additive white Gaussian noise (AWGN) with a two-sided power spectral density of $N_0/2$.
3. The noise output is approximately independent of the modulating signal.
4. The IF bandwidth is determined by Carson's rule, which defines the bandwidth with 98% of the signal power confinement. Note however, the FCC defines the bandwidth as 99% of the signal power confinement for wireless applications [Rap96].

The operating principle of an FM system with differentiation demodulation was developed in Section 2.3.1. Based on that system configuration, the input SNR and the output SNR of an FM differentiator are found to be [Cou93]

$$(\frac{S}{N})_{in} = \frac{A_c^2}{4N_0(\beta+1)B}, \tag{2.33}$$

and

$$(\frac{S}{N})_{out} = \frac{3A_c^2\beta^2\overline{(\frac{m}{V_p})^2}}{2N_0B}, \tag{2.34}$$

where

A_c is the amplitude of the carrier,

N_0 is related to the two-sided AWGN power spectral density $N_0/2$,

β is the FM modulation index,

B is the bandwidth of the baseband modulating signal,

m is the baseband modulating signal, and

V_p is the peak value of the modulating signal $m(t)$.

The expression of the output SNR indicates that the performance of an FM system can be improved by increasing the modulation index β, at the cost of a wider IF bandwidth occupancy. The increment of the modulation index β, however, reduces the input SNR of an FM demodulator as indicated by Eqn. (2.33). As we shall see later, an FM system exhibits a threshold phenomenon where the output power of the demodulator drops rapidly as the input SNR goes below the threshold. This tradeoff will be very important in the design of our hybrid FM/CDMA communication system.

2.4.2 FM Threshold

The FM threshold effect was analyzed in detail by Rice and Stumpers [Ric63]. The threshold was found to be related with the number of noise spikes ("clicks" as we may hear), when the input signal power is at a lower lever compared with the channel noise. Experiments as well as simulations show that there is a level of input SNR below which the output SNR rolls off quickly.

To understand the occurrence of spikes, let us consider the input signal to be an unmodulated carrier in the presence of white Gaussian noise [Tau86]. After passing through an IF filter, the white Gaussian noise becomes a narrowband noise process $n(t)$, which can be represented in the quadrature notation.

$$n(t) = x(t)cos\omega_c t - y(t)sin\omega_c t. \tag{2.35}$$

The input signal $v_i(t)$ is the narrow band noise plus the unmodulated carrier:

$$v_i(t) = A_c cos\omega_c t + x(t)cos\omega_c t - y(t)sin\omega_c t. \tag{2.36}$$

In complex representation,

$$v_i(t) = Re\{[A_c + x(t) + jy(t)]e^{j\omega_c t}\}. \tag{2.37}$$

Let $r(t) = \sqrt{x^2(t) + y^2(t)}$ and $\phi(t) = tan^{-1}[\frac{y(t)}{x(t)}]$. Then $r(t)$ is a Rayleigh distributed random variable [Sta94] and $\phi(t)$ is a random variable uniformly distributed between $[-\pi, \pi]$. The baseband signal of the demodulated input can be written as

$$g(t) = A_c + x(t) + jy(t) = A_c + r(t)e^{j\phi(t)} = R(t)e^{j\theta(t)}. \tag{2.38}$$

When the input SNR is high, the probability that $r(t) \gg A_c$ is very small. The phasor diagram of $g(t)$ is drawn in Fig. 2.9. Since $r(t) \ll A_c$, the resultant vector $R(t)$ has a very limited phase drift $\theta(t)$ around the vector A_c. Therefore spikes are very unlikely to occur at high input SNR level.

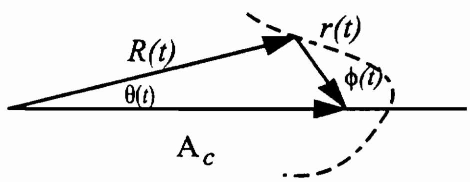

Figure 2.9: Phasor Diagram for High Input SNR

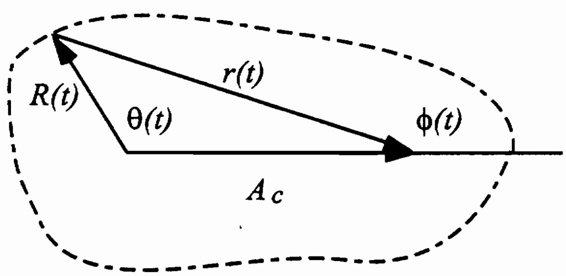

Figure 2.10: Phasor Diagram for Low Input SNR

However, if the input SNR is low, the probability that $r(t) > A_c$ is large. The phasor diagram of $g(t)$ in this case is drawn in Fig. 2.10. The resultant vector $R(t)$ may have a very large phase drift, and even rotate around the carrier vector A_c. Then there is a period of time when the angle $\theta(t)$ changes from 0 to 2π. Suppose the 2π phase transition occurs over a time interval between t_1 and t_2. Then before t_1 and after t_2, $r(t) \ll A_c$, only small random phase variations occur.

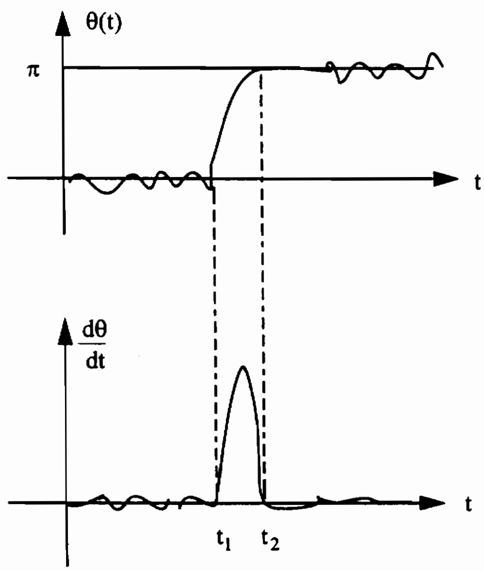

Figure 2.11: Occurance of a Spike

Fig. 2.11 shows an abrupt phase change of π of the phase signal. If the time duration from t_1 to t_2 is very small, the spike is more or less like a δ-function, in which case there is a strong spike of interference in the received FM signal.

Based on the assumption that the occurrence of spikes causes threshold effect in an FM demodulation, Taub and Shilling [Tau86] calculated the average time between spikes (spike occurring frequency), the total number of spikes occurring per second and the output SNR is related to the input SNR by a nonlinear relationship

$$(\frac{S}{N})_{out} = \frac{6\beta^2(\beta+1)\overline{(\frac{m}{V_p})^2}(\frac{S}{N})_{in}}{1 + 12\sqrt{\frac{2}{\pi}\overline{(\frac{m}{V_p})^2}}\beta(\beta+1)(\frac{S}{N})_{in} exp\{-(\frac{S}{N})_{in}\}}. \tag{2.39}$$

The exponential term of input SNR contributes significantly to the FM threshold. Fig.

2.12 uses Eqn. (2.39) to plot the output SNR versus the input SNR for a normalized input baseband signal power of 0.02, and β of 1.0, 2.0, 3.0 and 5.0. It can be seen from the figure that

1. The output SNR increases as the modulation index β increases.

2. The FM threshold increases as the modulation index β increases.

When a system is designed to operate in a wide dynamic range of input SNR, a lower threshold is desired. To achieve this goal, the system must operate with a smaller modulation index β, which in turn degrades the voice quality, or else a more complicated demodulation technique, such as a PLL, should be used for threshold extension.

2.5 Chapter Summary

In this chapter, we have reviewed the fundamental principles of FM modulation and demodulation. We have reviewed the derivation of the output SNR expression for the case of a simple differentiator demodulator. After reviewing te principles of CDMA in the next chapter, we will use these results to undertake a rigorous analysis of the hybrid FM/CDMA system in Chapter 4.

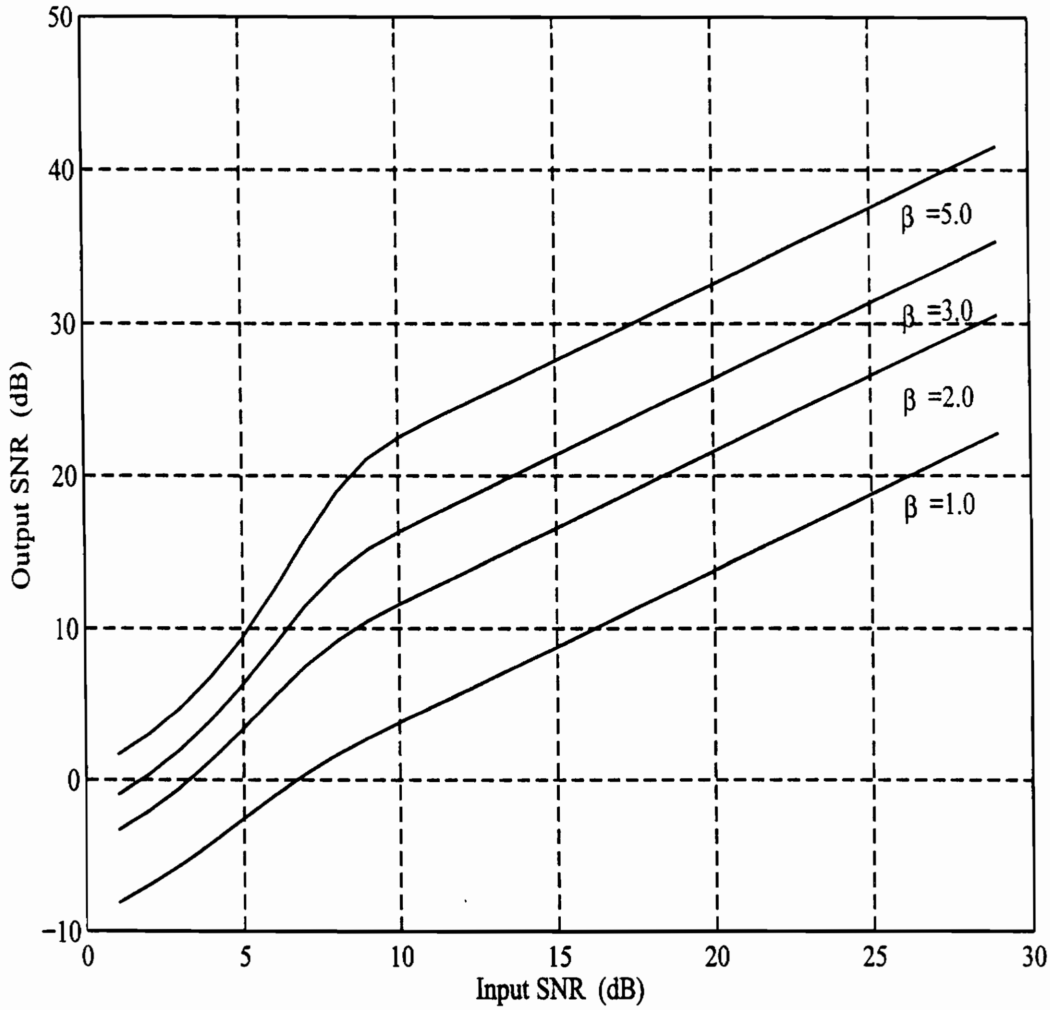

Figure 2.12: Theoretical Curve of Output SNR versus Input SNR for Differentiation Demodulation

Chapter 3

CDMA for Spread Spectrum Communication

The development of commercial CDMA systems has undergone tremendous progress in the past few years. Numerous field tests and trials have been conducted on the feasibility of CDMA systems for cellular and PCS applications. Direct Sequence Code Division Multiple Access (DS/CDMA) techniques have been proposed for cellular [Lee91], PCS [Mil92], indoor [Kav87] and satellite communications [Gil90]. CDMA is also a strong competitor for high data applications, such as wireless local area networks and video phones. Before delving further into CDMA technique, let us first review different multiple access schemes widely used in wireless communications.

3.1 Multiple Access Techniques

Multiple access schemes are used for the sharing of fixed communication resources, such as time, frequency, space, polarization, or code set. Depending on the statistical properties of each random arrival, the resource may be allocated according to specific needs. Variable transmission rate of the voice signal in a GSM cellular system and dynamic channel allocation in North America AMPS cellular system are two of such examples.

3.1.1 FDMA

Frequency Division Multiple Access (FDMA) was the earliest communication resource allocation scheme in telephony dating back to early 1900s. Due to the success of landline applications, it was adopted in the first generation cellular telephone standards, such as AMPS, ETACS and NTT.

Fig. 3.1 shows the utilization scheme of frequency bands as communication resources in an FDMA system. The channelized spectrum is assigned to a single user for a long time period.

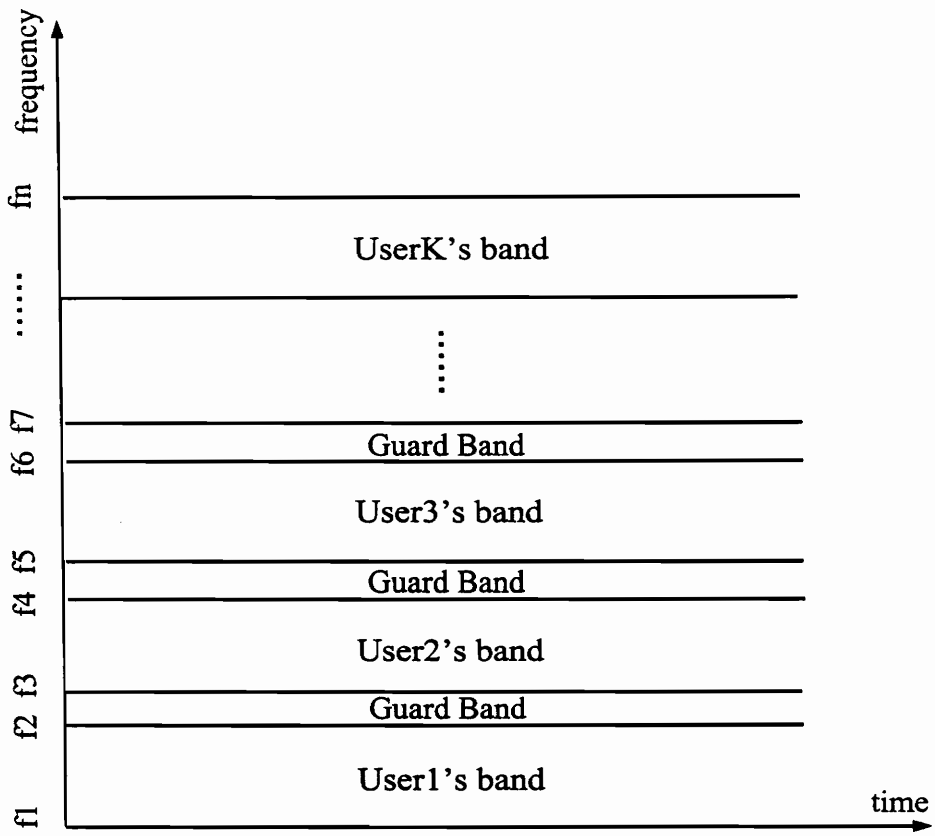

Figure 3.1: Illustration of FDMA Scheme

The major advantage of a FDMA system is its simplicity because each channel is almost independent of all other channels and therefore no coordination is necessary. The disadvantage, on the other hand, is the inefficiency in channel utilization. With this type of circuit switching technique, a channel may not be accessed by other users once it is assigned to one user, no matter whether the channel is active or not.

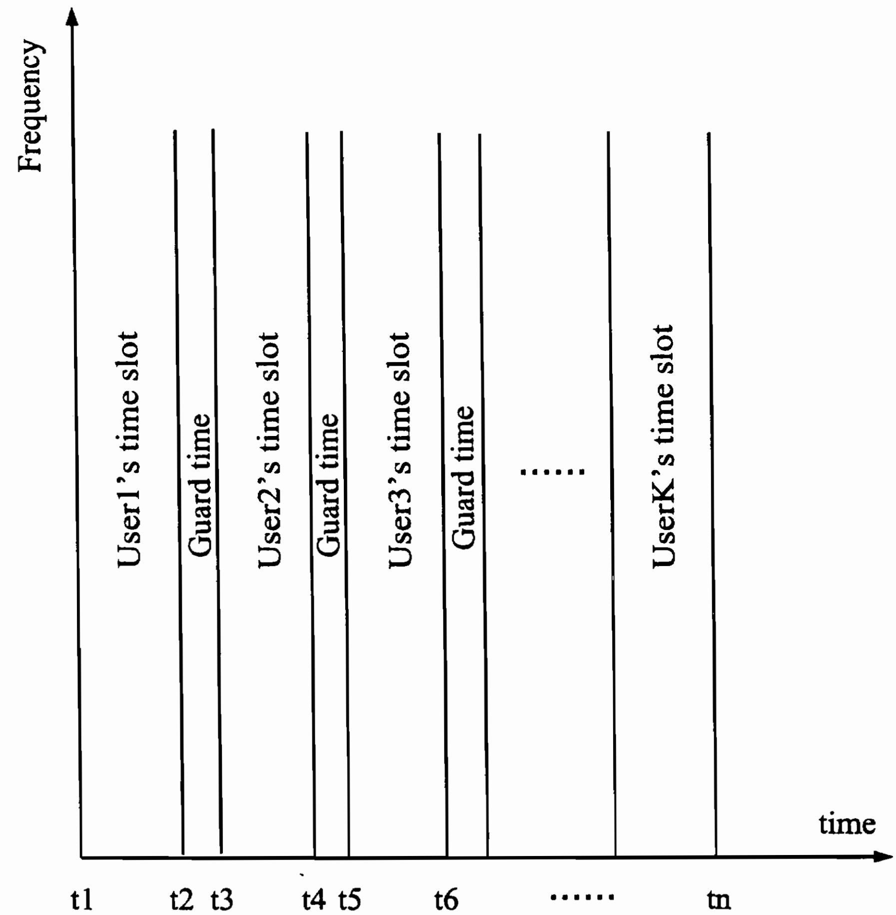

Figure 3.2: Illustration of TDMA Scheme

3.1.2 TDMA

Time Division Multiple Access (TDMA) was promoted as a result of the advances in digital communications based on VLSI technology. As a result, the second generation of cellular communication systems such as Global System for Mobile (GSM), IS-54, and cordless systems such as Digital European Cordless Telephone (DECT), and the PCS system such as Personal Access Communication System (PACS) are all developed and commercially deployed all over the world. Digital cellular systems were designed to co-exist with the analog cellular system in the dual mode operation. It is expected that the digital cellular systems will replace the analog cellular systems as the cost of VLSI chips drops.

In Fig. 3.2, sharing of the communication resource is accomplished via time slot assignment. Each channel is distinguished by assigning a finite time duration, which is separated by a guard time. Each TDMA frame contains a fixed number of time slots. This frame structure repeats so that a time slot assigned to a particular user appears periodically within each time frame. However, for a fixed assignment TDMA scheme, each time slot is pre-assigned to a particular user. If that user has no data to transmit during a pause in that time slot, the communication resource is wasted which results in a low channel utilization. When the channel assignment is unpredicatable, which is true for most digital communication systems with random signal accesses, a dynamic channel assignment strategy known as packet switching is more popular used to provide better channel utilization. Based on this idea, Extended-TDMA (E-TDMA) systems, have been developed as an example of dynamic allocation of TDMA time slots, assigning time slots based on digital speech interpolation to take advantage of voice activity [Kei95]. Another important advantage of TDMA system is the ability to reduce cost due to the sharing of RF equipment by multiple users assigned to the same frequency channel.

3.1.3 CDMA

Code Division Multiple Access (CDMA) is an application of spread spectrum communication technology which has been used in military systems for the past half century [Sch82]. Each signal occupies the same wide frequency band and transmits at the same time. Therefore, there is only one physical channel in the system. However, virtual channels may be identified by different signature sequences. Fig. 3.3 illustrates the CDMA concept in which all users share the same frequency spectrum for all time. Channels are formed by assigning each user a unique signature or code sequence. There are two primary ways of implementing CDMA, Direct Sequence Spread Spectrum (DS/SS) and Frequency Hopped Spread Spectrum (FH/SS).

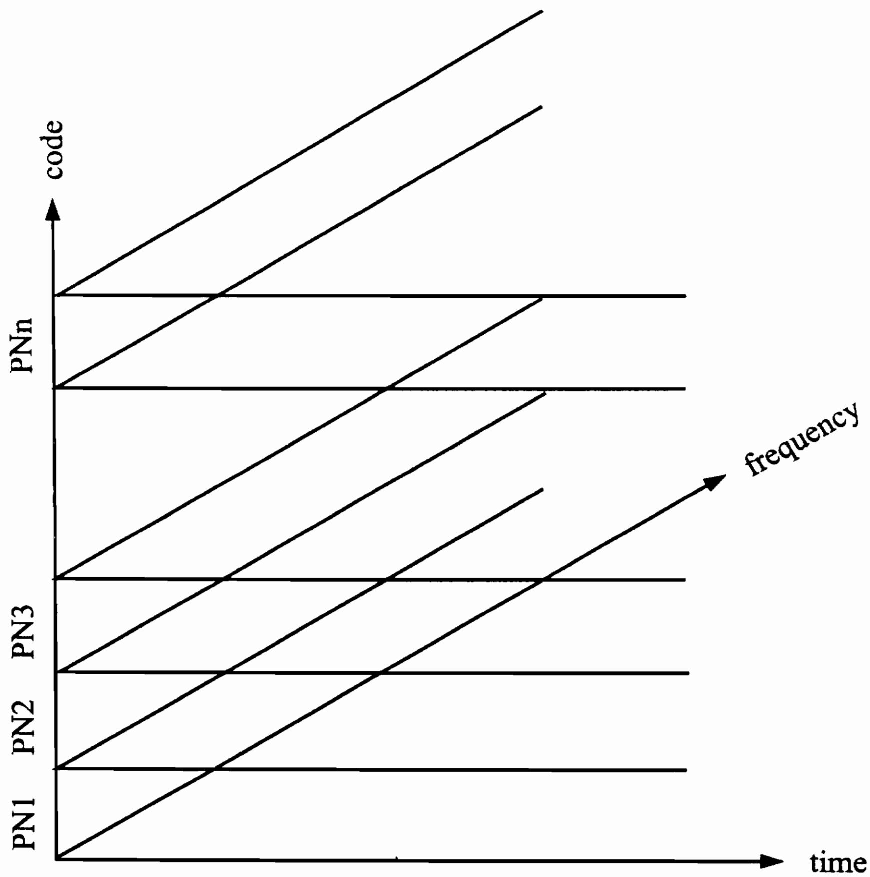

Figure 3.3: Illustration of CDMA Scheme

DS/SS

In DS/SS, the transmitted baseband signal is spread into a much wider bandwidth by multiplying with a noise-like signature sequence so that the signal power spectral density is so low that it is virtually indistinguishable from the background noise. The transmitted signal of each user is assigned a periodic spreading sequence with a bandwidth on the order of several MHz. The communications resource is specified by a set of orthogonal or nearly orthogonal code sequences. The Pseudo-Noise signature sequence, or PN sequence, consists of a pseudorandom series of 1's and 0's which repeats at a regular period. Fig. 3.4 and Fig. 3.5 show the transmitter and the receiver structures of a CDMA system.

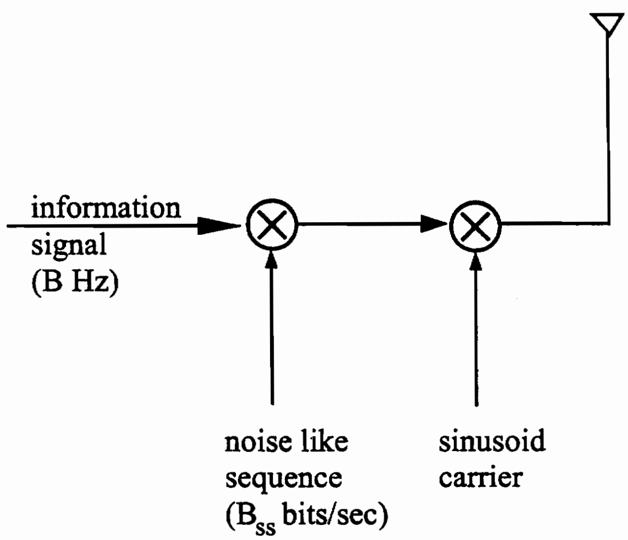

Figure 3.4: CDMA Modulator

The information signal can be either analog or digital, with a narrow band bandwidth being B Hz. The noise like spreading code is a period sequence using bipolar NRZ signaling with a bandwidth of B_{ss} Hz which is much much greater than that of the narrow band interference signal. The ratio B_{ss}/B is a very important parameter called "processing gain", which describes the ratio of the power spectral density function of the desired user to

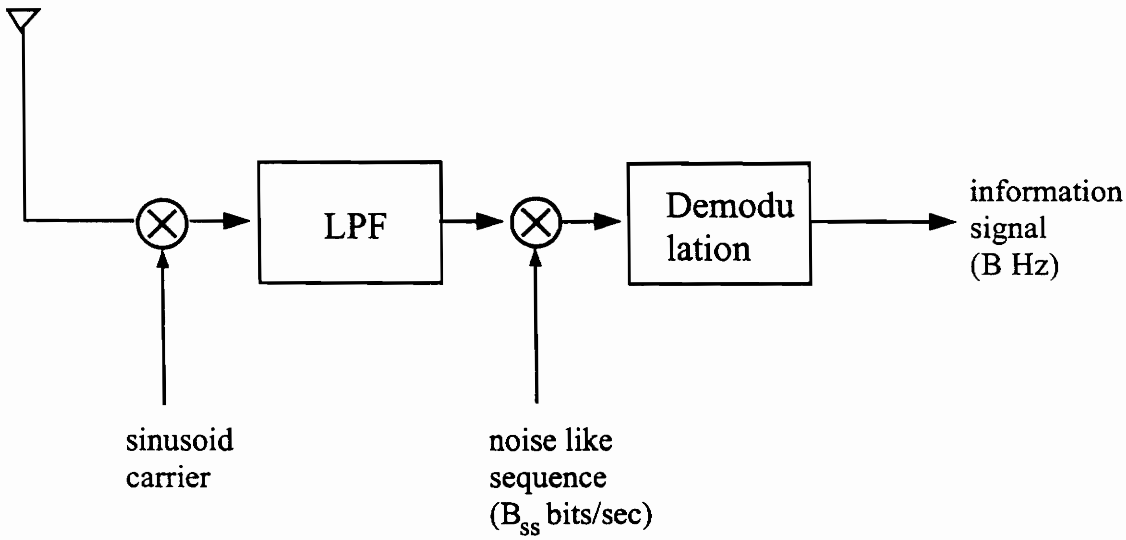

Figure 3.5: CDMA Demodulator

those of the interfering users. The higher the processing gain, the less the multiple access interference.

Fig. 3.6 shows the concept of a baseband CDMA signal in the time domain, where

$b(t)$ is the data information to be transmitted with the bit duration time of T_b,

$a(t)$ is the spreading sequence with the chip duration time of T_c,

$c(t)$ is the spread signal, $c(t) = b(t)a(t)$,

$d(t)$ is the despread signal, $d(t) = a(t)c(t)$.

From Fig. 3.6, it can be seen that the spread signal is much like random noise. Without the prior knowledge of the spreading sequence, it is almost impossible to reproduce the original data. However, with a synchronized despreading, the original data is perfectly recovered.

Fig. 3.7 shows the concept of CDMA in the frequency domain. Suppose the desired user and the interfering user have the same shape of baseband power spectral density as shown in (a). After being multiplied by user specified PN sequences, the signal power of both users is spread into the whole spread spectrum bandwidth. The level of each power

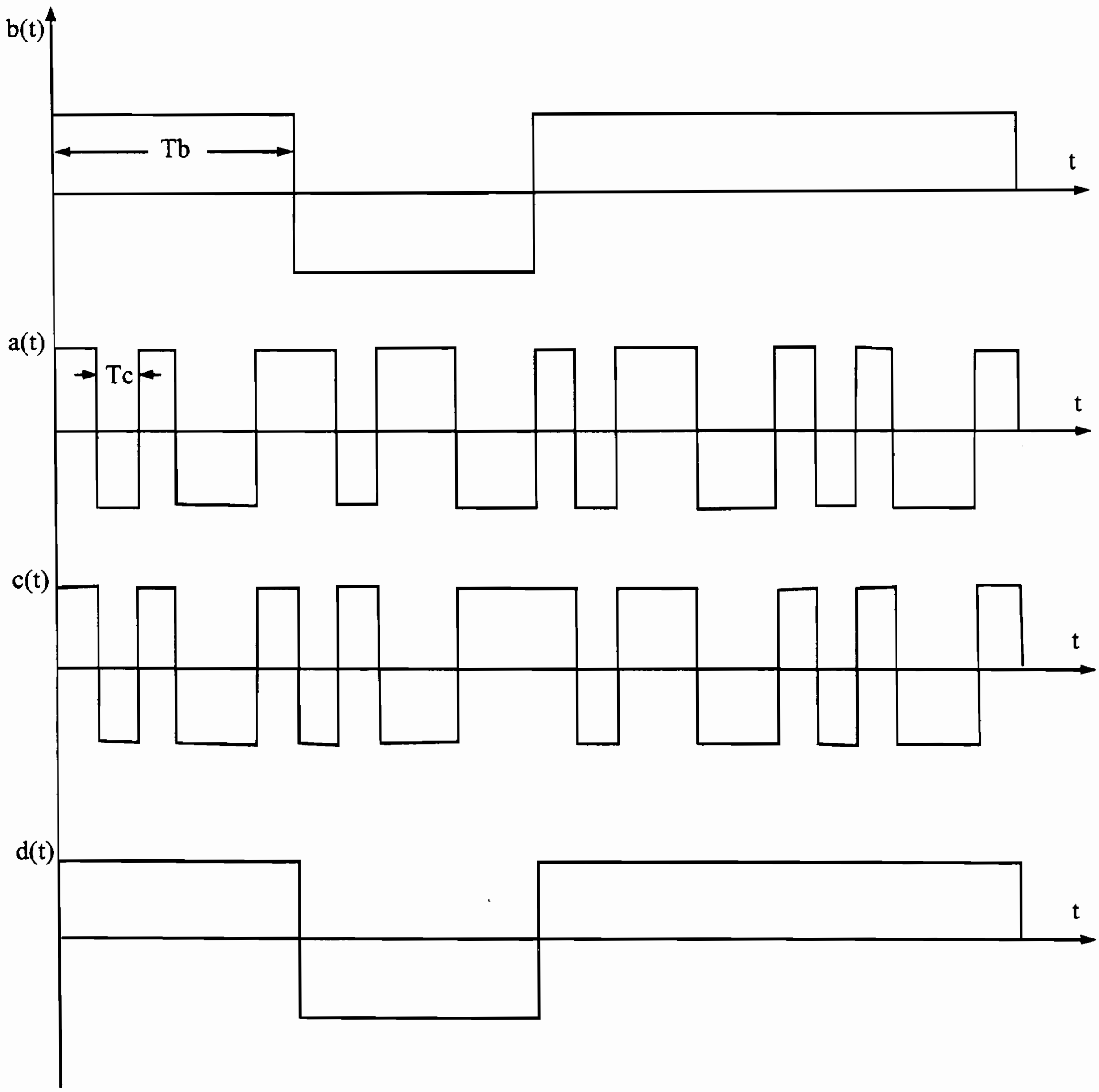

Figure 3.6: CDMA Concept in Time Domain

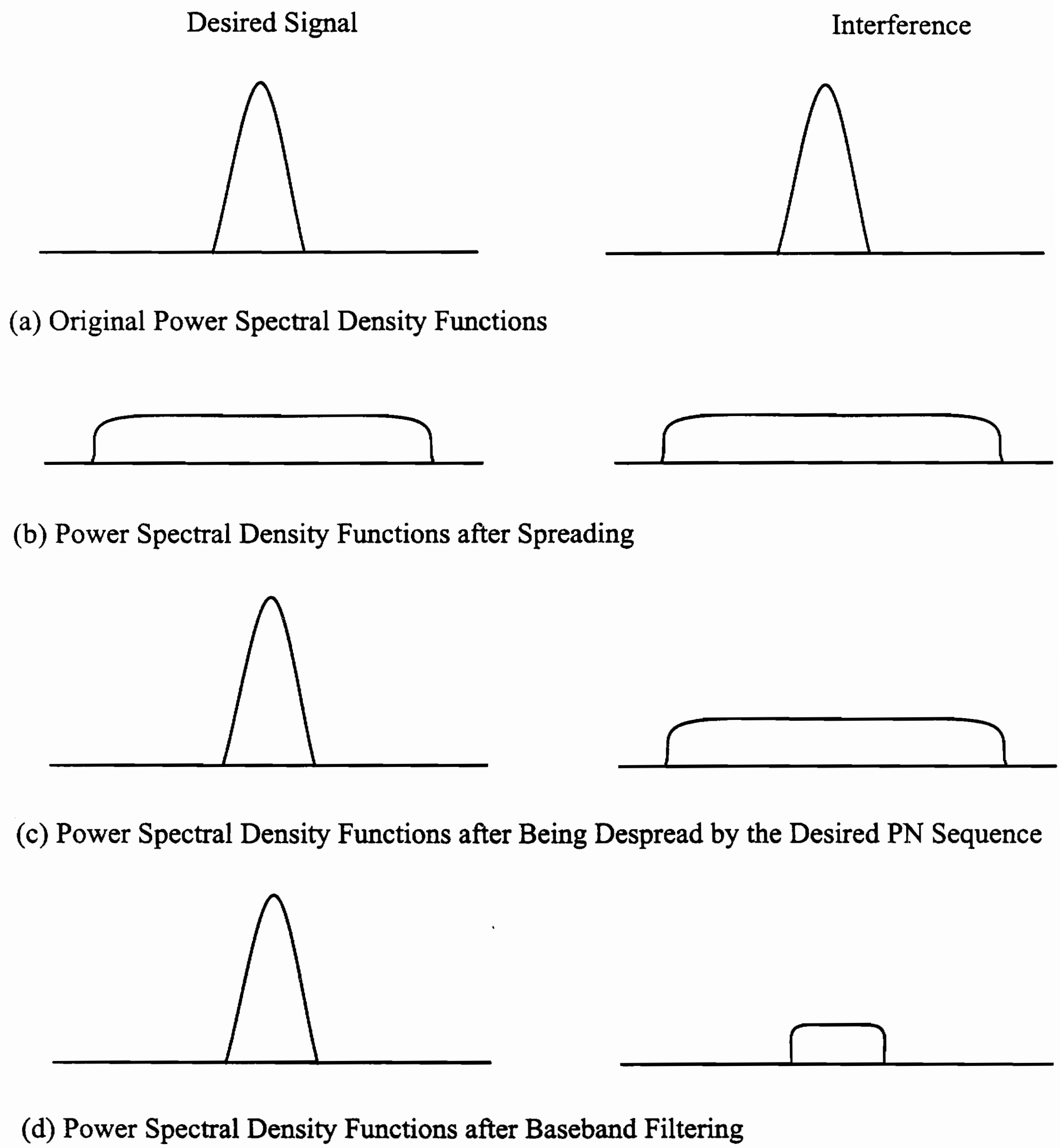

Figure 3.7: CDMA Concept in Frequency Domain

spectral density is significantly reduced by energy conservation as shown in (b). In (c), both of the spread signals are multiplied by the PN sequence of the desired user. The signal is fully recovered for the desired user, but not for the interfering user. In (d), a narrowband filter is used to reduce the out of band noise. The signal or interference power is the area under each shape. The signal to interference ratio in this simple case is approximately the processing gain.

For different users, the PN sequences are chosen such that the cross-correlations of the PN sequences assigned to different users are approximately zero, in order to reduce the multiple access interference. The auto-correlations of each PN sequence should ideally approximate a δ-function in order to reduce the effect of multipath components. At the receiver, when the received signal is multiplied by a signature sequence of a particular user to despread that user, only the desired signal spread by the same signature sequence contributes significantly to the despread signal, while other components spread by different signature sequences nearly vanish due to the approximate orthogonality of the signature sequences. This means of implementing CDMA is referred to as Direct Sequence Spread Spectrum (DS/SS).

FH/SS

Frequency Hopping is the other principle means of generating a CDMA signal [Sim94]. It differs from DS/SS in that the transmitted signal is a narrowband signal while the carrier frequency of a particular user varies over a wide range according to a preselected pseudo-random pattern. The transmitted signal resides on a particular narrow frequency band for only a short period of time. Depending on the duration of this residing time compared with the data period, FH/SS can be classified as fast frequency hopping and slow frequency hopping. If the carrier frequency changes at a rate greater than the data rate, the system is referred to as a fast frequency hopping system; if the carrier frequency changes at a rate smaller or equal to the data rate, the system is referred to as a slow frequency hopping system. Due to the limitations of present VLSI technology, fast frequency hopping systems

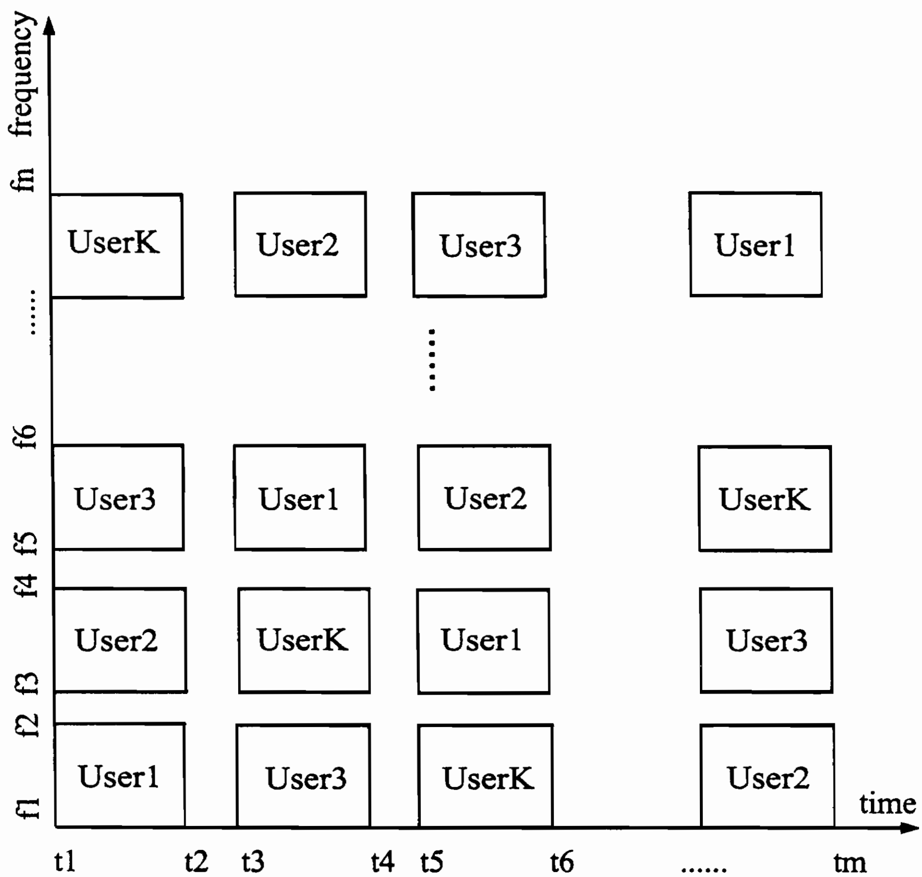

Figure 3.8: Block Diagram of FH/SS Scheme

are not commercially available at the present time.

Fig. 3.8 shows the utilization of communication resources (time, frequence) in frequency hopping system. In each time slot, a different user occupies different frequency band. From one time slot to another, a user's carrier frequency hops from one narrow band to another. Frequency collisions might occur when two users hop on the same frequency band at the same time.

One advantage of a Frequency Hopping system is the resistance to narrowband fading. Typically, the total spread spectrum bandwidth is much greater than the coherent bandwidth of the transmitted signal. The frequency band a particular user occupies during one time slot, is usually far from that at another time slot and hence it suffers uncorrelated fading. In other word, when a user suffers severe fading during one time slot, the user may not during another time slot.

There are various hybrids of the above four types of basic multiple access schemes which make better resource utilization or improve system performance in the wireless communication environment. The GSM standard allows the TDMA based cellular system to employ a slow frequency hopping technique when a particular channel experiences severe fading [Mou92]. Omnipoint developed a TDMA/CDMA hybrid digital system which uses a 9 MHz bandwidth at 900 MHz or 2 GHz and 8 time slots per TDMA frame. A FDMA/CDMA hybrid system has also been proposed to operate within a wideband spectrum which is divided into a set of sub-spectra. Each user's signal is first spread into a narrowband CDMA system and then is modulated by different carrier frequencies to generate the desired FDMA/CDMA signal [Eng93]. FDMA/CDMA, now commonly referred to as multicarrier CDMA has demonstrated advantages in robustness to multipath fading, suppression of narrowband interference and lower demand of chip rate [Shi96][Sou96].

Because of the costs of generating a frequency hopped signal, most commercial CDMA systems favor the DS/SS technique. We will consider DS/SS systems exclusively for this reason.

Advantages of CDMA

Compared with TDMA and FDMA schemes, a CDMA system has unique advantages due to its wideband modulation by a noise-like signature sequence. In recent years, a growing body of work has documented the advantages of CDMA for wireless applications, such as cellular telephone, PCS and WLL. We briefly review these key characteristics of CDMA systems as a means of justifying the use of CDMA technology in our WLL system design. For the reasons enumerated below, we will focus on a CDMA WLL in the remainder of this thesis.

(1) Capacity Improvement

In a multiple cell system, some researchers have claimed that CDMA is able to achieve up to 6 times the capacity of TDMA and 15-20 times of capacity of FDMA due to the frequency reuse in each cell of the system [Lee83][Gil91]. In CDMA, each user is assigned a unique noise like wideband signature sequence which occupies the entire frequency band allowed. Time and frequency resource allocations are not restricted. All the users share the same frequency band and transmit at the same time. In FDMA and TDMA systems, frequency spectrum must be allocated according to a frequency reuse pattern in order to achieve acceptable co-channel interference levels. This in turn reduces the number of channels available in any given cell of the system and thus reduces the system capacity.

Another feature of CDMA system is its soft capacity limit. There is no definite number of users the system is able to accommodate. Increasing the number of users merely raises the noise level in the system. Therefore, admitting more users into the system will in turn degrade the voice quality of all other users gradually.

(2) Voice Activity

During a two way telephone conversion, a voice is typically active for about 3/8 of the time [Bra68]. A system based on CDMA is able to exploit this voice activity phenomenon. During the pause of the speech, the transmitter can be switched off so that the number of multiple access interference is reduced as the system load decreases. Generally speaking, the system can more than double its capacity as this result.

(3) Multipath Fading Resistance

In CDMA, the spread spectrum bandwidth is chosen to be much greater than the coherent bandwidth of the channel. The amplitude and phase of each multipath component is uncorrelated with the anothers. The envelope of each arriving signal obeys a Rayleigh distribution [Sta94]. It has been shown that with an asymptotically large number of independent Rayleigh components, the system achieves the same BER as the system suffering unfaded propagation [Vit96]. Even for finite number of multipath arrivals, a CDMA system still shows greater fading resistance than a TDMA or a FDMA system.

A CDMA system is able to exploit high chip rate to resolve multipath components. When the chip duration time is smaller than the channel delay spread in a frequency selective fading channel, which is true for most of the outdoor CDMA systems, multipath components arrive at different chips. Since the signature sequences are designed to have low auto-correlation, the demodulation of other multipath components results in an increased noise background. However, with pilot-aided coherent multipath demodulation scheme [Vit96], each multipath component can be tracked by locking each user to the pilot sequence and multipath delays can be searched by synchronizing to the pilot sequence present in each multipath component. A RAKE receiver can be employed to exploit multipath components, since the system is able to synchronize the signature sequence to different delayed versions of the desired signal. Each "finger" of the RAKE consists of a correlation demodulator. A pilot sequence tracking loop is able to determine the timing delay and synchronizes the signature sequence to that of one of the multipath components. Different "fingers" are locked to different multipath versions and the decision statistic is the weighted combination of different multipath demodulation outputs. For example, in IS-95, a base station has four correlator RAKE receivers while a mobile user has a three correlator RAKE receiver [Qua92].

(4) Sectoring

In CDMA, the frequency bands are reused within the same cell and in adjacent cells as well (known as universal frequency reuse). Sectoring reduces the amount of interference affecting a desired user in a particular sector. However, sectoring will not reduce the number of channels available to each sector since there is only one channel in the spread spectrum technique. But for channelized schemes, such as TDMA and FDMA, each sector is assigned only a portion of the total number of channels of the cell. The break-up of all the available channels decreases the trunking capacity of the system. In CDMA, sectoring reduces only the interference, since CDMA capacity is limited by the number of MAI. Sectoring is commonly used in a CDMA cellular system for this purpose.

(5) Near-Far Effect

If CDMA technology is adopted for the WLL application, a key problem to be overcome is the so called near-far problem caused by self-jamming, which arises when the signature sequences are not perfectly orthogonal. For a system with a correlation receiver, the performance is heavily dependent on the selection of PN sequences [Non94]. There are several criteria in determining how to choose a good PN sequence. The least-sidelobe criterion was proposed to reduce the spilled energy outside the bandwidth of the PN sequence [Per79]. Another criterion is to reduce the ratio of the received signal power normalized by the power of the intersymbol interference [Non96]. This criterion can be applied to a frequency selective fading channel with either coherent or noncoherent demodulation.

In the reverse channel, when two users locate at different distances away from the base station, the near user may dominate the signal reception because of less propagation path loss. When the interferer is much closer than the desired user, it may be impossible to detect the desired signal.

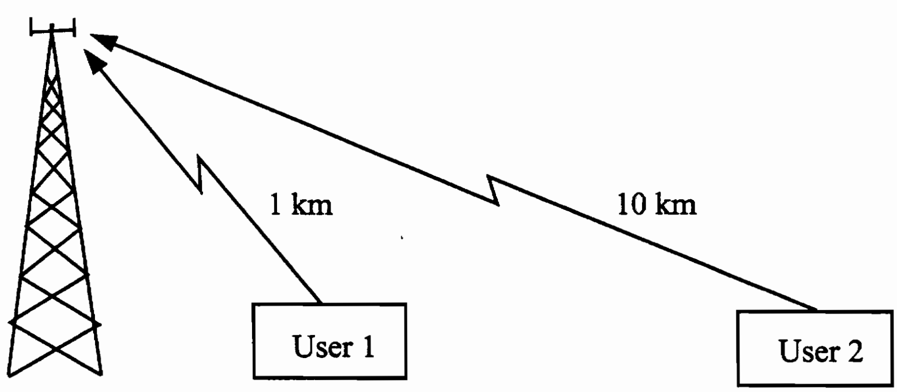

Figure 3.9: Near-Far Scenario

Fig. 3.9 illustrates the near-far scenario. Suppose user 1 and user 2 deliver the same transmitted power. User 1 is 1 km away from the base station and user 2 is 10 km away from the base station. For propagation path loss of 4, which is a typical value for the far field beyond the Frauenhofer distance, the received power at the base station for user 1 will be 40 dB higher than that of user 2, according to the following path loss formula [Rap96]:

$$\frac{P(d)}{P(d_0)} = (\frac{d}{d_0})^4. \tag{3.1}$$

The usual approach to compensating the near-far effect is to employ a power control mechanism. The power control scheme is essential to maximize the system capacity and has been proved both in theoretical analysis [Vit96][Woe92][Sal91] and experimental measurement [Pad94][Vit92]. The benefit of power control is of twofold. First power control can overcome the near-far problem. Second, power control can significantly reduce the standard deviation of the log-normal shadowing distribution. Without power control scheme, the typical value of the standard deviation of the log-normal shadowing is 8 - 10 dB while a good power control scheme is able to reduce the that value to 1.5 dB for an open environment and 2.3 dB for an urban environment [CTI91]. Note, however, that these limitations on the effectiveness of power control are primarily due to the mobile nature of a cellular system. For a WLL system which does not need to support mobility, power control should be much more effective at mitigating the near-far problem.

The basic idea of power control is to measure the received signal power and inversely adjust the transmit power of the mobile according to the measurement. There are two primary approaches to implement this, namely an open loop mode and a closed loop mode [Qua92]. A hybrid scheme of above two was also proposed by SigTek [Sig95]. In an open loop mode, the mobile measures the received signal power in every a few milliseconds. If the mobile measures a weaker signal level, it increases the transmit power to a desired level. If, on the other hand, the mobile measures a strong signal level, it decreases the transmitting power accordingly. This adjustment is based on the reciprocity principle which states that the signal level received at the base station transmitted from the mobile unit is the same as it is received at the mobile unit transmitted from the base station if the transmitted power levels are the same. This is true when the signals are transmitted at the same frequency.

However, the frequency band allocated to the forward channels is separated from the reverse channels (45 MHz in current North America cellular standards). The coherence bandwidth, which defines the range of frequencies over which the amplitude of two signals experience the same fading characteristics, is much less than the band separation. Therefore, the signal suffers uncorrelated fading in the forward channel and reverse channel. As a result, the open loop scheme achieves only limited control accuracy, although it is attractive because of its simplicity. In a closed loop mode, the base station measures the received signal energy per bit over interference power E_b/I_0, instead of merely received signal power, to estimate the bit-error-rate (BER) [Vit96]. The base station instructs the mobile unit to adjust its transmit power based on the best estimation of BER for a measured E_b/I_0. This approach eliminates the uncorrelated fading dilemma but introduces extra time delay for the mobile to adjust its transmit power.

CDMA System Performance

In a traditional digital CDMA system employing binary modulation, performance may be analyzed by applying the central limit theorem [Hen94] to model the cumulative effects of many interfering chips from many multiple access user as a Gaussian random variable [Pur77]. This leads to the following expression for the SNR at the output of the matched filter correlation receiver:

$$SNR = \left[\frac{\sum_{k=2}^{K} E_b^{(k)}}{3E_b^{(1)} PG} + \frac{N_0}{2E_b^{(1)}} \right]^{(-1)}, \tag{3.2}$$

where K is the total number of users, $E_b^{(k)}$ is the energy per bit for the k_{th} user, PG is the processing gain, $N_0/2$ is the power spectral density of AWGN. Assuming a perfect power control for the interference limited CDMA system, and $E_b^{(k)} = E_b^{(1)}$, then the AWGN term can be ignored.

$$SNR = \frac{3PG}{K-1} \tag{3.3}$$

This can be used to obtain an analytical expression for the BER:

$$BER = Q\left(\sqrt{SNR}\right), \tag{3.4}$$

where $Q(x) = \int_x^\infty \frac{1}{\sqrt{2\pi}} e^{-u^2/2}\, du$.

As we shall see later in Chapter 4, the expression of SNR in Eqn. (3.3) is identical to the input SNR of an FM demodulator. In fact, frequency modulation is analogous to error correction coding in digital communications, where the output SNR of a matched filter is just the input SNR for an error correction decoding. There should be an agreement of SNRs between the analog FM and digital error correction coding.

3.2 Chapter Summary

In this chapter, we have reviewed the basic principles of CDMA techniques and discussed why the CDMA is desirable for a WLL system. The model for a digital CDMA system has led to a simple analytical technique for the BER. For an FM/CDMA system, the performance is measured by the output SNR. As we shall find later in the next chapter on the theoretical analysis of the FM/CDMA system, the analog FM/CDMA system exhibits close similarities in SNR and equivalent power spectral density.

Chapter 4

FM/CDMA System Performance

In this chapter, the performance of the reverse link of a hybrid FM/CDMA system is examined. In mobile cellular and WLL communication systems, the reverse link is a many-to-one transmission. Under perfect power control, the received power at the base station from each user can be assumed to be identical. As discussed in the previous chapter, good power control is a reasonable assumption for a WLL system. The received signal is the sum of white Gaussian noise and Multiple Access Interference (MAI). MAI dominates the system performance under heavily loaded conditions. First, the system is modeled in the presence of white Gaussian noise. However, we are interested in the case where white Gaussian noise has little effect and when the system is operating at a input signal to interference ratio above the FM threshold in order to achieve a good voice quality. The Gaussian noise term is ignored in the SIR calculations.

4.1 Analytical Model

Note that the conventional approach for a digital CDMA receiver is to model the decision statistic as a Gaussian random variable. However, since the desired output signal here is a continuous time signal, this approach is no longer rigorous. Instead, we derive the SIR here through examination of the auto-correlation functions of the resulting signal.

Fig. 4.1 shows the FM/CDMA receiver structure at the base station. This is a simplified version of the receiver structure where the de-emphasis, expander and RF downconvesion are not included in the diagram. The FM demodulation is implemented by a differentiator because an analytically tractable closed form system performance may be obtained with

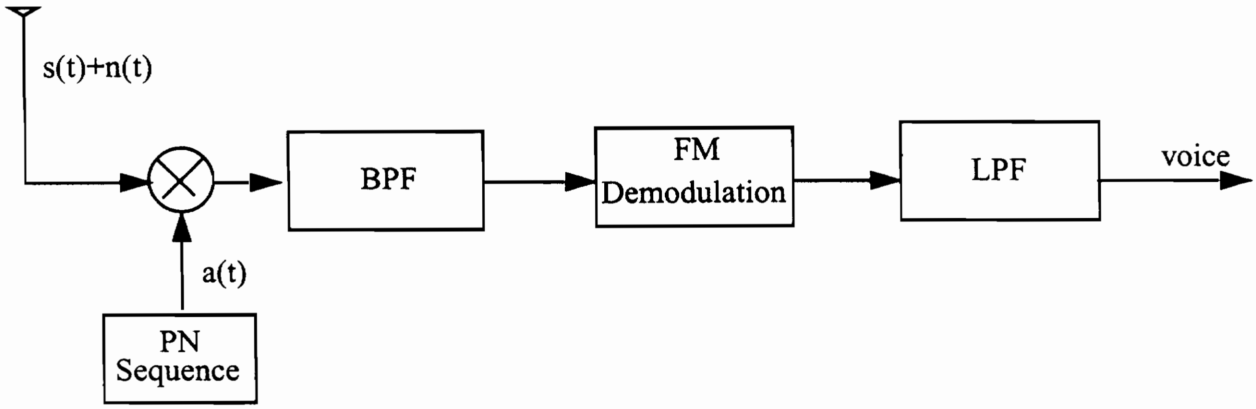

Figure 4.1: Simplified Receiver Structure of FM/CDMA System

reasonable assumptions. In Fig. 4.1, $s(t)$ is the received signal of the desired user, $i(t)$ is the received signal from other interfering users, and $n(t)$ is the white Gaussian noise. The combination of these signals is first despread using the signature sequence of the desired user. Since the signature sequences have low cross-correlations, the interference signals are further spread. The power spectral density of the interference becomes even smaller. The Gaussian noise is not spread, which will be proved later, and is still a white Gaussian noise process. After passing through the band pass filter, the FM signal is extracted from the Gaussian noise and the noise-like interference.

4.2 Basic Approach

In this section, we wish to derive a closed form for the input signal to interference ratio and the output signal to interference ratio for FM/CDMA system. In order to simplify the procedure without losing insight into the operation of the system, the theoretical analysis is based on the following assumptions.

1. The propagation channel is an AWGN channel with two sided noise power spectral density of $N_0/2$.

2. The system operates under perfect power control so that the received signal powers are the same for all the users.

3. Different signature sequences are uncorrelated with one another.

4. The signature sequence and the FM signal are uncorrelated.

Let $a(t)$ be the cyclical signature sequence, A_c be the amplitude of the carrier, and $m(t)$ be the modulating signal.

$$a(t) = \sum_{j=-\infty}^{\infty} \sum_{i=0}^{M-1} a_{k,i} \Pi\left(\frac{t-(i+jM)T_c}{T_c}\right) \qquad a_{k,i} \in \{-1,1\}, \tag{4.1}$$

where M is the number of chips within a CDMA frame. T_c is the chip period, $\Pi(t)$ is the unit pulse function given by

$$\Pi(t) = \begin{cases} 1 & 0 \leq t \leq T \\ 0 & \text{otherwise.} \end{cases}$$

Define $\theta(t) = D_f \int_{-\infty}^{t} m(x)\,dx$, where D_f is the frequency deviation constant. The transmitted signal of user k is

$$s_k(t) = A_c a_k(t) cos[\omega_c t + \theta_k(t) + \phi_k]. \tag{4.2}$$

Let the received signal be $r(t)$, where

$$r(t) = \sum_{k=1}^{K} s_k(t-\tau_k) + n(t). \tag{4.3}$$

Suppose user 1 is the user of interest. The received signal $r(t)$ is despread by multiplying by the signature sequence of user 1. Without loss of generality, assume the random phase and random delay of user 1 to be zero.

Let $d_1(t)$ be the despread signal of the desired user at the receiver.

$$\begin{aligned} d_1(t) &= r(t)a_1(t) \\ &= a_1(t)\sum_{k=1}^{K} s_k(t-\tau_k) + a_1(t)n(t) \end{aligned}$$

$$\begin{aligned}
&= A_c a_1^2(t) cos[\omega_c t + \theta_1(t)] \\
&\quad + A_c \sum_{k=2}^{K} a_1(t) a_k(t-\tau_k) cos[\omega_c(t-\tau_k) + \theta_k(t-\tau_k) + \phi_k] \\
&\quad + a_1(t) n(t).
\end{aligned} \tag{4.4}$$

Notice that the signal $a_1(t)$ is a BPSK modulated binary sequence. Therefore, $a_1^2(t) = 1$. The above equation can be simplified as

$$\begin{aligned}
d_1(t) &= A_c cos[\omega_c t + \theta_1(t)] \\
&\quad + A_c \sum_{k=2}^{K} a_1(t) a_k(t-\tau_k) cos[\omega_c(t-\tau_k) + \theta_k(t-\tau_k) + \phi_k] \\
&\quad + a_1(t) n(t).
\end{aligned} \tag{4.5}$$

Define

$$R(t) = A_c cos[\omega_c t + \theta_1(t)], \tag{4.6}$$

$$I(t) = A_c \sum_{k=2}^{K} a_1(t) a_k(t-\tau_k) cos[\omega_c(t-\tau_k) + \theta_k(t-\tau_k) + \phi_k], \tag{4.7}$$

and

$$N(t) = a_1(t) n(t), \tag{4.8}$$

where $R(t)$ is the signal of the desired user, $I(t)$ is the multiple access interference from other users, and $N(t)$ is the noise introduced by the AWGN channel.

4.3 White Gaussian Noise

Suppose the power spectral density of AWGN is $S_n(f) = N_0/2$, then the auto-correlation of AWGN is the inverse Fourier transform of the power spectral density, which is known to be $R_n(\tau) = \frac{N_0}{2}\delta(\tau)$. The auto-correlation of noise $N(t)$ is

$$\begin{aligned}
R_N(t) &= E[N(t)N(t+\tau)] = E[a_1(t)n(t)a_1(t+\tau)n(t+\tau)] \\
&= E[a_1(t)a_1(t+\tau)]E[n(t)n(t+\tau)] \\
&= R_1(\tau)R_n(\tau) = R_1(\tau)\frac{N_0}{2}\delta(\tau) = \frac{N_0}{2}R_1(0)\delta(\tau),
\end{aligned} \tag{4.9}$$

where $R_1(\tau)$ is the auto-correlation function of user 1's signature sequence. Since $R_1(0)$ is the power of the binary signature sequence $a_1(t)$, it is obvious that $R_1(0) = 1$. The auto-correlation function of the noise term is

$$R_N(\tau) = \frac{N_0}{2}\delta(\tau). \tag{4.10}$$

The auto-correlation function of $N(t)$ is the same as that of AWGN. Therefore, the power spectral density function of $N(t)$ is the same as AWGN as well. This shows that the Gaussian noise is not spread by the signature sequence. Hence

$$S_N(f) = N_0/2. \tag{4.11}$$

4.4 Multiple Access Interference

We are interested in the case where the CDMA system is an interference limited system in which the power of multiple access interference is greater than the Gaussian channel noise. In this section, the channel noise is ignored. Once an expression of power spectral density of multiple access interference is obtained, it is a trivial step to combine the Gaussian channel noise into the final results.

Define the phase ψ_k of the received signal from the k_{th} user as

$$\psi_k = \omega_c\tau_k + \phi_k. \tag{4.12}$$

Rewrite $I(t)$ as

$$I(t) = A_c \sum_{k=2}^{K} a_1(t)a_k(t-\tau_k)\cos[\omega_c t + \theta_k(t-\tau_k) + \psi_k]. \tag{4.13}$$

Therefore, the auto-correlation function of the multiple access interference term $R_I(\tau)$ is

$$\begin{aligned} R_I(\tau) &= E\{I(t)I(t+\tau)\} \\ &= A_c^2 E\{\sum_{k=2}^{K} a_1(t)a_k(t-\tau_k)\cos[\omega_c t + \theta_k(t-\tau_k) + \psi_k] \times \end{aligned}$$

$$
\begin{aligned}
& \sum_{l=2}^{K} a_1(t+\tau)a_l(t+\tau)\cos[\omega_c t + \theta_l(t+\tau-\tau_l) + \psi_l]\} \\
= \; & A_c^2 E\{\sum_{k=2}^{K}\sum_{l=2}^{K} a_1(t)a_1(t+\tau)a_k(t-\tau_k)a_l(t+\tau-\tau_l) \times \\
& \cos[\omega_c t + \theta_k(t-\tau_k) + \psi_k]\cos[\omega_c t + \theta_l(t-\tau_l) + \psi_l]\} \\
= \; & \sum_{k=2}^{K}\sum_{l=2}^{K} E\{a_1(t)a_1(t+\tau)\}E\{a_k(t-\tau_k)a_l(t+\tau-\tau_l)\} \times \\
& E\{A_c^2\cos[\omega_c t + \theta_k(t-\tau_k) + \psi_k]\cos[\omega_c t + \theta_l(t+\tau-\tau_l) + \psi_l]\} \\
= \; & \sum_{k=2}^{K}\sum_{l=2}^{K} R_1(\tau)R_{kl}(\tau)R_{c,kl}(\tau),
\end{aligned}
\tag{4.14}
$$

where

$$R_1(\tau) = E\{a_1(t)a_1(t+\tau)\} \tag{4.15}$$

is the auto-correlation function of PN sequence of the desired user. Let

$$R_{kl}(\tau) = E\{a_k(t-\tau_k)a_l(t+\tau-\tau_l)\} \tag{4.16}$$

be the cross-correlation function of the PN sequences of the undesired users when $k \neq l$, and is the auto-correlation function when $k = l$. Furthermore, let

$$R_{c,kl}(\tau) = E\{A_c^2\cos[\omega_c t + \theta_k(t-\tau_k) + \psi_k]\cos[\omega_c t + \theta_l(t+\tau-\tau_l) + \psi_l]\} \tag{4.17}$$

be the cross-correlation function of the FM signals of the undesired users when $k \neq l$, and the auto-correlation function when $k = l$.

By definition,

$$R_{kl}(\tau) = \lim_{T\to\infty}\frac{1}{T}\int_{-T/2}^{T/2} a_k(t-\tau_k)a_l(t+\tau-\tau_l)\,dt. \tag{4.18}$$

If $k \neq l$, the above integral is zero because a_k and a_l are uncorrelated random sequences with the probabilities $P\{a_k(t) = 1\} = P\{a_k(t) = -1\} = 1/2$. Therefore, only the terms with $k = l$ remain.

Therefore

$$R_{kl}(\tau) = R_k(\tau)\delta_{kl}, \tag{4.19}$$

where the auto-correlation function of the kth user is given by

$$\begin{aligned} R_k(\tau) &= E\{a_k(t-\tau_k)a_k(t+\tau-\tau_k)\} \\ &= \lim_{T\to\infty}\frac{1}{T}\int_{-T/2}^{T/2} a_k(t-\tau_k)a_k(t+\tau-\tau_k)\,dt. \end{aligned} \tag{4.20}$$

Now $R_I(\tau)$ can be simplified as

$$R_I(\tau) = \sum_{k=2}^{K} R_1(\tau)R_k(\tau)R_{c,kl}(\tau). \tag{4.21}$$

If we let $\lambda = t - \tau_k$, then

$$R_k(\tau) = \lim_{T\to\infty}\frac{1}{T}\int_{-T/2-\tau_k}^{T/2-\tau_k} a_k(\lambda)a_l(\lambda+\tau)\,d\lambda. \tag{4.22}$$

Since $T \to \infty$, hence for small τ_k, $T/2 - \tau_k \approx T/2$, therefore

$$\begin{aligned} R_k(\tau) &= \lim_{T\to\infty}\frac{1}{T}\int_{-T/2}^{T/2} a_k(\lambda)a_k(\lambda+\tau)\,d\lambda \\ &= \frac{1}{NT_c}\int_{-NT_c/2}^{NT_c/2} a_k(\lambda)a_k(\lambda+\tau)\,d\lambda \\ &= \frac{1}{T_c}\int_{-T_c/2}^{T_c/2} a_k(\lambda)a_k(\lambda+\tau)\,d\lambda, \end{aligned} \tag{4.23}$$

where T_c is the chip duration time of the CDMA PN sequence, NT_c is the period of the PN sequence. It is easy to show that

$$R_1(\tau) = R_k(\tau) = \sum_{n=-\infty}^{\infty} \Lambda\left(\frac{\tau - nNT_c}{T_c}\right), \tag{4.24}$$

where $\Lambda(\cdot)$ is the triangle function given by

$$\Lambda(\frac{\tau}{T}) = \begin{cases} \dfrac{T-|\tau|}{T} & 0 \le |\tau| \le T \\ 0 & \text{otherwise.} \end{cases}$$

Since the power spectral density is the Fourier transform of the auto-correlation, and it is easy to show that the Fourier transform of a triangle waveform is a squared $sinc(\cdot)$ function, where

$$sinc(x) = \frac{sin(\pi x)}{\pi x}. \tag{4.25}$$

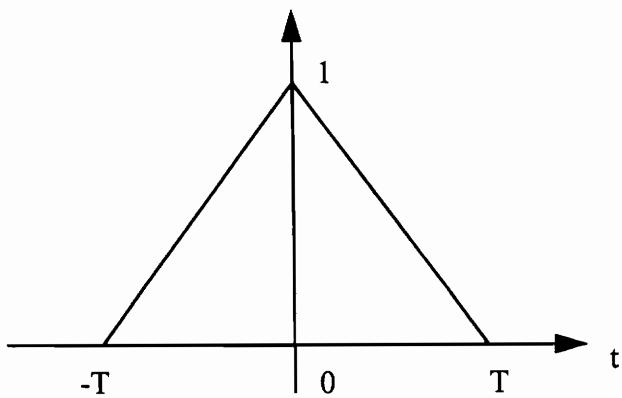

Figure 4.2: Triangular Function

Here, the Fourier series takes the place of the Fourier transform for periodic waveform. Therefore

$$S_1(f) = S_k(f) = \frac{1}{N} \sum_{n=-\infty}^{\infty} sinc^2(fT_c)\delta(f - nf_0), \tag{4.26}$$

where $S_1(f)$ and $S_k(f)$ are the power spectral density function of user 1 and user k, respectively, $f_0 = 1/NT_c$.

Let the power spectral density of the FM signal be $S_{fm}(f)$, which is identical for all users. In the case of wide band FM(WBFM), the modulation index $\beta > 1$, the power spectral density is given by

$$S_{fm}(f) = \frac{\pi A_c^2}{2D_f} \left\{ f_m \left[\frac{2\pi}{D_f}(f - f_c) \right] + f_m \left[\frac{2\pi}{D_f}(-f - f_c) \right] \right\}, \tag{4.27}$$

where D_f is the FM frequency deviation constant, and f_m is the probability distribution function of the modulating signal. Define the base band equivalence of FM power spectral density to be $S_{fm\_b(f)}$:

$$S_{fm\_b} = \frac{\pi A_c^2}{D_f} \left\{ f_m \left(\frac{2\pi}{D_f} f \right) \right\}. \tag{4.28}$$

According to Eqn. (4.21), the power spectral density $S_I(f)$ of the multiple access interference $I(t)$ can be written as

$$S_I(f) = \sum_{k=2}^{K} S_1(f) \otimes S_k(f) \otimes S_{fm}(f), \tag{4.29}$$

where $\otimes$ denotes the convolution. We may simplify the term $S_1(f) \otimes S_k(f)$ as follows:

$$\begin{aligned}
S_1(f) \otimes S_k(f) &= \int_{-\infty}^{\infty} S_1(f-\nu) S_k(\nu)\, d\nu \\
&= \frac{1}{N^2} \int_{-\infty}^{\infty} \sum_{n=-\infty}^{\infty} sinc^2[(f-\nu)T_c]\delta(f-v-nf_0) \sum_{m=-\infty}^{\infty} sinc^2(\nu T_c)\delta(\nu - mf_0)\, d\nu \\
&= \frac{1}{N^2} \sum_{n=-\infty}^{\infty} \sum_{m=-\infty}^{\infty} \int_{-\infty}^{\infty} sinc^2[(f-\nu)T_c] sinc^2(\nu T_c)\delta(f-\nu-nf_0)\delta(\nu-mf_0)\, d\nu \\
&= \frac{1}{N^2} \sum_{n=-\infty}^{\infty} \sum_{m=-\infty}^{\infty} sinc^2[(f-mf_0)T_c] sinc^2(mf_0T_c)\delta(f-mf_0-nf_0) \\
&= \frac{1}{N^2} \sum_{n=-\infty}^{\infty} \sum_{m=-\infty}^{\infty} sinc^2(nf_0T_c) sinc^2(mf_0T_c)\delta(f-mf_0-nf_0).
\end{aligned} \tag{4.30}$$

Let $l = m+n$, then Eqn. (4.30) becomes

$$\begin{aligned}
&S_1(f) \otimes S_k(f) \\
&= \frac{1}{N^2} \sum_{l=-\infty}^{\infty} \sum_{n=-\infty}^{\infty} sinc^2(nf_0T_c) sinc^2[(l-n)f_0T_c)]\delta(f-lf_0).
\end{aligned} \tag{4.31}$$

Now look at the term of $l = 0$ in Eqn. (4.31)

$$\begin{aligned}
&\frac{1}{N^2} \sum_{n=-\infty}^{\infty} sinc^2(nf_0T_c) sinc^2[(-n)f_0T_c)]\delta(f) \\
&= \frac{1}{N^2} \sum_{n=-\infty}^{\infty} sinc^4(nf_0T_c)\delta(f) \\
&= \frac{1}{N^2} \sum_{n=-\infty}^{\infty} sinc^4(\frac{n}{N})\delta(f).
\end{aligned} \tag{4.32}$$

Since N is the number of chips in one period of the PN sequence, we may assume that $N \gg 1$. In this case the sum of the series can be calculated by integration.

$$\frac{1}{N} \sum_{n=-\infty}^{\infty} sinc^4(\frac{n}{N}) = \int_{-\infty}^{\infty} sinc^4(x)\, dx. \tag{4.33}$$

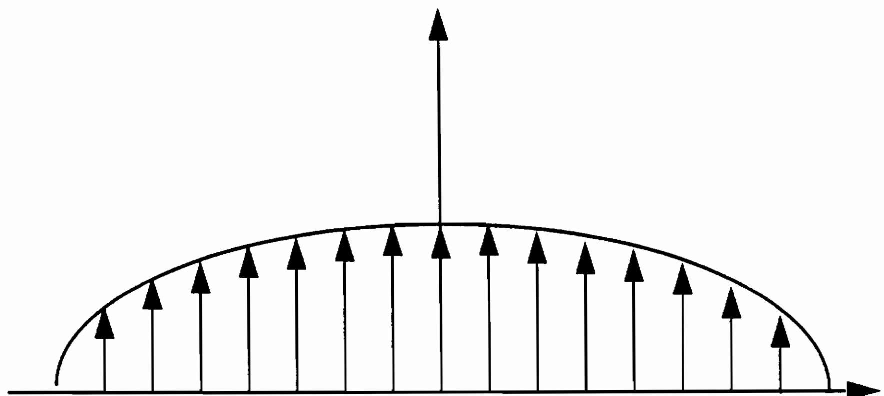

Figure 4.3: Disecrete Spectrum of Multiple Access Interference

where $\Delta x = 1/N$ in Riemann sum [Olm61].

Since the following definite integral is known:

$$\int_{-\infty}^{\infty} \frac{sin^4(x)}{x^4}\, dx = \frac{2\pi}{3}. \tag{4.34}$$

A simple manipulation yields the relation

$$\int_{-\infty}^{\infty} sinc^4(x)\, dx = \frac{2}{3}. \tag{4.35}$$

Then the $l = 0$ term in the summation of Eqn. (4.31) is simplified as

$$\begin{aligned} &\frac{1}{N^2} \sum_{n=-\infty}^{\infty} sinc^2(nf_0T_c) sinc^2[(-n)f_0T_c)]\delta(f) \\ &= \frac{1}{N^2} \sum_{n=-\infty}^{\infty} sinc^4(nf_0T_c)\delta(f) = \frac{2}{3N}\delta(f). \end{aligned} \tag{4.36}$$

Eqn. (4.36) is illustrated by Fig. 4.3. The left hand side of Eqn. (4.36) is the summation of the frequency components at $0, \pm\frac{1}{NT_c}, \pm\frac{2}{NT_c}, \pm\frac{3}{NT_c}, \cdots$.

Now consider the second term of $l = 1$ in Eqn. (4.31)

$$\frac{1}{N^2} \sum_{n=-\infty}^{\infty} sinc^2(nf_0T_c) sinc^2[(1-n)f_0T_c)]\delta(f - f_0). \tag{4.37}$$

From Fig. 4.3, we can see that the summation of the second term is the frequency component at $f = 0$ multiplied by itself, plus the frequency components at $f = \frac{n}{NT_c}$ multiplied by its mirrored adjacent component on the right, where $n = \pm 1, \pm 2, \cdots$, or equivalently, the frequency component multiplied by its left adjacent component since the signal spectrum is symmetric for real signals. In spread spectrum technology, the system parameters are so chosen that the spread spectrum bandwidth is much much larger than the FM bandwidth, or the processing gain is very large. And the period of the PN sequence is in the order of 10^3 or larger. Therefore, the line spectrum is densely spaced within the main lobe of the spread spectrum. Within our band of interest, which is determined by the FM bandwidth, the spectrum of $S_1(f) \otimes S_k(f)$ can be considered "flat", especially when Nyquist pulse shaping is used. This concludes each line spectrum has the same amplitude. The power spectral density of the multiple access interference is also "flat". Therefore, the summation of n for each l in Eqn. (4.31) is approximately equal to the result given by Eqn. (4.36). This is a very good approximation for $l \ll N$, which is true for a well designed FM/CDMA system. Therefore

$$S_1(f) \otimes S_k(f) = \sum_{n=-n'}^{n'} \frac{2}{3N} \delta(f - nf_0), \tag{4.38}$$

where n' is determined by the FM bandwidth BW_{FM}.

Let the chip rate R_c be reciprocal of the chip duration, i.e.

$$R_c \equiv \frac{1}{T_c}. \tag{4.39}$$

Define the system processing gain PG to be the ratio of the chip rate and the FM bandwidth, i.e.

$$PG \equiv \frac{R_c}{BW_{FM}}. \tag{4.40}$$

The maximum value of n (n') can be expressed in terms of the system processing gain PG and the CDMA frame length N

$$f \leq BW_{FM}/2. \tag{4.41}$$

Then

$$nf_0 \leq BW_{FM}/2. \tag{4.42}$$

Therefore

$$n \leq \frac{BW_{FM}}{2f_0} = \frac{BW_{FM}NT_c}{2} = \frac{NBW_{FM}}{2R_c}. \tag{4.43}$$

Therefore

$$n' = n_{max} = \lfloor \frac{NBW_{FM}}{2R_c} \rfloor = \lfloor \frac{N}{2PG} \rfloor, \tag{4.44}$$

where $\lfloor \cdot \rfloor$ represents the integer part of a real number.

Now Eqn. (4.29) can be simplified to a finite summation of n from $-n'$ to n'.

$$\begin{aligned}
S_I(f) &= \sum_{k=2}^{K} \sum_{n=-n'}^{n'} \left[\frac{2}{3N} \delta(f - nf_0) \right] \otimes S_{fm}(f) \\
&= \sum_{k=2}^{K} \sum_{n=-n'}^{n'} \frac{1}{3N} \int_{-BW_{FM}/2}^{BW_{FM}/2} \delta(\nu - nf_0) S_{fm_b}(f - \nu)\, d\nu \\
&= \sum_{k=2}^{K} \sum_{n=-n'}^{n'} \frac{1}{3N} \int_{-BW_{FM}/2}^{BW_{FM}/2} \delta(\nu - nf_0) \frac{2P_k}{D_f} f_m \left[\frac{2\pi(f - \nu)}{D_f} \right] d\nu \\
&= \frac{2\pi}{3ND_f} \sum_{k=2}^{K} P_k \sum_{n=-n'}^{n'} \int_{-BW_{FM}/2}^{BW_{FM}/2} f_m \left[\frac{2\pi(f - \nu)}{D_f} \right] \delta(\nu - nf_0)\, d\nu \\
&= \frac{2\pi}{3ND_f} \sum_{k=2}^{K} P_k \sum_{n=-n'}^{n'} f_m \left[\frac{2\pi(f - nf_0)}{D_f} \right],
\end{aligned} \tag{4.45}$$

where BW_{FM} is the FM bandwidth of the transmitted signal, which is equal for all users.

Assume each received multiple access interference has equal signal power due to perfect power control. Then $P_k = A_c^2/2$.

Therefore,

$$S_I(f) = \frac{\pi(K-1)A_c^2}{3ND_f} \sum_{n=-n'}^{n'} f_m \left[\frac{2\pi(f - nf_0)}{D_f} \right]. \tag{4.46}$$

Substituting Eqn. (4.28) into Eqn. (4.46), yields

$$S_I(f) = \frac{K-1}{3N} \sum_{n=-n'}^{n'} S_{fm\_b}(f - nf_0). \tag{4.47}$$

At this point, we consider the following two cases:

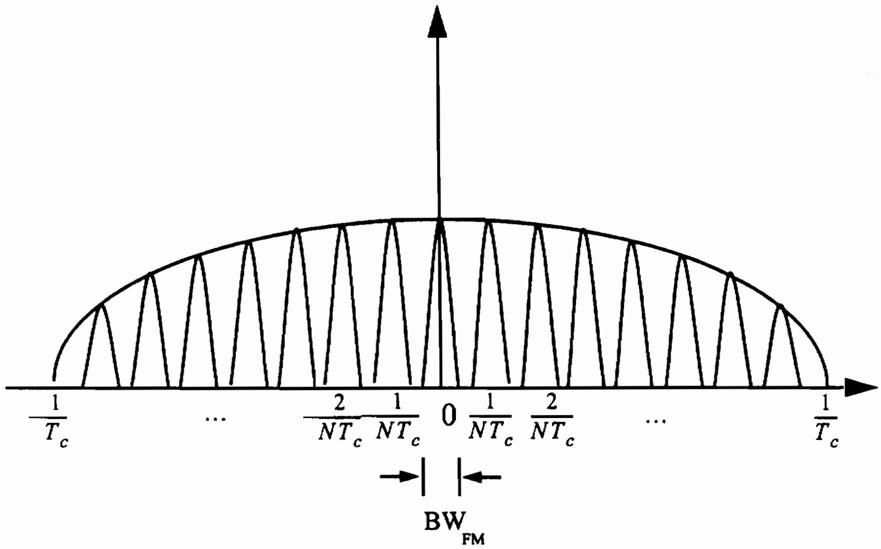

Figure 4.4: PSD of MAI in the Upper Bound

4.5 Upper Bound (Non-Overlapping Spectra)

The FM/CDMA parameters are chosen such that the multiple access interference spectra do not overlap between adjacent discrete components as shown in Fig. 4.4. In this case the following relationship must be satisfied:

$$\frac{1}{NT_c} \geq \frac{BW_{FM}}{2}. \tag{4.48}$$

From Eqn. (4.39), the above equation can be written as:

$$\frac{R_c}{N} \geq \frac{BW_{FM}}{2}. \tag{4.49}$$

Or equivalently

$$N \leq \frac{2R_c}{BW_{FM}} = 2PG. \tag{4.50}$$

As long as the processing gain PG is larger than half of the CDMA frame length N, the FM spectra will not overlap with one another. Each discrete frequency component occupies the same spectrum bandwidth, which equals the FM bandwidth. This implies $n' = 0$ in Eqn. (4.38), where only the term with $n = 0$ survives. By Eqn. (4.47), the power spectral density of the multiple access interference is just the replica of the FM power spectral density, with only a difference of a constant, so

$$S_I(f) = \frac{K-1}{3N} S_{fm\_b}(f). \tag{4.51}$$

In this case, the power spectral density of the multiple access interference is actually the summation of the power spectral density functions of all the interferers. It is inversely proportional to the CDMA frame length N. For system operating near the upper bound point, N cannot be too large in order to satisfy Eqn. (4.50). but if N is too small, the multiple access interference will increase.

4.6 Lower Bound (Full-Overlapping Spectra)

The FM/CDMA parameters are such chosen that the FM spectra overlap not only with the adjacent discrete frequency components, but also overlap with other discrete frequency components all over the FM spectrum as shown in Fig. 4.5. In this case, the resulting spectrum is continuous and flat. The following condition must be satisfied:

$$\frac{1}{NT_c} \ll \frac{BW_{FM}}{2}. \tag{4.52}$$

Equivalently

$$\frac{R_c}{N} \ll \frac{BW_{FM}}{2}, \tag{4.53}$$

or

$$N \gg \frac{2R_c}{BW_{FM}} = 2PG. \tag{4.54}$$

When the CDMA frame length N is greater than twice the system processing gain PG, the resulting power spectral density function of multiple access interference is characterized by a continuous and flat spectrum. By Eqn. (4.47),

$$S_I(f) = \frac{K-1}{3N} \sum_{n=-n'}^{n'} S_{fm\_b}(f - nf_0). \tag{4.55}$$

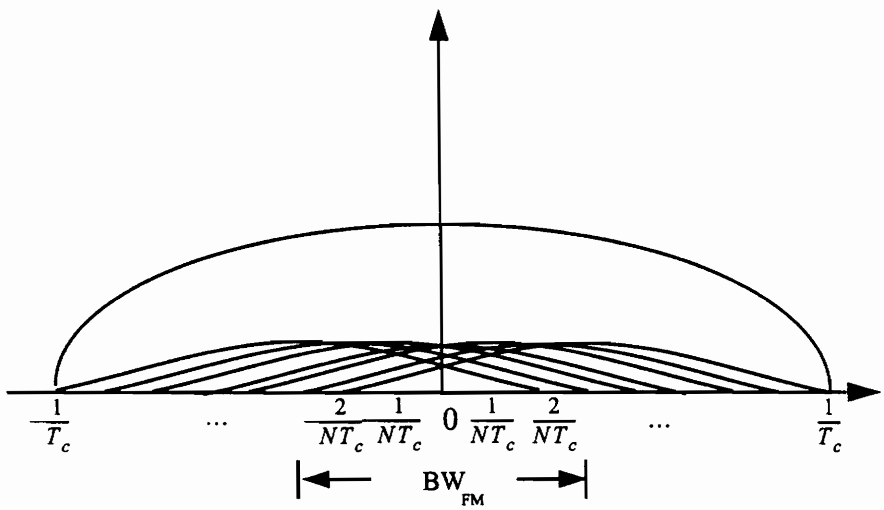

Figure 4.5: PSD of MAI in the Lower Bound Case

The power spectral density function of the multiple access interference is the summation of the sampled version of the FM spectrum at $f = 0, \pm\frac{R_c}{N}, \pm\frac{2R_c}{N}, \pm\frac{3R_c}{N}, \cdots$, multiplied by a constant, which is proportional to the number of interferers $K-1$ and inversely proportional to the CDMA frame length N. The parameter n' is given by Eqn. (4.44). Now n' is very large according to Eqn. (4.54). For simplicity, let $n' \to \infty$. Then Eqn. (4.55) becomes

$$S_I(f) = \frac{K-1}{3N} \sum_{n=-\infty}^{\infty} S_{fm\_b}(f - nf_0). \tag{4.56}$$

The summation can be evaluated by integration

$$\frac{R_c}{N} \sum_{n=-\infty}^{\infty} S_{fm\_b}(f - nf_0) = \int_{-\infty}^{\infty} S_{fm\_b}(f - x)\, dx, \tag{4.57}$$

where $\Delta x = R_c/N$ in Riemann sum [Olm61].

Let $\nu = x - f$, then

$$\int_{-\infty}^{\infty} S_{fm\_b}(f - x)\, dx = \int_{-\infty}^{\infty} S_{fm\_b}(-\nu)\, d\nu = \int_{-\infty}^{\infty} S_{fm\_b}(\nu)\, d\nu. \tag{4.58}$$

The last step is deduced from the property that the power spectral density of a real signal is an even function in the frequency domain. The integral of Eqn. (4.58) is obviously the power of FM signal, $P_k = A_c^2/2$. Therefore, the power spectral density function of the multiple access interference in the lower bound case can be written as:

$$\begin{aligned} S_I(f) &= \frac{K-1}{3R_c} P_k && (4.59) \\ &= \frac{(K-1)A_C^2}{6R_c} && (4.60) \\ &= \frac{1}{3R_c} \sum_{k=2}^{K} P_k. && (4.61) \end{aligned}$$

The power spectral density of the multiple access interference is proportional to the total power of all the interferers and inversely proportional to the chip rate. In this case the CDMA frame length has little effect on the system performance if it is chosen to be long enough. The line spectrum is very densely spaced in the main lobe of the PN sequence spectrum. The larger the N, the more interference power is filled into the FM bandwidth. As $N \to \infty$, the worst case occurs, and the lower bound of the system capacity is reached.

4.7 Input and Output SIR for Upper Bound

The spectrum of angular modulated signal had been a subject of much investigation [Pra69], [Jak93]. Prabhu calculated the angular modulation spectra for Gaussian Modulation. Gans calculated the spectra of angular modulation spectra by means of Poisson's sum formula. Both resulted in an identical power spectral density curve at baseband frequency. The power spectral density curve is almost flat within the baseband bandwidth. Assume the power spectral density function is rectangular shaped within the FM spectrum.

$$S_{fm\_b}(f) = \frac{A_c^2}{2BW_{FM}} \Pi\left(\frac{f}{BW_{FM}}\right), \qquad (4.62)$$

where

$$\Pi\left(\frac{f}{W}\right) = \begin{cases} 1 & \frac{-W}{2} \leq f \leq \frac{W}{2} \\ 0 & \text{otherwise.} \end{cases}$$

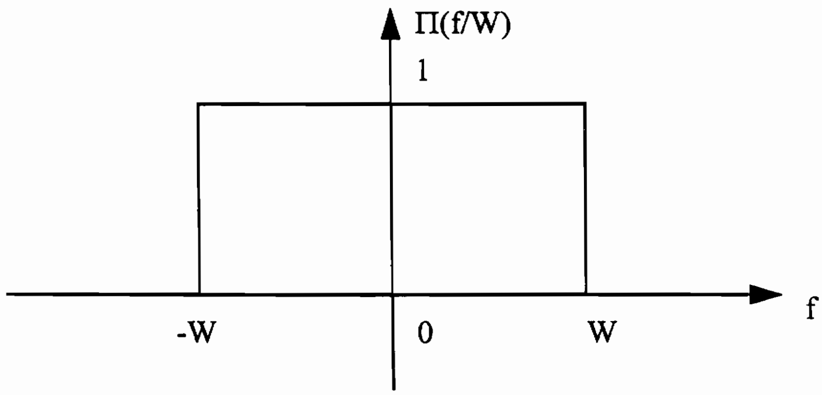

Figure 4.6: Rectangular FM Spectrum

Following the approach of Couch [Cou93], the power of the multiple access interference can be calculated.

$$\begin{aligned}\overline{i_o^2} &= \int_{-B}^{B} [\frac{C^2}{2\pi A_c}]^2 \, |j2\pi f|^2 \, \frac{K-1}{3N} S_{fm}(f)\, df \\ &= \frac{(K-1)\pi C^2}{3NA_c^2} \int_{-B}^{B} f^2 S_{fm}(f)\, df \\ &= \frac{(K-1)C^2B^3}{9NBW_{FM}}, \end{aligned} \tag{4.63}$$

where $\overline{i_o^2}$ is the received power of multiple access interference, B is the bandwidth of the speech signal, and C is a constant introduced by the FM demodulation.

After FM demodulation, the received baseband voice signal power can be easily calculated

$$\overline{s_o^2} = \left(\frac{CD_f}{2\pi}\right)^2 \overline{m^2(t)}, \tag{4.64}$$

where $m(t)$ is the recovered baseband signal.

Therefore, the output signal to interference ratio $(\frac{S}{I})_{out}$ can be expressed as:

$$(\frac{S}{I})_{out} = \frac{\overline{s_o^2}}{\overline{i_o^2}} = \frac{(\frac{CD_f}{2\pi})^2 \overline{m^2}}{\frac{(K-1)C^2B^3}{9NBW_{FM}}}. \tag{4.65}$$

Note that

$$\frac{D_f}{2\pi} = \frac{\beta B}{V_p}, \tag{4.66}$$

where V_p is the peak voltage of the modulating signal. Then

$$\begin{aligned}(\frac{S}{I})_{out} &= \frac{9NBW_{FM}B^2\beta^2\overline{(\frac{m}{V_p})^2}}{(K-1)B^3} \\ &= \frac{9NBW_{FM}\beta^2\overline{(\frac{m}{V_p})^2}}{(K-1)B}.\end{aligned} \tag{4.67}$$

By Carson's rule

$$BW_{FM} = 2B(\beta+1), \tag{4.68}$$

then

$$(\frac{S}{I})_{out} = \frac{18N(\beta+1)\beta^2}{(K-1)}\overline{(\frac{m}{V_p})^2}. \tag{4.69}$$

Rewriting the above equation in terms of the chip rate R_c and the processing gain PG yields

$$BW_{FM} = 2B(\beta+1) = \frac{R_c}{PG}, \tag{4.70}$$

or

$$(\beta+1) = \frac{R_c}{2BPG}. \tag{4.71}$$

Therefore

$$(\frac{S}{I})_{out} = \frac{9N}{(K-1)PG}(\frac{R_c}{B})(\frac{R_c}{2PGB}-1)^2\overline{(\frac{m}{V_p})^2}. \tag{4.72}$$

For a fixed chip rate R_c, the larger the processing gain, or the narrower the FM bandwidth, the smaller the output signal to interference ratio. The output signal to interference ratio is proportional to the CDMA frame length N. The longer the CDMA frame length, the larger the output signal to interference ratio. However, N can not be arbitrarily large because Eqn. (4.50) has to hold in the upper bound case.

The input signal to interference ratio is

$$(\frac{S}{I})_{in} = \frac{\overline{s_i^2}}{\overline{i_i^2}}. \tag{4.73}$$

The input signal is the constant envelope FM signal

$$\overline{s_i^2} = \frac{A_c^2}{2}. \tag{4.74}$$

The input interference power is

$$\begin{aligned}
\overline{i_i^2} &= \int_{-\infty}^{\infty} S(f)\,df \\
&= \int_{-BW_{FM}/2}^{BW_{FM}/2} \frac{(K-1)}{3N} S_{fm_b}(f)\,df \\
&= \frac{K-1}{3N} \int_{-BW_{FM}/2}^{BW_{FM}/2} S_{fm_b}(f)\,df \\
&= \frac{K-1}{3N}\frac{A_c^2}{2}.
\end{aligned} \tag{4.75}$$

Therefore, the input signal to interference ratio can be written as:

$$(\frac{S}{I})_{in} = \frac{3N}{K-1}. \tag{4.76}$$

Note that this input SIR is similar to the digital case given by Eqn. (3.3), where PG is the processing gain and here N is the frame length or code repeat period of the code sequence. The input signal to interference ratio is inversely proportional to the number of interferers. The input S/I has to be large enough above the FM threshold. However, a good FM/CDMA system design should guarantee a large output S/I. Normally, it is around 20 dB. And the input S/I is not too far away for the FM threshold. For FM demodulation without threshold extension, the threshold value is about 8 dB. If the system operating point is around 12 dB, the output S/I is still 8 dB higher than the input S/I. Therefore, the system capacity is determined by the output S/I. Both the input S/I and the output S/I is in proportional to N, the CDMA frame length. N should be chosen according to Eqn. (4.50)

$$N = 2PG. \tag{4.77}$$

Combining Eqn. (4.69) and Eqn. (4.76), we obtain the output and input S/I ratio

$$\begin{aligned}
\frac{(S/I)_{out}}{(S/I)_{in}} &= 6(\beta+1)\beta^2\overline{(\frac{m}{V_p})^2} \\
&= (\frac{3R_c}{PGB})(\frac{R_c}{2PGB}-1)^2\overline{(\frac{m}{V_p})^2}.
\end{aligned} \tag{4.78}$$

4.8 Input and Output SIR for Lower Bound

When the multiple access interference passes through the differentiator, the power spectral density function is multiplied by $|j2\pi f|^2$

$$S_{i_o}(f) = (\frac{C}{2\pi A_c})^2 |j2\pi f|^2 S(f). \tag{4.79}$$

The receiver output contains the low-pass filtered version of the multiple access interference. Combining Eqn. (4.60) and Eqn. (4.79), the interference power is

$$\begin{aligned} \overline{i_o^2} &= \int_{-B}^{B} S_{i_o}(f)\, df = \frac{C^2}{3A_c^2} B^3 \frac{(K-1)A_c^2}{3R_c} \\ &= \frac{(K-1)C^2B^3}{9R_c}. \end{aligned} \tag{4.80}$$

With Eqn. (4.64) and Eqn. (4.66), the output S/I is

$$(\frac{S}{I})_{out} = \frac{\overline{s_o^2}}{\overline{i_o^2}} = \frac{9\beta^2}{K-1} \frac{R_c}{B} \overline{(\frac{m}{V_p})^2}. \tag{4.81}$$

By using Eqn. (4.71), the output S/I is

$$(\frac{S}{I})_{out} = \frac{9}{K-1} (\frac{R_c}{B}) (\frac{R_c}{2PGB} - 1)^2 \overline{(\frac{m}{V_p})^2}. \tag{4.82}$$

The lower bound output SIR, Eqn. (4.82), and the upper bound SIR, Eqn. (4.72), are extremely similar. The only difference is N is replaced by PG in the first fraction term. However, since N is greater than twice of PG as confined by Eqn. (4.54) for the lower bound approximation, the output S/I is actually smaller than the upper bound case. The deduction of the output S/I is a factor of the ratio of the CDMA frame length and the processing gain N/PG. Combining Eqn. (4.60) and Eqn. (4.74),the input signal to interference ratio is

$$\begin{aligned} (\frac{S}{I})_{in} &= \frac{\overline{s_i^2}}{\overline{i_i^2}} = \frac{A_c^2/2}{B(\beta+1)\frac{(K-1)}{3R_c}A_c^2} \\ &= \frac{3}{2(K-1)(\beta+1)} (\frac{R_c}{B}). \end{aligned} \tag{4.83}$$

With Eqn. (4.71)

$$(\frac{S}{I})_{in} = \frac{3PG}{K-1}. \tag{4.84}$$

Note that this input SIR is the same as the SNR for the interference limited case of a digital CDMA system given by Eqn. (3.3). The input SIR in the lower bound case is closer to the FM threshold than in the upper bound case. The output and input S/I ratio is

$$\frac{(S/I)_{out}}{(S/I)_{in}} = 6(\beta+1)^3\overline{(\frac{m}{V_p})^2} = (\frac{3R_c}{PGB})(\frac{R_c}{2PGB}-1)^2\overline{(\frac{m}{V_p})^2}. \tag{4.85}$$

4.9 Comparison of Upper Bound and Lower Bound

It is desirable to compare the output SIR in the upper bound and lower bound cases. Rewriting the left hand side of Eqn. (4.72) and Eqn. (4.82) yields

$$(\frac{S}{I})_{outU} = \frac{9N}{K-1}(\frac{R_c}{PGB})(\frac{R_c}{2PGB}-1)^2\overline{(\frac{m}{V_p})^2}, \tag{4.86}$$

and

$$(\frac{S}{I})_{outL} = \frac{9PG}{K-1}(\frac{R_c}{PGB})(\frac{R_c}{2PGB}-1)^2\overline{(\frac{m}{V_p})^2}. \tag{4.87}$$

Therefore

$$\frac{(S/I)_{outU}}{(S/I)_{outL}} = \frac{N}{PG}. \tag{4.88}$$

By Eqn. (4.76) and Eqn. (4.84)

$$\frac{(S/I)_{inU}}{(S/I)_{inL}} = \frac{N}{PG}. \tag{4.89}$$

Since the CDMA frame length N is usually greater than the processing gain PG, the upper bound case can obtain larger output SIR than the lower bound case. However, by Eqn. (4.77), the maximum SIR difference is 3 dB. For input SIR, the system operates further away from the FM threshold for the upper bound case. Again, the input SIR difference between the upper bound case and the lower bound case is 3 dB. Still this 3 dB SIR difference is not guaranteed when the cross-correlation between the PN sequences of different users can not be neglected. Pursley etc. [Pur79] studied the properties of the auto-correlation function and the cross-correlation function of the random PN sequences.

Table 4.1: System Parameters

Spread Spectrum Bandwidth B_{ss} (MHz)	10
PN Sequence Chip Rate R_c (Mcps)	8
Typical Voice Bandwidth B (Hz)	3400
IF Bandwidth BW_{FM} (kHz)	25
Processing Gain PG	320
PN Sequence Frame Length N (chips)	2000
Number of Users K	24

A lower bound of the cross-correlation was obtained, which relates the lower bound of the cross-correlation to the CDMA frame length. From this analysis, the cross-correlation is inversely proportional to the CDMA frame length N. The shorter the frame period, the larger the cross-correlation, and thus the larger the multiple access interference. For orthogonal spreading sequences, the cross-correlation is always zero if good synchronization is achieved. However, orthogonal codes have poor performance in multipath fading channel environment. Only one bit of change in the orthogonal code caused by the channel fading can eliminate the orthogonality, and the cross-correlation functions contribute significantly to the total received signal and thus increase the interferences level.

Fig. 4.7 compares the upper bound and the lower bound output SIR versus the number of users. Fig. 4.8 compares the upper bound and the lower bound output SIR versus the IF bandwidth. These plots are drawn for the following parameters listed in Table 4.1, unless specified otherwise. In Fig. 4.7, the number of users is not fixed at 24 but varies from 10 to 60 while keeping the IF bandwidth to be 25 kHz. In Fig. 4.8, the number of users is 24, while the IF bandwidth varies from 15 kHz to 60 kHz and the processing gain varies from 533 to 133. In both two plots, the upper bound output SIR outperforms the lower bound SIR by 3 dB by choosing the upper bound CDMA frame length N to be twice the processing gain PG. The same 3 dB advantage shows in the upper input SIR as illustrated in Fig. 4.9 and Fig. 4.10. In Fig. 4.9, the input SIR is 16.2 dB for 24 users for a 25 kHz IF bandwidth. It is still above 12 dB when the system is loaded with 60 uses. The save observation holds in Fig. 4.10 where the input SIR reaches 16.2 dB at 25 kHz IF bandwidth and 12.5 dB at 60 kHz IF bandwidth with 24 users.

4.10 Comparison of FM/CDMA to Fully Digital CDMA

The performance of digital CDMA has been extensively studied using the Gaussian approximation [Pur77], according to the central limit theorem [Sta94], or using the improved Guassian approximation [Mor89] to improve the accuracy at low Bit Error Rate (BER). A simplified expression for the improved Gaussian approximation was obtained to reduce the computational intensity [Lib95].

By Gaussian approximation, the variance σ^2 of multiple access interference plus Gaussian noise is given by

$$\sigma^2 = \frac{PGT_c^2}{6}\sum_{k=2}^{K} P_k + \frac{N_0 T_b}{4} = \frac{T_b}{2}\left(\frac{T_c}{3}\sum_{k=2}^{K} P_k + \frac{N_0}{2}\right), \tag{4.90}$$

wherer T_c is the chip period of the signature sequence, T_b is the data bit period, PG is the processing gain defined as $PG = T_b/T_c$, K is the number of users, and P_k is the received signal power of user k.

In FM/CDMA system, now consider the lower bound case in the presence of Gaussian noise process. According to Eqn. (4.61) and Eqn. (4.11), the power spectral density of interference plus noise $S(f)$ can be written as:

$$S(f) = S_I(f) + S_N(f) = \frac{1}{3R_c}\sum_{k=2}^{K} P_k + \frac{N_0}{2} = \frac{T_c}{3}\sum_{k=2}^{K} P_k + \frac{N_0}{2}. \tag{4.91}$$

Compare Eqn. (4.91) with Eqn. (4.90), the FM/CDMA system is very similar to the fully digital CDMA system, characterized by the common equivalent power spectral density term $\frac{T_c}{3}\sum_{k=2}^{K} P_k + \frac{N_0}{2}$. A factor of 2 difference arises from the manipulation that signal is first downconverted from bandpass to baseband before despreading and passing through a correlation receiver in the digital CDMA system.

4.11 Chapter Summary

In this chapter, we have derived expressions for the input and output SIRs for a hybrid FM/CDMA system. The derivation made use of the assumption that the signature sequences of different users were uncorrelated. Expressions for two separate cases were considered, corresponding to the cases where the spectral replicas of the FM signal overlapped and did not overlap with one another. Although both cases resulted in similar expressions, it was found that the SIRs for the two cases could differ by as much as 3 dB. The performance of FM/CDMA is compared with that of the fully digital CDMA system and both systems have similar performance. In the next chapter, we consider the implications of this theoretical FM/CDMA system for WLL applications.

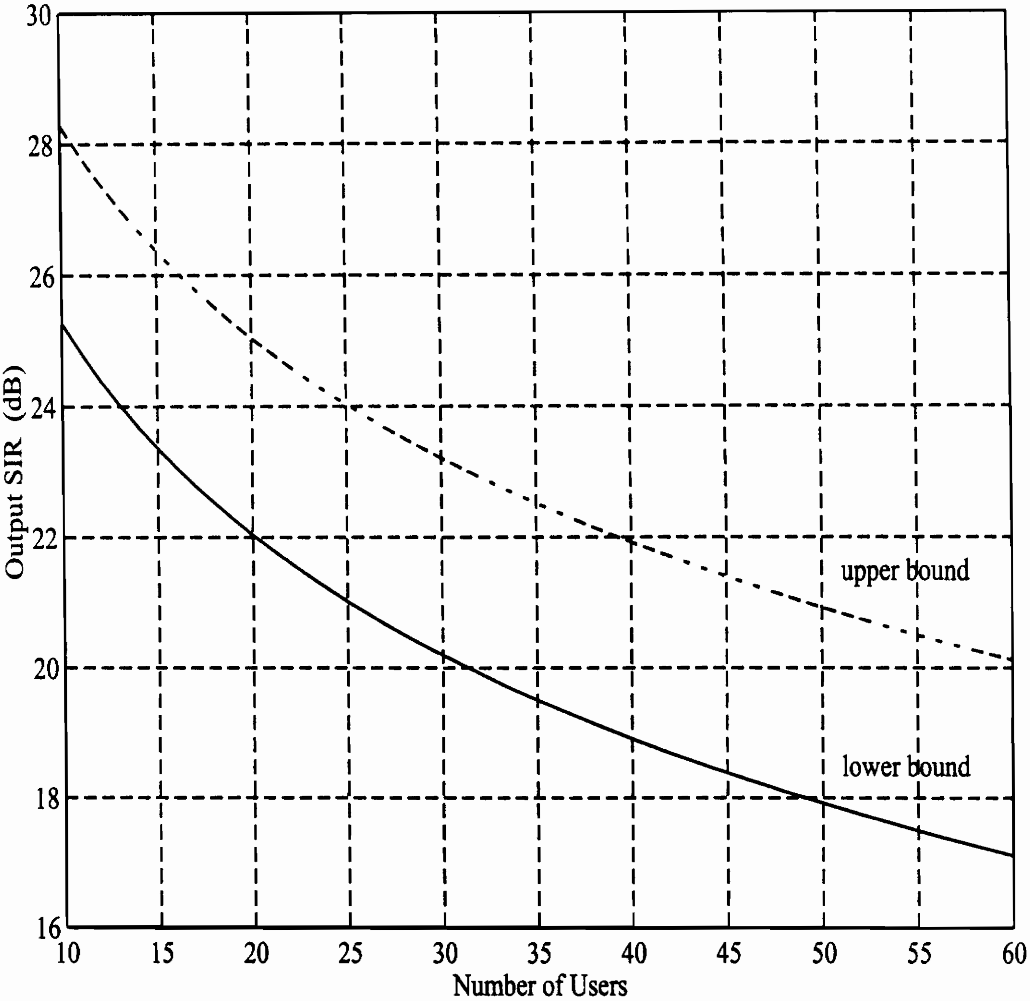

Figure 4.7: Output SIR versus Number of Users for the Upper Bound and Lower Bound for a 25 kHz IF Bandwidth

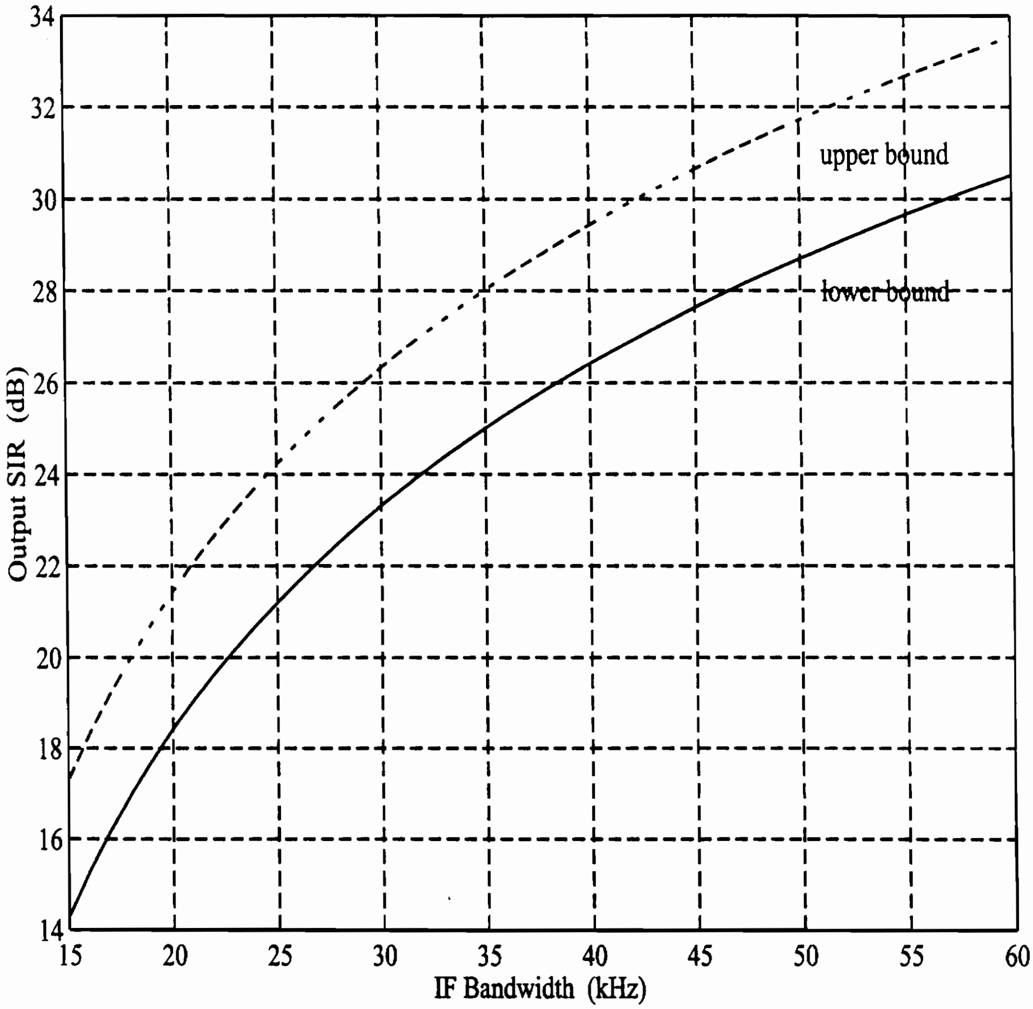

Figure 4.8: Output SIR versus IF Bandwidth for the Upper Bound and Lower Bound with 24 Users

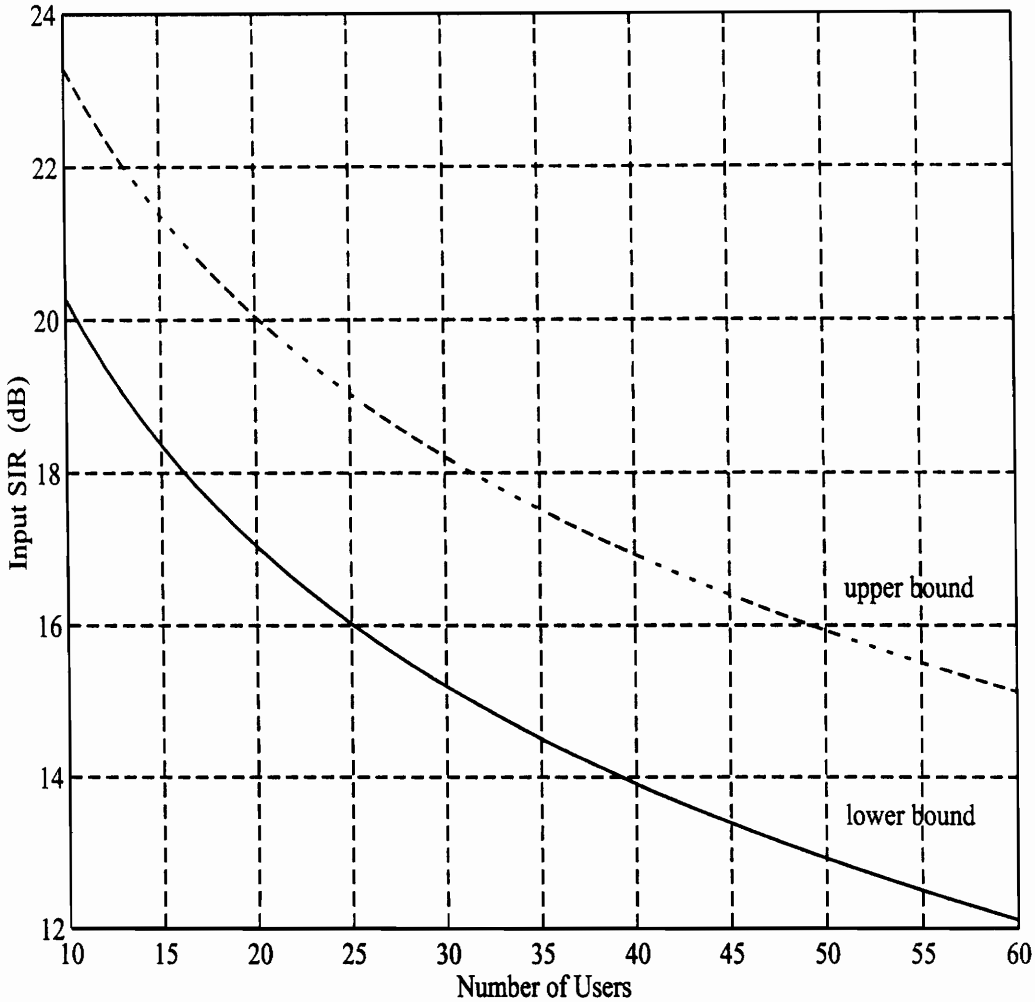

Figure 4.9: Input SIR versus Number of Users for the Upper Bound and Lower Bound for a 25 kHz IF Bandwidth

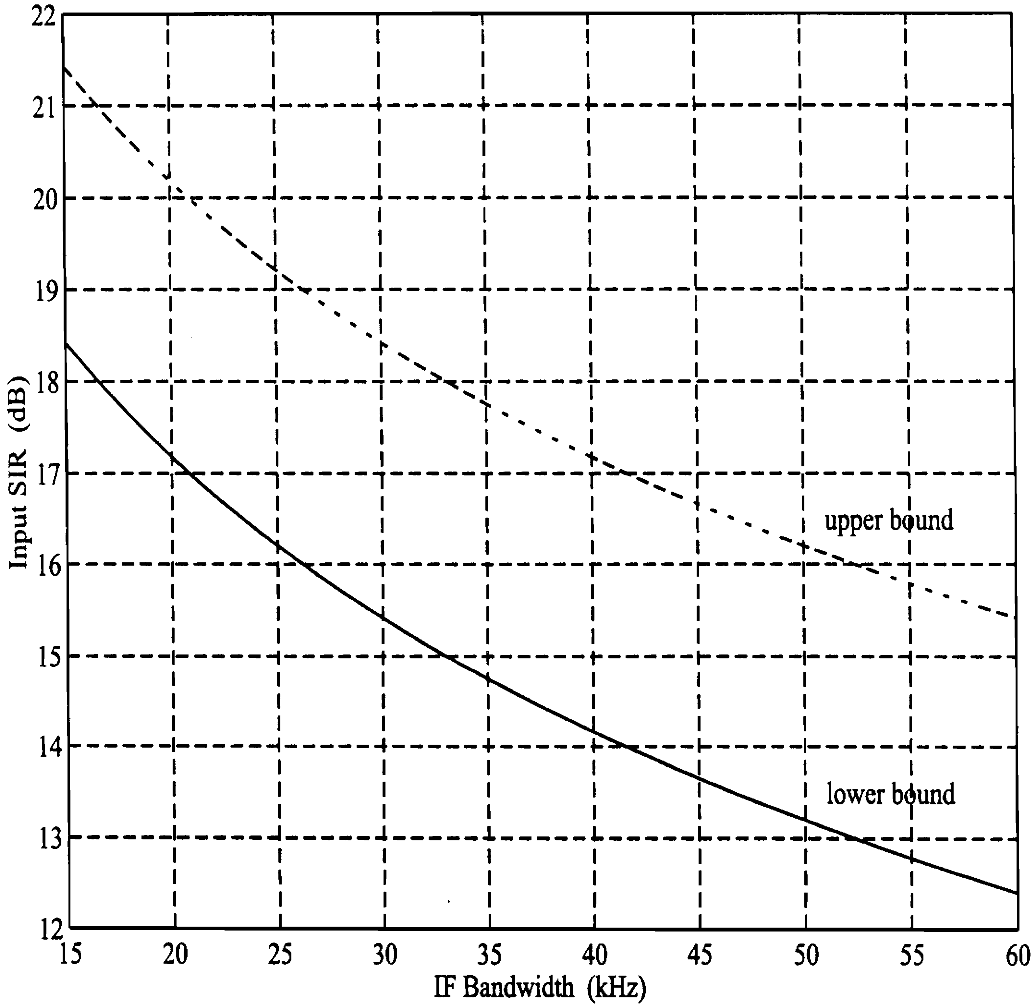

Figure 4.10: Input SIR versus IF Bandwidth for the Upper Bound and Lower Bound with 24 Users

Chapter 5

A Model for a Hybrid FM/CDMA WLL System

5.1 Background

The research described in this thesis has been performed for a telecommunication company that is targeting telephone service for developing countries where no wireline service is available. This system employs a unique hybrid FM/CDMA system, with its advantages of low cost of handsets and base stations, landline grade voice quality, ease of system implementation, and potential for further capacity growth. The system is initially designed for fixed user phones with a potential for a smooth transition to fully mobile system by replacing the current DSP chips with more sophisticated ones which incorporate a vocoder, QPSK modulator, and error correction coding. The capacity growth can be implemented by employing sectored antennas, cell splitting and full digital demodulation.

5.2 System Description

The complete system operating protocols for the WLL system are proposed in [Sig95] including the network management. This research, however, focuses primarily on the physical layer operating principles of traffic channels. Inspired by the success of AMPS and IS-95 cellular standards, the WLL system structure is shown in Fig. 5.1 and Fig. 5.2.

5.2.1 Transmitter Structure

The input voice is first converted from analog into digital signal by an A/D converter, which samples at 8 kHz. The digitized voice signal is compressed by a 2:1 dB compressor to accommodate a large speech dynamic range. The compressed signal is filtered by a pre-

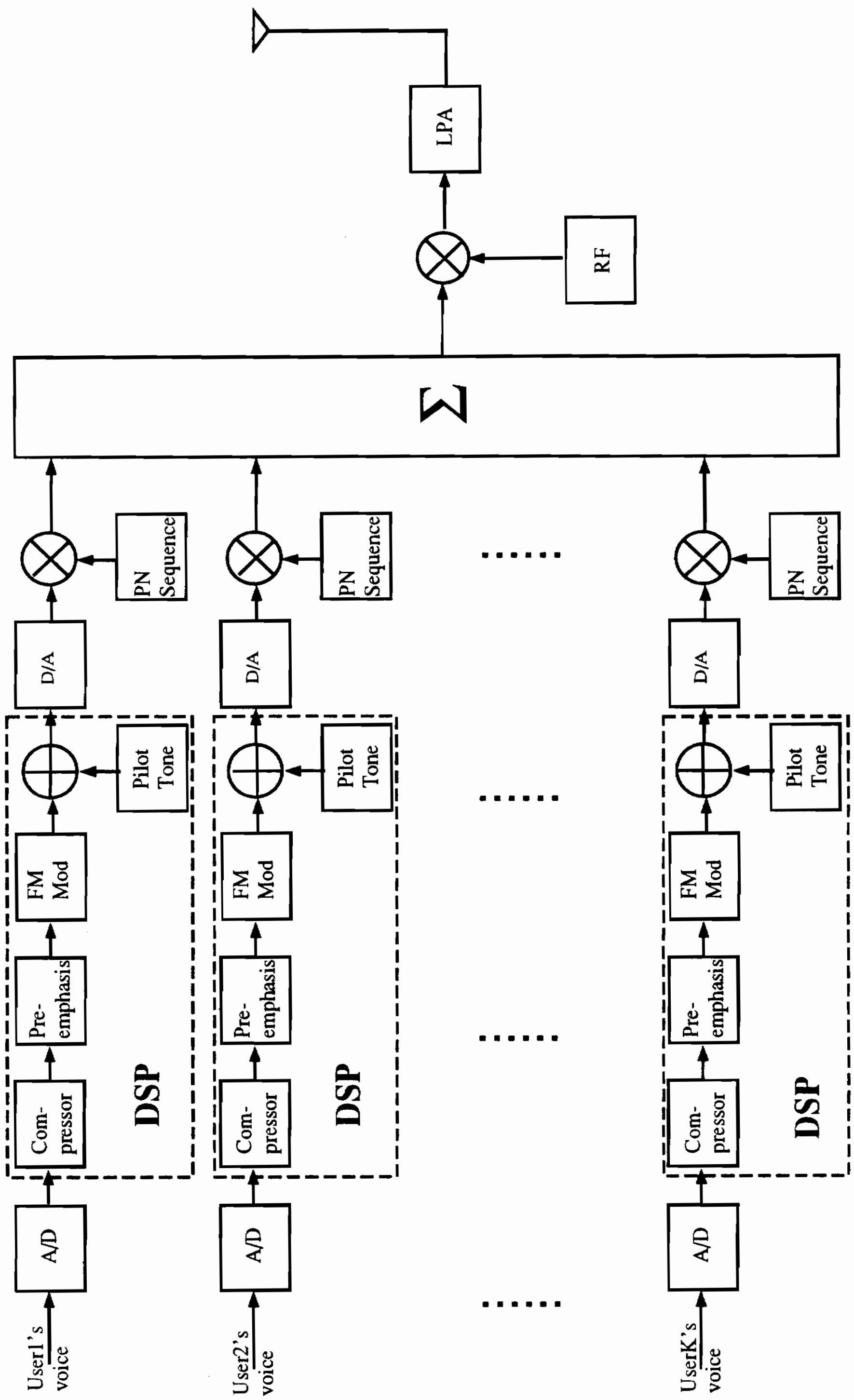

Figure 5.1 WLL Transmitter Structure

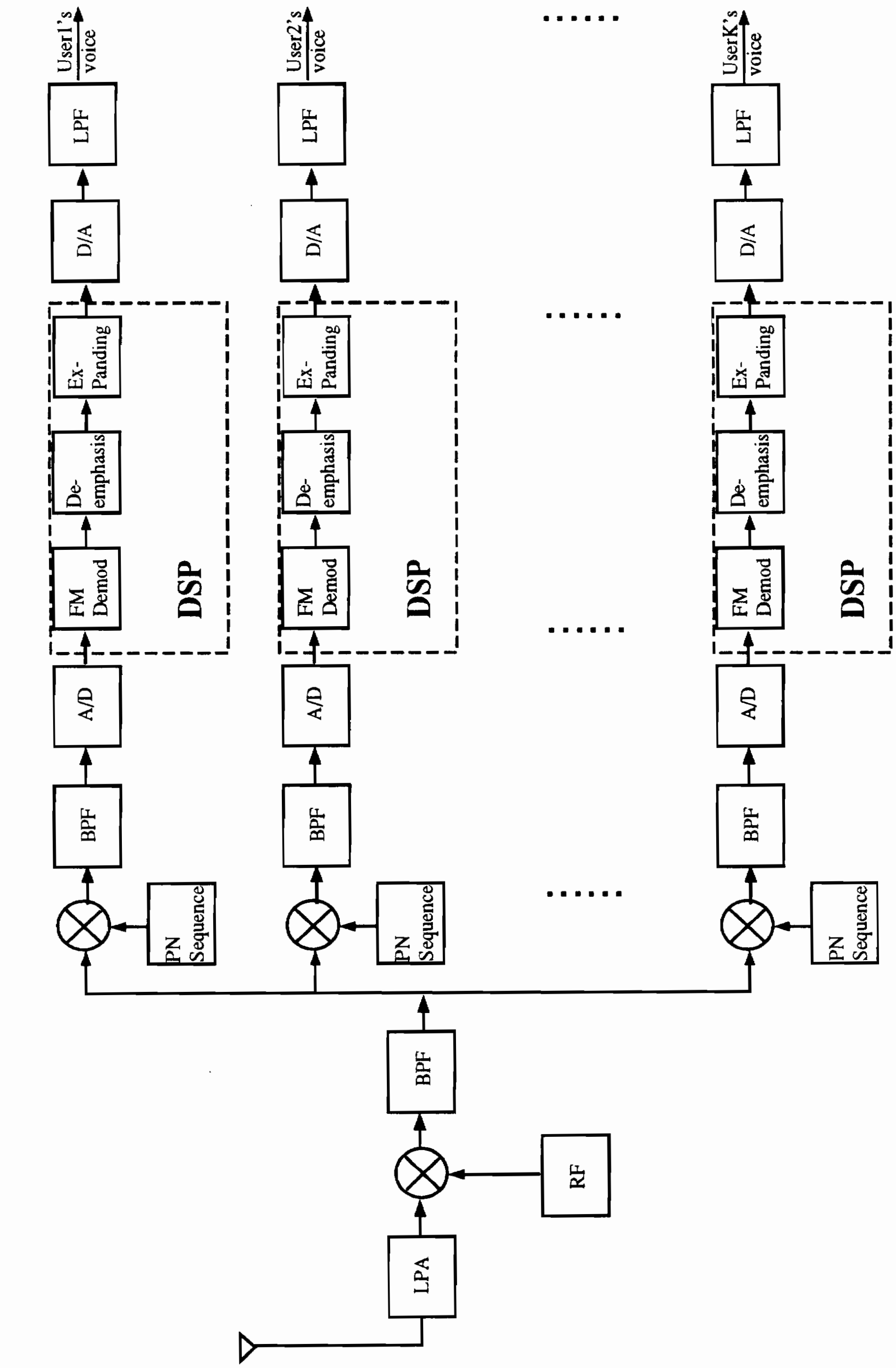

Figure 5.2 WLL Receiver Structure

emphasis filter which has a 6 dB/octave highpass frequency response between 300 Hz and 3.4 kHz. The output of the pre-emphasis filter drives an FM modulator which samples at 64 kHz with a 16 kHz carrier frequency and an IF bandwidth of 25 kHz. A digital pilot tone is used as a frequency reference to achieve synchronization and a power level indicator to implement the power control. The combined FM signal and pilot tone are converted from digital form into analog form by a D/A converter. The FM signal is multiplied by a 8 Mcps spreading sequence which is repeated every 2000 chips. The PN sequence is pulse shaped by a square root raised cosine filter with a roll-off factor of 0.35 to conserve the bandwidth. In the forward channel, i.e. from the base station to the users, the base station handles a number of calls simultaneously. The spread signals from different channels are summed up and then up-converted to RF at 2 GHz. The RF signal is amplified by a linear power amplifier in order to reduce the phase distortion and preserve the pulse shape.

The system is designed to implement companding, pre-emphasis/de-emphasis, FM modulation/demodulation and pilot tone in a DSP chip. This allows further upgrading to QPSK modulation/demodulation and sophisticated coding/decoding and interference cancellation for further capacity improvement by employing new DSP chips so that little change of system configuration is necessary.

5.2.2 Receiver Structure

The received signal is amplified, and filtered at RF frequency. Then it is downconverted to IF frequency after passing through a bandpass filter. The desired user's signal is extracted from the composite signal by multiplying the uniquely assigned PN sequence of the desired user and passing through an IF bandpass filter. The FM signal is demodulated in digital form. After passing through a de-emphasis filter, expander and baseband low pass filter, the original baseband signal is recovered.

5.3 System Performance

The tentative operating parameters for the WLL system are summarized in Table 5.1. The remainder of the results in this chapter employs these parameters unless otherwise specified. Since $N \gg 2PG$, the system is operating near the lower bound. Without pre-emphasis/de-emphasis and companding, the input SIR and the output SIR can be calculated according to Eqn. (4.84) and Eqn. (4.82), assuming a differentiation FM demodulation scheme is used.

Table 5.1: Tentative System Parameters

Spread Spectrum Bandwidth B_{ss} (MHz)	10
PN Sequence Chip Rate R_c (Mcps)	8
Typical Voice Bandwidth B (Hz)	3400
IF Bandwidth BW_{FM} (kHz)	25
Processing Gain PG	320
PN Sequence Frame Length N (chips)	2000
Number of Users K	24

In Eqn. (4.84), the input SIR is proportional to the PG, whereas in Eqn. (4.82), the output SIR decreases as PG increases. The operating point is selected based on the following tradeoff:

1. The system should be working in an input SIR range well above the FM threshold $T_h = 12$ dB.

2. The voice quality must be acceptable, which is measured by an output SIR being greater than $\gamma = 18$ dB.

By Eqn. (4.84), let

$$\frac{3PG}{K-1} \geq T_h. \tag{5.1}$$

Or

$$PG \geq \frac{(K-1)T_h}{3}. \tag{5.2}$$

For 24 users

$$PG \geq 122. \tag{5.3}$$

By Eqn. (4.82), let

$$\frac{9}{K-1}\frac{R_c}{B}(\frac{R_c}{2PGB}-1)^2\overline{(\frac{m}{V_p})^2} \geq \gamma. \tag{5.4}$$

Solving for PG, given a typical value of the normalized power of a voice signal $\overline{(\frac{m}{V_p})^2} = 0.02$, yields

$$\begin{aligned} PG &\leq \frac{R_c}{2B}\left[\sqrt{\frac{\gamma(K-1)B}{9R_c}\frac{1}{\overline{(\frac{m}{V_p})^2}}}+1\right]^{-1} \\ &\leq 413. \end{aligned} \tag{5.5}$$

Combining Eqn. (5.3) and Eqn. (5.5),

$$122 \leq PG \leq 413. \tag{5.6}$$

For tentative parameters, $PG = 320$. The input and output SIR's are:

$$(\frac{S}{I})_{in} = 16.21dB, \tag{5.7}$$

and

$$(\frac{S}{I})_{out} = 21.20dB. \tag{5.8}$$

If the IF bandwidth is 30 kHz, the processing, in this case, $PG = 266.67$. According to Eqn. (4.84) and Eqn. (4.82),

$$(\frac{S}{I})_{in} = 15.41dB, \tag{5.9}$$

and

$$(\frac{S}{I})_{out} = 23.31dB. \tag{5.10}$$

Fig. 5.3 plots the theoretical curve of output SIR versus the number of users based on the parameters above with sinusoid modulation, where $\overline{(\frac{m}{V_p})^2} = 0.5$. It can be seen from Fig. 5.3 that the output SIR in dB drops fast as the number of users increase from 1 to 20.

But it is fairly slow when the number of users is within 40 to 60. For the number of users being 25, the output SIR can reach as high as 35 dB.

Fig. 5.4 plots the theoretical curve of output SIR versus the IF bandwidth based on the parameters above with a sinusoid modulation. The output SIR in dB increases as the IF bandwidth increases. For an IF bandwidth of 25 kHz, the output SIR can reach as high as 35 dB.

For human voice, the normalized power of baseband signal is usually smaller than that of a sinusoid. The output SIR is smaller than the sinusiod modulation case. However, with pre-emphasis/de-emphasis technique, the output SIR can be increased by about 16 dB [Cou93], which greatly enhances the voice quality.

Fig. 5.3 and Fig. 5.4 are valid only when the input SIR is above the threshold of FM modulation. A typical value for the FM threshold in the presence of AWGN is about 8 dB. However, the multiple access interference for FM/CDMA modulation is not identical to a Gaussian noise. The threshold might be slightly different from that of a conventional FM demodulator.

Fig. 5.5 plots the input SIR versus the number of users in the system for an IF bandwidth of 25 kHz. The input SIR drops very fast as the number of users increases from 2 to 20. When the number of users increases above 30 but less than 60, the input SIR is still above a typical threshold value, which is approximately 8 dB for differentiation demodulation.

Fig. 5.6 plots the input SIR versus the IF bandwidth for 24 users per cell. The input SIR decreases almost linearly as the IF bandwidth increases. For a 25 kHz IF bandwidth the input SIR is about 16.2 dB. When the IF bandwidth increases from 35 kHz to 60 kHz, the input SIR is still above the desired operating point of 12 dB input SIR, but still above the FM threshold value.

5.4 Chapter Summary

In this chapter, we have described a model for a hybrid FM/CDMA WLL system. We have analyzed this system using the analytical method developed in Chapter 4 in order to find the operating point for the system which maximizes the capacity given a desired set of performance requirements. It was shown that the optimum choice of the IF bandwidth was 30 kHz and the optimum choice of the processing gain was 267, which is fairly consistent with the value $PG = 320$ chosen by SigTek in their initial system design. In the next chapter, we undertake a more detailed simulation study to confirm these analytical results.

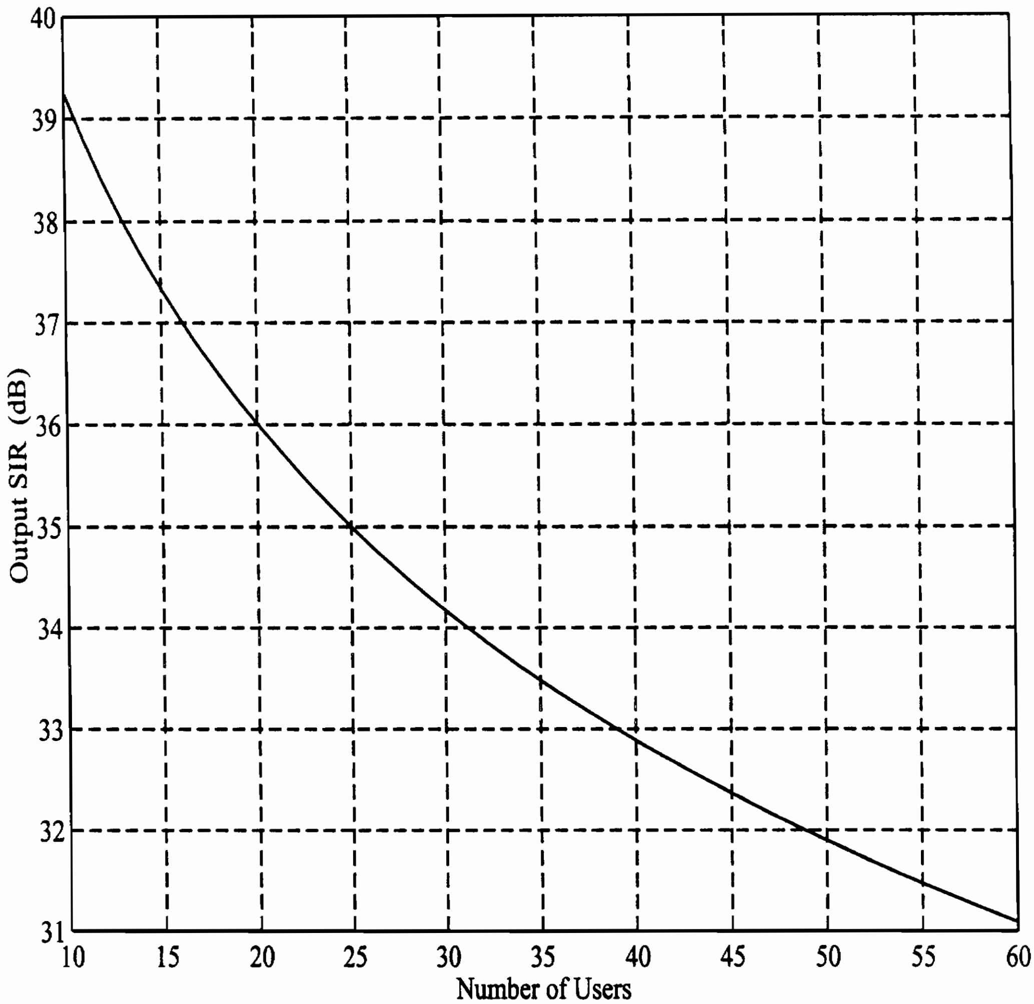

Figure 5.3: Theoretical Curve of the Output SIR versus the Number of Users without Gaussian Noise for 25 kHz IF Bandwidth with Sinusoid Modulation

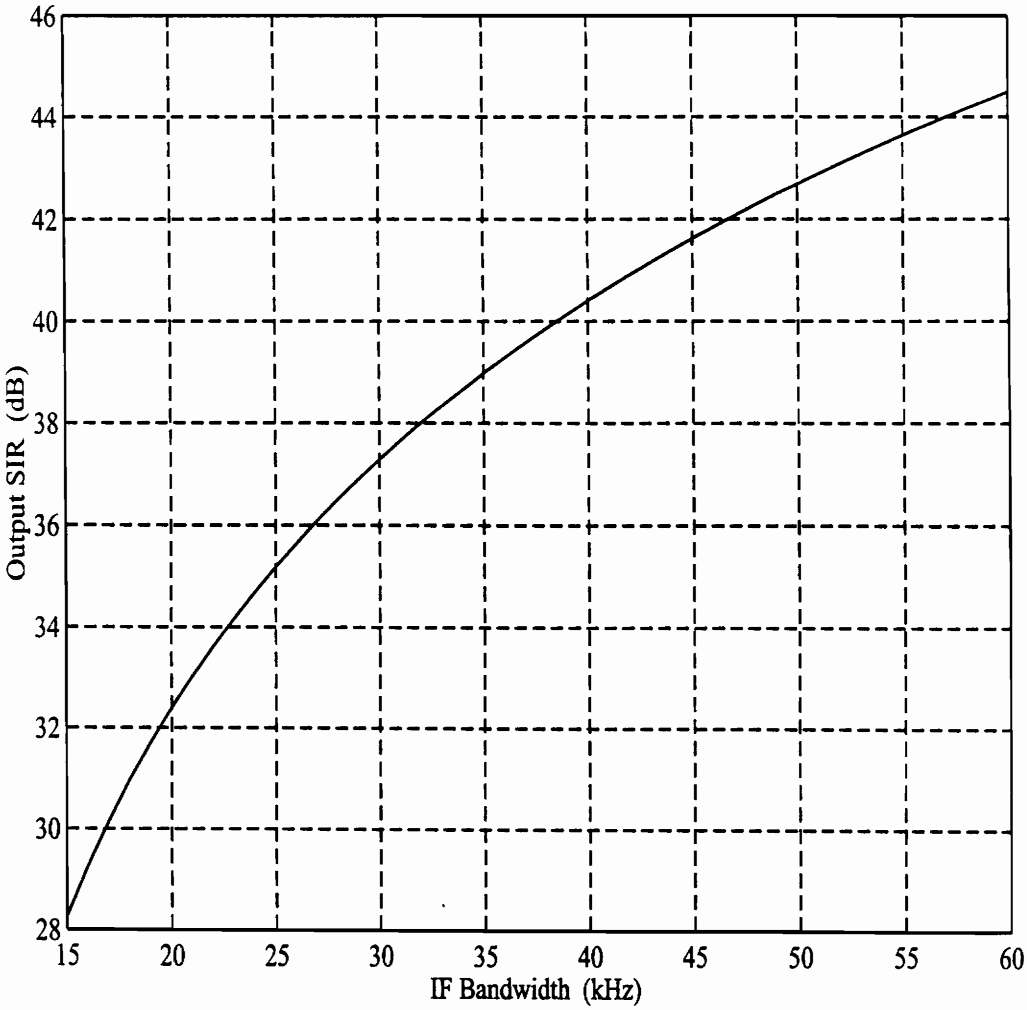

Figure 5.4: Theoretical Curve of the Output SIR versus the IF Bandwidth without Gaussian Noise for 24 Users with Sinusoid Modulation

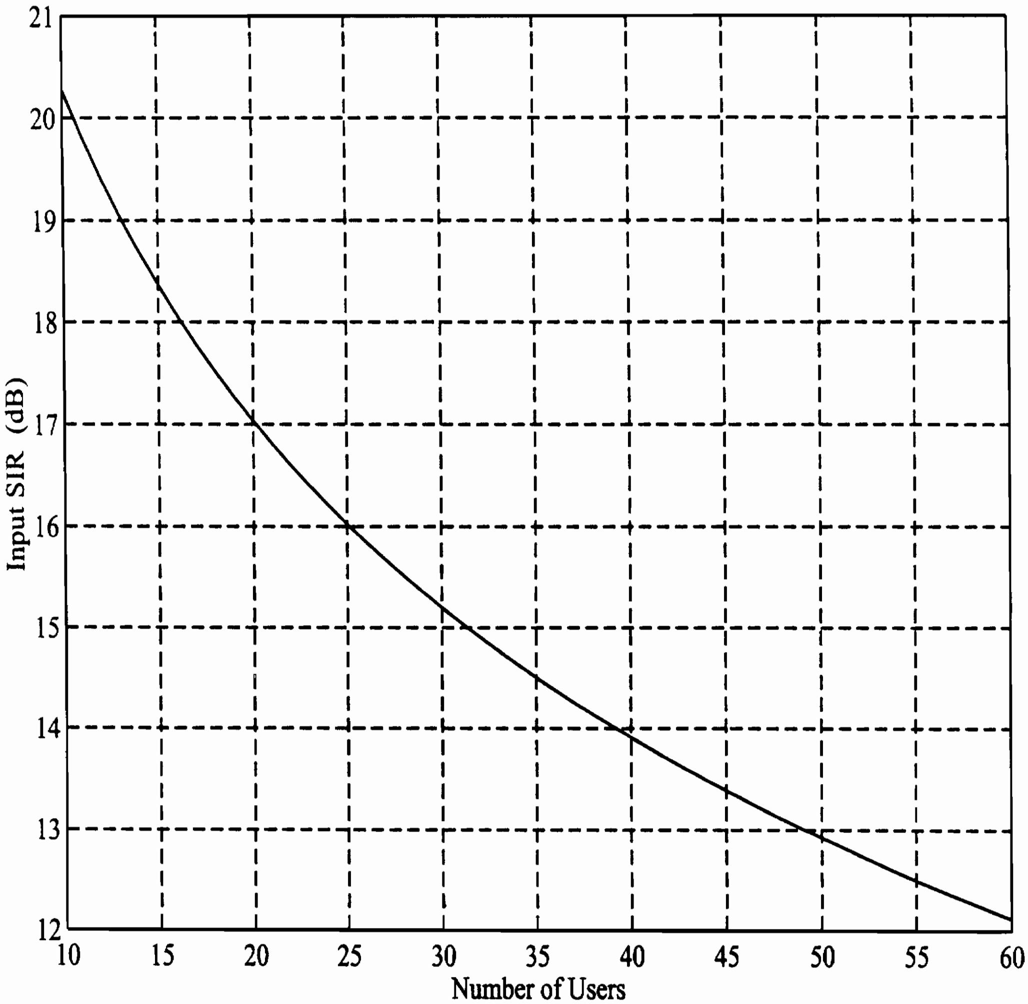

Figure 5.5: Theoretical Curve of the Input SIR versus the Number of Users without Gaussian Noise for 25 kHz IF Bandwidth with Sinusoid Modulation

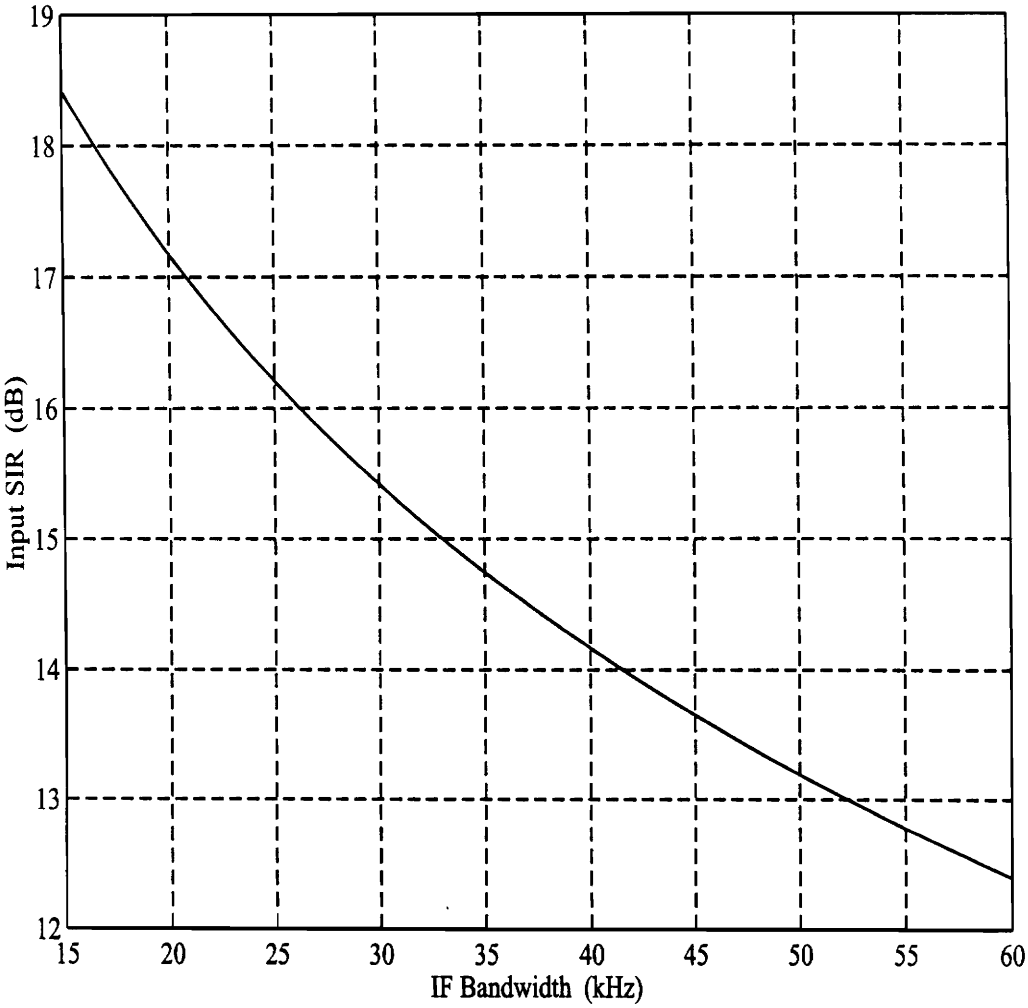

Figure 5.6: Theoretical Curve of the Input SIR versus the IF Bandwidth without Gaussian Noise for 24 Users with Sinusoid Modulation

Chapter 6

Simulation Approach and Results

Since the changes in hardware structure are very expensive and time consuming, while changes in software can be implemented quickly and easily, at early stages of a practical system development, a software test-bed is often generated to evaluate the effect of parameter changes on the system performance [Jer92]. Based on the system model of Chapter 5 and the communication fundamentals presented in Chapter 2 and Chapter 3, a modular program was developed in Matlab on Sun SPARC station platform to model this FM/CDMA system. The speech quality was also examined via an audio tool on the workstation.

The purposes of developing the software test-bed are:

1. To establish an FM/CDMA model to investigate the system mechanism and demonstrate the system performance.

2. To optimize the system performance through the selection of FM demodulation schemes and the tradeoffs in the frequency modulation index and the spread spectrum processing gain.

3. To investigate the system tolerance to overloading and unexpected interference.

In this chapter, four types of FM demodulation schemes - differentiator, quadrature, arctangent and phase locked loop were examined by calculating the output SNR in a white Gaussian noise channel environment. The effect of 2:1 dB companding on FM modulation/demodulation was also investigated. Major emphasis was placed on the simulation of FM/CDMA system performance because of the high calculation-intensity nature of CDMA simulation. The simulation based on the tentative parameters of an FM/CDMA system takes much memory and CPU time even for a few seconds of speech samples. We are primarily concerning two aspects of FM/CDMA system performance. One is how the system performance is affected by the choice of IF bandwidth of FM modulation. The other is how the system performs as the number of users increases. The system performance is investigated for both the forward link and the reverse link.

6.1 Simulation Approach

The system model is developed in Chapter 4 and Chapter 5. Results from the theoretical analysis of Chapter 4 and Chapter 2 are used as a guidance to organize the simulation.

All the simulation are carried out using a voice sample recorded by the audio tool on the work station. The male-tone voice is sampled at 8 kHz. The voice lasts about two seconds. Fig. 6.1 plots part of the voice signal. The normalized signal power of this voice sample $\overline{(\frac{m}{V_p})^2} = 0.02$. Prior to the frequency modulation, the voice sampling frequency is interpolated to 64 kHz to reduce aliasing. In order to match the chip rate of the PN sequence, the 64 kHz FM signal is further interpolated to 8 MHz. The spread signal is sampled at 32 MHz to reduce aliasing in signal processing.

For FM, information is contained in the signal phase. It is very important to avoid the phase distortion when using DSP techniques. An FIR filter exhibits a linear phase response and is favored in the simulation. Matlab also provides another powerful filtering technique which filters the signal sequence from two opposite directions and thus eventually eliminates phase distortion.

Memory management is crucial due to the high chip rate of the PN sequence. The voice sample of each user is divided into several smaller segments. Simulations are run on each segment and the final output voice is the combination of all the segmented outputs. One side effect of segmentation is introduced by the imperfect estimation of the final conditions of each segment, which in turn degrades the simulated results. The longer a segment of samples, the better the simulated results. In order to hear to examine the output voice quality, two seconds of output voice are desired. A two second voice sample for each user would require excessive computation resources when the FM/CDMA system is heavily loaded. However, like other CDMA systems, the output voice quality of all users in the FM/CDMA WLL system are identical to one another if perfect power control is achieved. Based on this observation, instead of examining the output voice quality of only one user, the output voice of all users is examined by concatenating each output voice into a whole series. This technique saves valuable computation resources.

Signal to noise ratio is calculated based on the estimation theory given in [Jer92]. After a signal passes through a system, it is corrupted by noise. The output signal $y(t)$ is a Least Square Estimation (LSE) of the input signal $x(t)$. The condition gives

$$(\frac{S}{N})_{out} = \frac{R_{xy}^2}{P_x P_y - R_{xy}^2}, \tag{6.1}$$

where R_{xy} is the maximum value of the cross-correlation function between the input signal $x(t)$ and the output signal $y(t)$ of the system: $R_{xy} = max\{E[x(t)y(t+\tau)]\}$, P_x is the power of the input signal $x(t)$: $P_x = E\left[x^2(t)\right]$, P_y is the power of the output signal $y(t)$: $P_y = E\left[y^2(t)\right]$.

Another approach to calculate the output SNR/SIR is by signal subtraction. Suppose the original baseband signal is $m(t)$, the recovered baseband signal is $\tilde{m}(t)$. Assume the signal and the noise are independent through the modulation/demodulation process. The recovered signal can be expressed as the original signal multiplied by a constant plus the channel noise:

$$\tilde{m}(t) = cm(t) + n(t), \tag{6.2}$$

where c is a constant and $n(t)$ is the noise. Normalizing the constant c yields

$$\hat{m}(t) = m(t) + \hat{n}(t). \tag{6.3}$$

The noise power is calculated by $E\{[\hat{m}(t) - m(t)]^2\}$. Note the normalization is done by dividing the maximum absolute value of $\tilde{m}(t)$ because we have no prior knowledge of $cm(t)$. The original signal is also normalized to one. However, since the noise is a random process, there is a probability that a particular sample of noise is larger than the signal amplitude at that particular time and the sum of the signal and the noise is the extreme value of the sequence. For this instance, the rest of the recovered sequence may differ from the original sequence by a noticeable factor. The subtraction cannot remove all the information signal but correspondingly increased the noise power. On the other hand, when the signal and the noise are not independent, as in the case of the arctangent demodulation, the normalization tends to introduce larger error. For these considerations, the SNR/SIR calculations are carried out based on the first approach throughout this thesis.

6.2 Simulation Results for FM System

In the following simulation of FM demodulation schemes, the IF bandwidth is fixed at 25 kHz, The bandwidth of the voice signal is assumed to be 3400 Hz. The normalized signal power is measured to be 0.02.

6.2.1 Differentiator Demodulation

Fig. 6.2 plots the curve of the output SNR versus the input SNR for the differentiation demodulation scheme and compares with the theoretical curve given by Eqn. (2.40). Companding is not used in this case. The theoretical curve agrees very well with the simulation curve. In Fig. 6.2, a threshold is observed at about 8 dB of input SNR. Below the threshold, the output signal quality deteriorates significantly. Above the threshold, the output SNR approximately increases linearly to the input SNR with a unity slope. This is verified by listening to and comparing with the output sound quality. The output SNR is 17.3 dB for a input SNR of 12 dB.

Fig. 6.3 plots the output SNR versus the input SNR and evaluate the effect of companding. It is clear that companding does not affect the threshold value. The output SNR with companding is greater than that without companding case at low input SNR values, but smaller at high input SNR values. Saturation of output SNR is observed when companding is applied. In our simulation, the 2:1 dB compressing is implemented by taking the square root of the signal and expanding is implemented by squaring the signal. Simulation concludes that the nonlinear operation leads to the saturation of output SNR.

Investigation of the companding process is significant because, with the knowledge of this effect, the FM/CDMA system performance is able to be predicted from one case to the other. For an input SNR of 12 dB, the output SNR reaches 19.5 dB, which is 2.2 dB superior to the no companding case. Therefore, companding is able to improve the system performance at the desired 12 dB operating point.

6.2.2 Quadrature Demodulation

Fig. 6.4 compares the output SNR of quadrature demodulation to that of differentiation demodulation when no companding is applied. The quadrature demodulation performs as well as the differentiation demodulation. Fig. 6.5 plots the output SNR versus the input SNR with companding. The quadrature again performs almost identical to the differentiation demodulation.

6.2.3 Arctangent Demodulation

Fig. 6.6 compares the output SNR of arctangent demodulation to that of differentiation demodulation without companding. The threshold is observed to be 8 dB, the same value as a differentiation or quadrature demodulation. However, the output SNR value is about 3-5 dB less than the previous two demodulation schemes. Fig. 6.7 plots the output SNR versus the input SNR with companding. The nonlinear effect is observed again but a 5 dB lower saturation level-only 17 dB.

6.2.4 PLL Demodulation

Simulation of PLL is run on a sample by sample basis. The choice of parameters such as loop gain and sampling period has very subtle effect in simulation results. A second order

PLL is studied. The low pass filter is described by the following difference equation:

$$y(n) = a_0 x(n) + a_1 x(n-1) - b_1 y(n-1), \tag{6.4}$$

where the coefficients of the transfer function are:

$$a_0 = \frac{T_s + 2\tau_2}{\alpha_1 T_s + 2\tau_1}, \tag{6.5}$$

$$a_1 = \frac{T_s - 2\tau_2}{\alpha_1 T_s + 2\tau_1}, \tag{6.6}$$

and

$$b_1 = \frac{\alpha_1 T_s - 2\tau_1}{\alpha_1 T_s + 2\tau_1}. \tag{6.7}$$

The transfer function of the filter is described by

$$F(s) = \frac{s\tau_2 + 1}{s\tau_1 + \alpha_1}, \tag{6.8}$$

where $\alpha_1 = 1$ for active filters and $\alpha_1 = 0$ for passive filters, T_s is the sampling period. τ_1 and τ_2 are determined by the cut-off frequency of the low pass filter.

The difference equation of VCO is given by the trapezoidal integration:

$$\hat{\theta}(n) = \frac{T_s}{2}[\nu(n) + \nu(n-1)] + \hat{\theta}(n-1), \tag{6.9}$$

where ν is the input signal of the VCO, $\hat{\theta}$ is the output of the VCO, which is used as a feedback into the phase detector. The error output of the phase detector, $e(n)$, is

$$e(n) = sin[\theta(n) - \hat{\theta}(n)], \tag{6.10}$$

where θ is the phase of the received signal.

Fig. 6.8 plots the second order PLL demodulation without companding. Compared with the differentiator on the same plot, the threshold is observed to be 6 dB, a threshold extension of 2 dB is achieved. Fig. 6.19 plots the PLL demodulation with companding. The output SNR is saturated at about 25 dB.

Compared with the four FM demodulation schemes, the differentiator and the quadrature implementation show the same performance. The arctangent implementation shows a low level of system performance. The PLL is able to achieve threshold extension and performs the best.

6.3 Simulation Results for FM/CDMA System

Having established a baseline model for FM demodulator performance, we now investigate the results for the hybrid FM/CDMA system.

6.3.1 Forward Link

The forward link is a one to many transmission. The spreading sequence can be synchronized for different users. It is possible in this case that orthogonal codes be used. SIR is examined for both PN sequences and Walsh sequences.

The effect of the number of users on output SIR is examined. Fig. 6.10 plots the output SIR versus the number of users with PN sequence spreading. The output SIR decreases from 22.5 dB for 10 users down to 14 dB for 60 users. Since the minimum acceptable SIR level is 18 dB, the system is able to accommodate up to 38 users. When the system is loaded with 24 users, the output SIR reaches 20.5 dB. Compared with the theoretical curve given by Fig. 4.7, the plot approaches the lower bound case.

Fig. 6.11 plots the output SIR versus different IF bandwidth with PN sequence spreading. The output SIR increases from 14.2 dB at 15 kHz IF bandwidth and reaches a peak of 19.8 dB at 25 kHz. The output SIR drops all the way down to 8.2 dB at 60 kHz. For a desired output signal quality of 18 dB, the optimal bandwidth is 25 kHz for PN sequence spreading. Compared with the theoretical curve given by Fig. 4.8, the system is operating closely to the lower bound case for the IF bandwidth between 15 kHz and 25 kHz. Above 25 kHz, the theory predicts a continuous output SIR increase because the input SIR is always above the 8 dB FM threshold as illustrated in Fig. 4.10, assuming the MAI of FM/CDMA system in lower bound exhibits the same FM threshold. Three important factors contribute to this discrepancy. First, the non-zero cross-sorrelations between different users increase the background noise when the PN sequence frame is short. Second, as mentioned earlier in the description of our simulation approach, the samples are broken into segments to fit the computer memory. For 24 users, two baseband voice samples are processed each time.

To achieve a final 32 MHz sampling rate after spreading, the baseband 8 kHz voice have to be interpolated by 4000. Since the interpolation and decimation implemented in Matlab are not completely inverse processes, errors may occur during these manipulations. Third, the IF bandwidth is calculated by Carson's rule, which promises 98% energy confinement. However, distortion may occur for worse and worse as the IF bandwidth increases. The SNR/SIR calculation approach described in Section 6.1 is based on the cross-correlation between the input and the output voice signal. Any distortion will introduce dissimilarity between the two voice signals. The output SIR is degraded by the distortion rather than the noise. This conclusion is further supported by listening to the output voice quality. As a result, the output SIR falls below the FM threshold. As the IF bandwidth increases, the distortion caused by the interpolation/decimation and the Carson's rule also increases. Therefore the output SIR decreases. These factors will also affect other results in the rest of simulation.

Fig. 6.12 plots the output SIR versus the number of users with Walsh code spreading. SIR does not degrade as the number of users increases from 10 to 60. This is verified via the audio tool. The sound quality of 10 users and 60 users are very good and indistinguishable from one another. As analyzed in Section 4.3, the Gaussian noise could not be spread by a signature sequence. PN sequence exhibits some similarity to a white Gaussian noise. Therefore when despreading, the power spectral density of the received signal is little affected due to the uncorrelated property of PN sequences. But for Walsh sequence spreading/despreading, the spectra of the interfering signals are further spread by the Walsh sequence of the desired user. The contribution of the interfering spectra after IF band filtering is much less than that spread by a PN sequence.

Fig. 6.13 plots the output SIR versus different IF bandwidth with Walsh code spreading. The output SIR increase from 23.8 dB of 15 kHz IF bandwidth to a peak of 26 dB at 35 kHz. The output SIR falls off quickly down to 12.5 dB at 60 kHz. For 24 users, the IF bandwidth can extend to 35 kHz with a best output voice quality. Again the same reason as in Fig. 6.11 causes the voice degradation below threshold. Noting that the FM signal is modulated by the Walsh sequence, orthogonality will not hold when phase reversal of FM signal occurs.

6.3.2 Reverse Link

The reverse link is a many to one transmission. The received signal is not synchronized on a chip period level. It is well known that Walsh code is not a good choice in reverse link spreading due to the random delay of signals' arrival. In IS-95, Walsh code is used in the reverse link as data modulation instead of spreading. Our primary concern is the system performance under PN sequence spreading.

Fig. 6.15 plots the output SIR versus the number of users in the system. The output SIR decreases from 23.5 dB for 10 users down to 17.3 dB for 60 users. Compared with Fig. 6.11, the output SIR is slightly better than the synchronous case. This is due to the fact that the multiple access interference is averaged if the PN sequences are not aligned to each other.

Fig. 6.16 plots the output SIR versus the IF bandwidth with PN sequence spreading. The output SIR increases from 9.5 dB at 15 kHz to a maximal value of 21.8 dB at 25 kHz. The output SIR decreases slightly as the IF bandwidth increases up to 60 kHz. Therefore, for asynchronous reception, the IF bandwidth does not effect the system performance very much.

Power control is another key issue in CDMA applications. The system capacity is significantly affected by the variance of the received signal power. In this section, the FM/CDMA system performance under imperfect power control scheme was examined. Fig. 6.17 plots the ability of FM/CDMA system to tolerate interference. The output SIR was measured based on the system parameters proposed in Section 5.3. The variance of the received power of 24 users varies from 0 dB to 8 dB. For the variance of the received power less than 2.3 dB, the output SIR falls within the range of good voice quality. The output SIR suffers a sharp roll-off when the variance further increases. As for a variance of 5 dB, the output voice quality becomes unacceptable.

6.4 Chapter Summary

In this chapter, we have discussed a simulation of an hybrid FM/CDMA system for the WLL application. For the forward link, we found that Walsh code achieves extremely high capacity. For the reverse link, it was found that the system design could support up to 30 users with acceptable output voice quality. One key use of the simulations is to verify the operating point of the system. An IF bandwidth in the range of 25-40 kHz was found to be optimal over most cases, a value which agrees well with both the design value of 25 kHz and the analytically computed value of 30 kHz.

Figure 6.1: Voice Sample

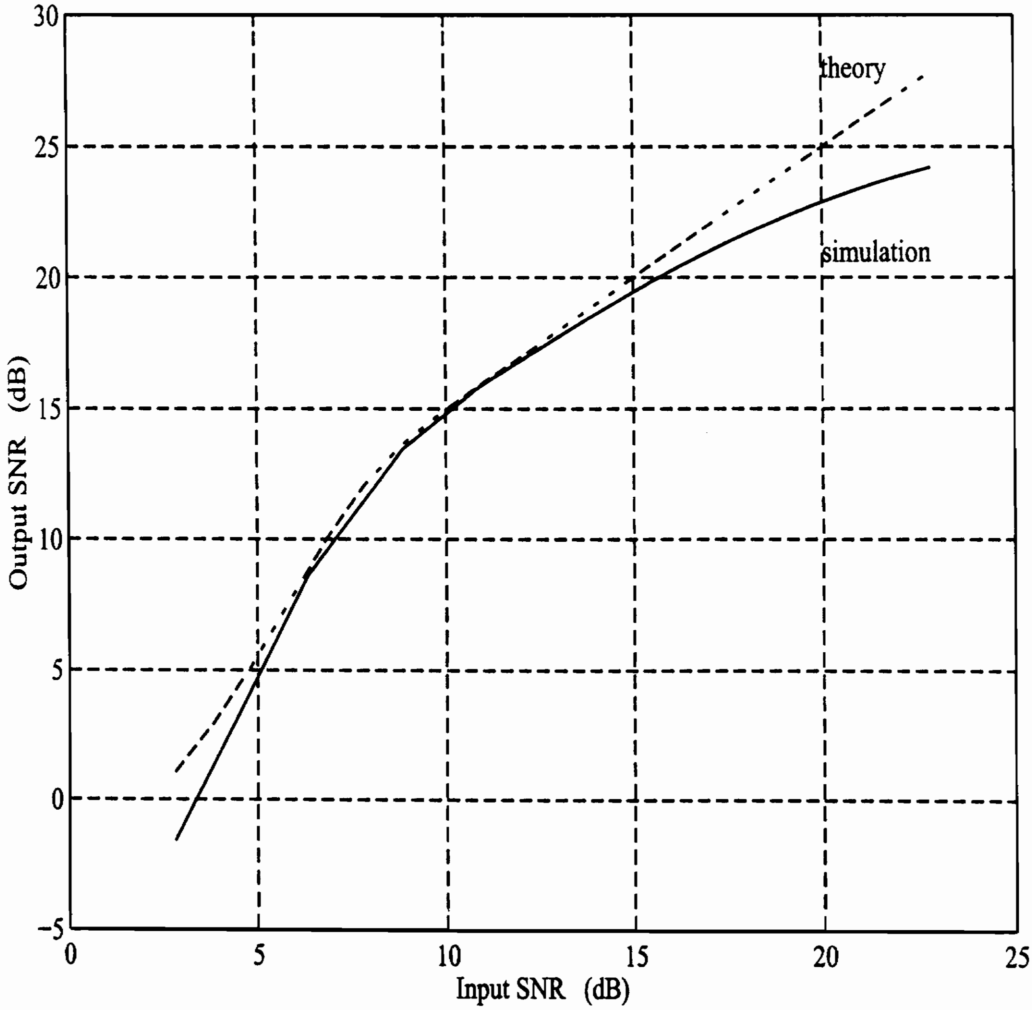

Figure 6.2: Output SNR versus Input SNR for Differentiation Demodulation without Companding

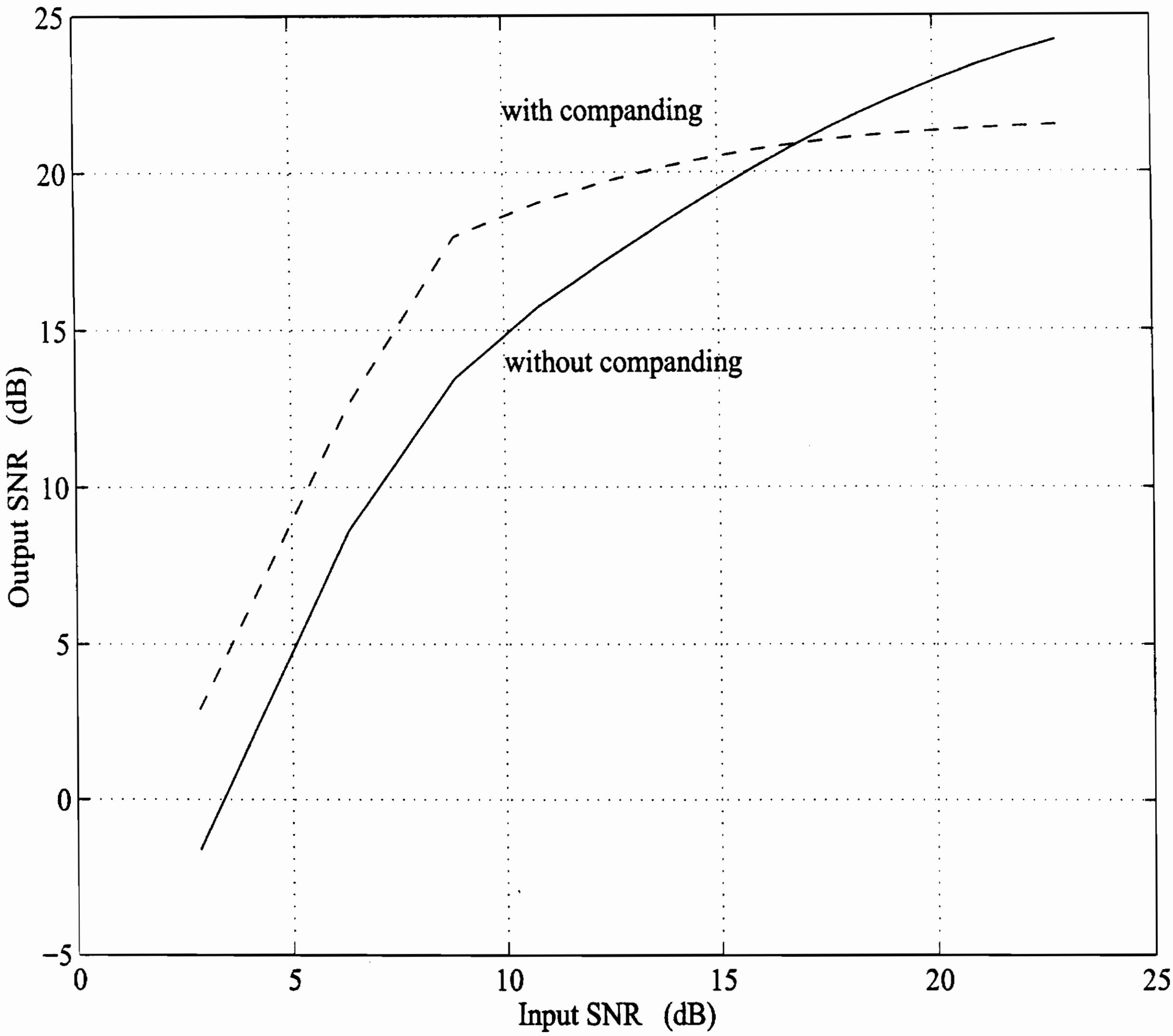

Figure 6.3: Output SNR versus Input SNR for Differentiation Demodulation with Companding

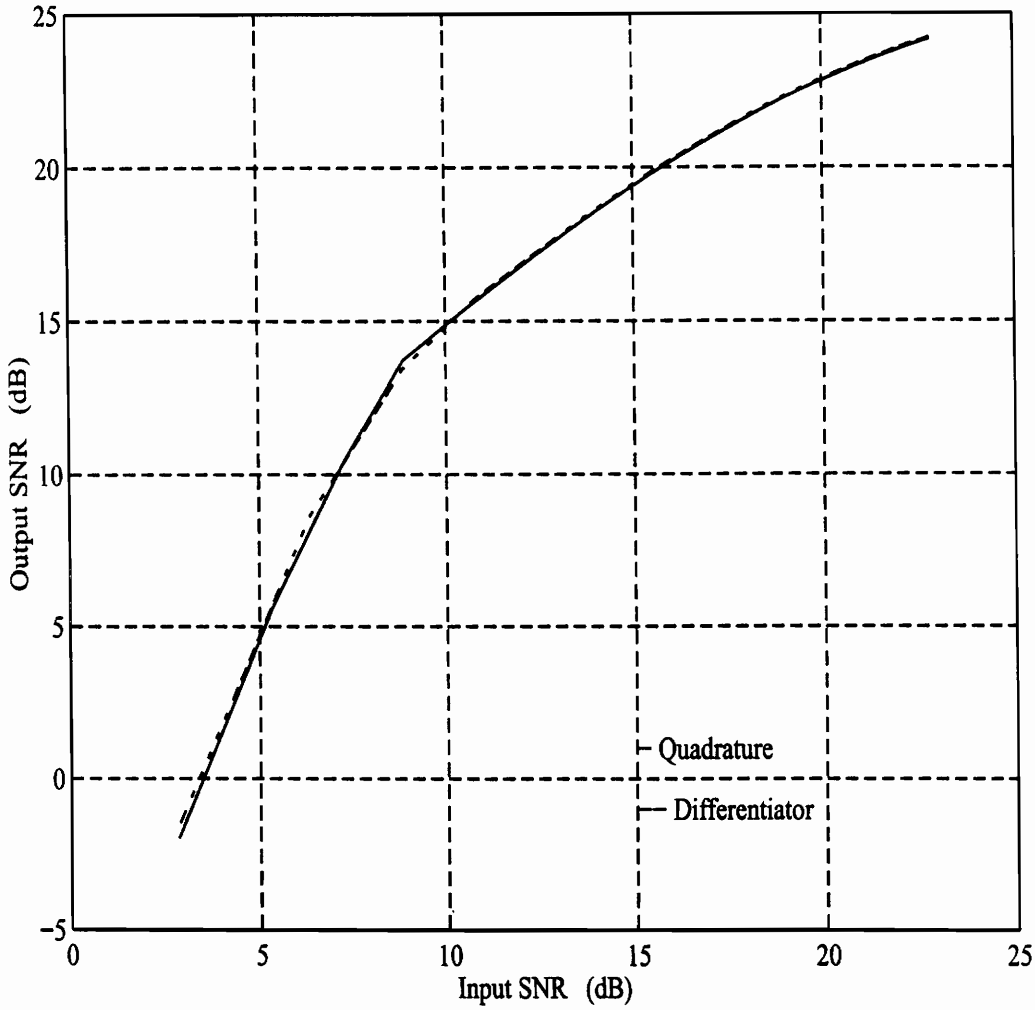

Figure 6.4: Output SNR versus Input SNR for Quadrature and Differentiation Demodulation without Companding

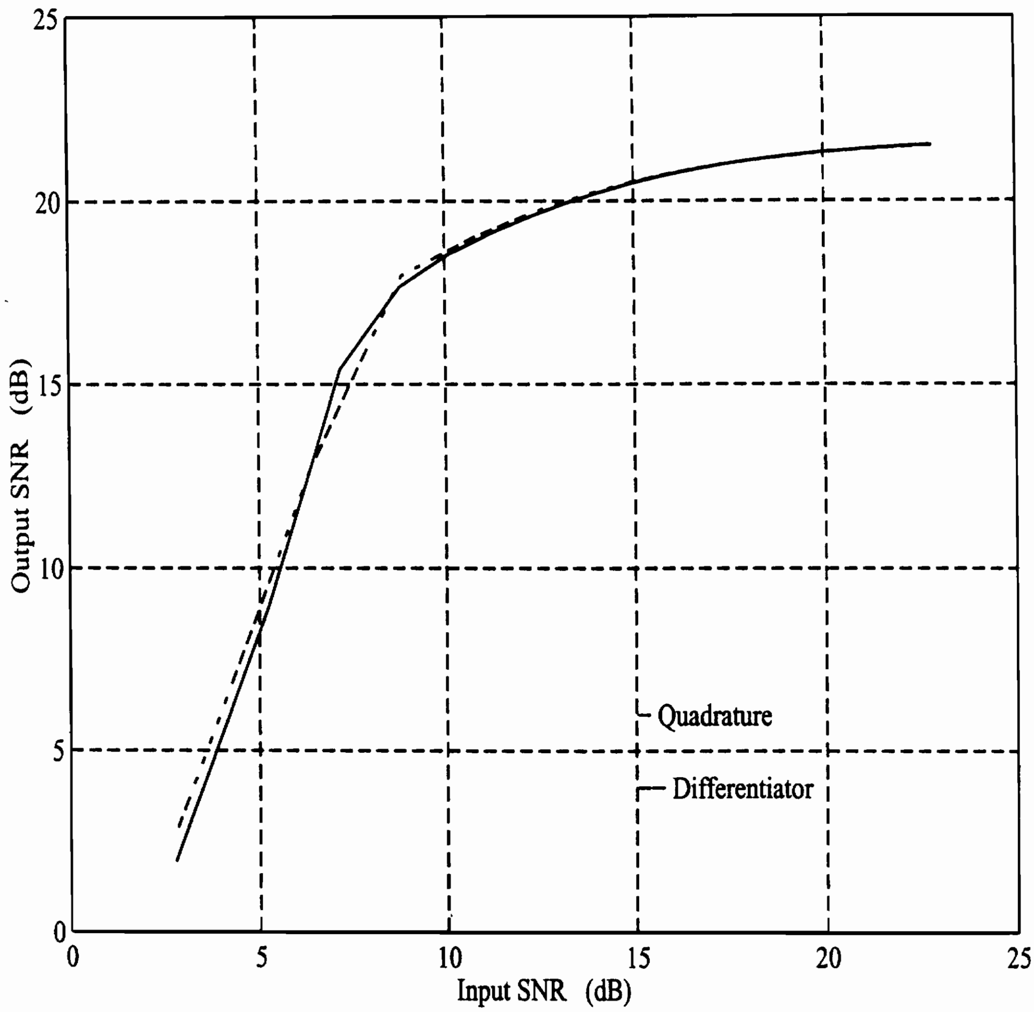

Figure 6.5: Output SNR versus Input SNR for Quadrature and Differentiation Demodulation with Companding

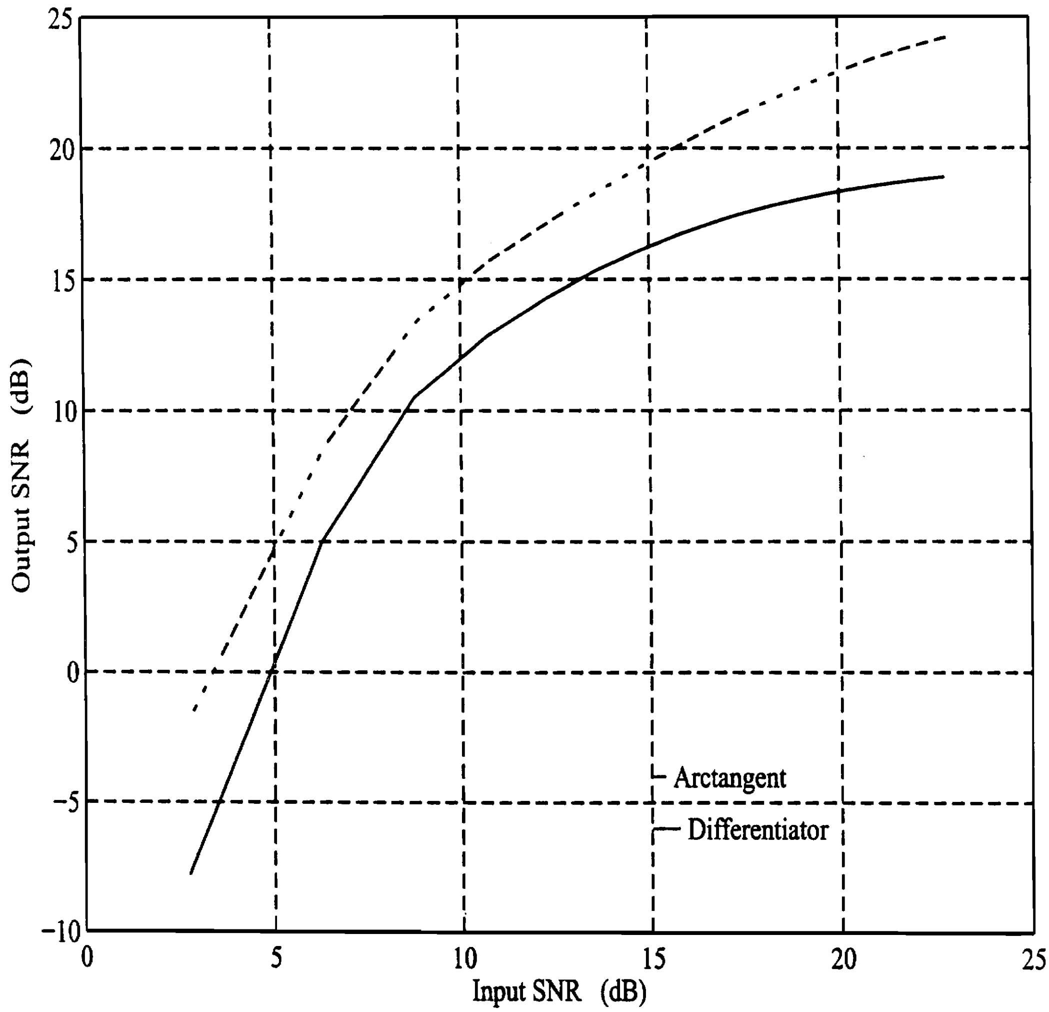

Figure 6.6: Output SNR versus Input SNR for Arctangent and Differentiation Demodulation without Companding

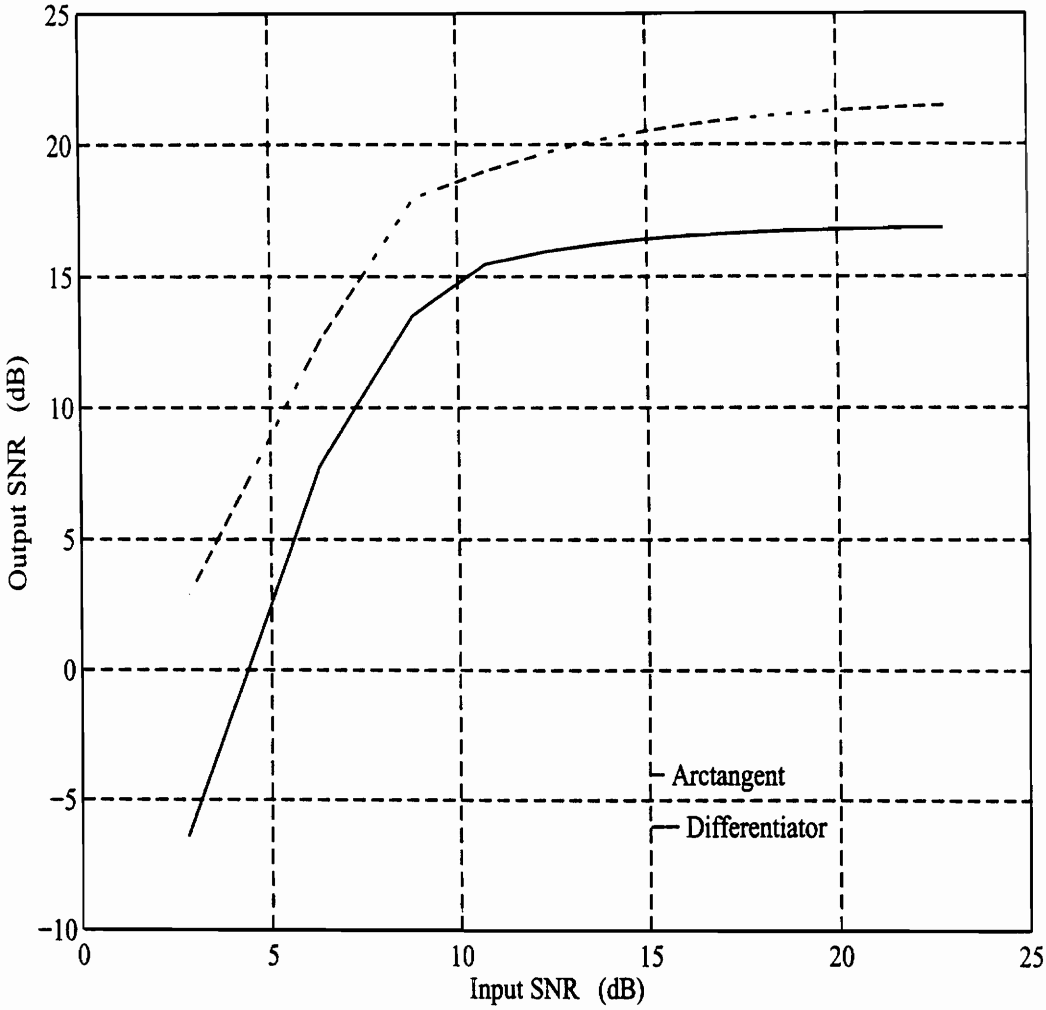

Figure 6.7: Output SNR versus Input SNR for Arctangent and Differentiation Demodulation with Companding

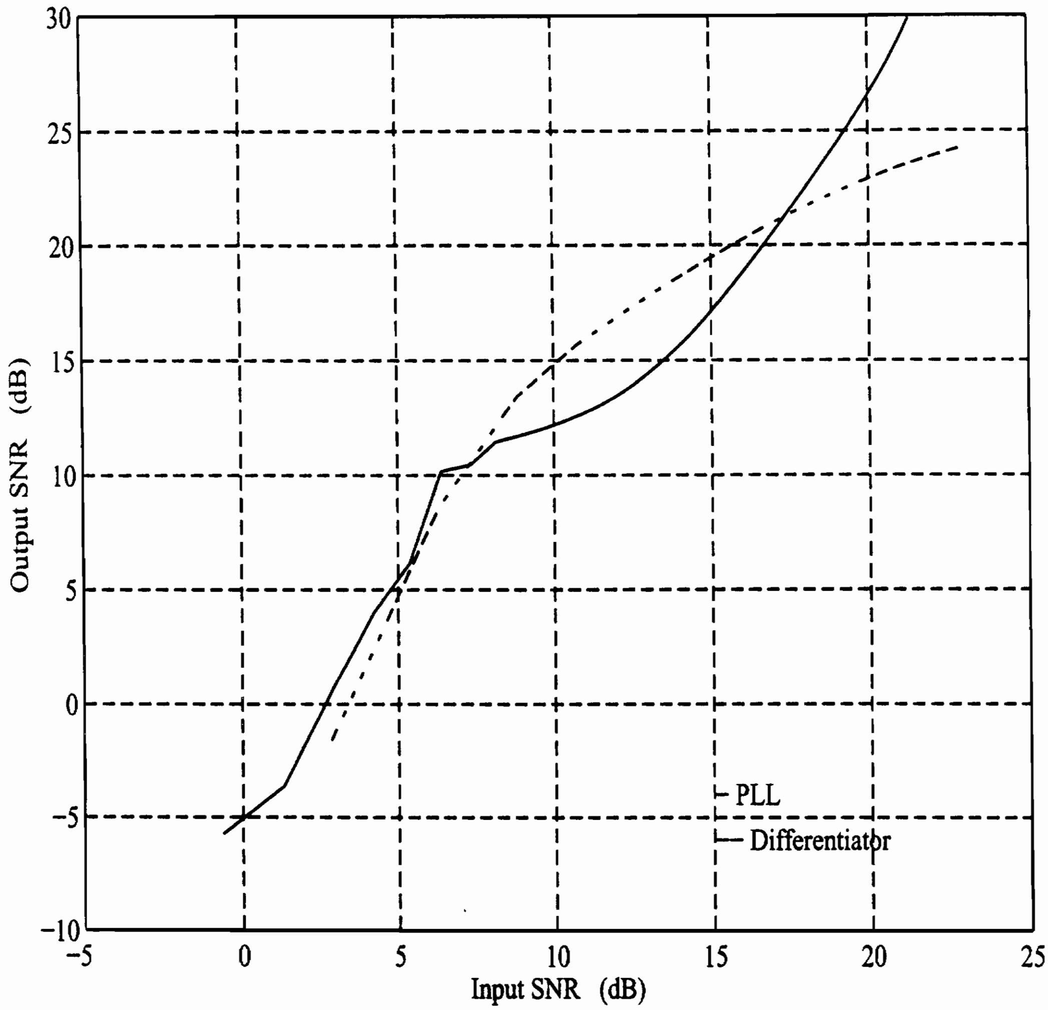

Figure 6.8: Output SNR versus Input SNR for PLL and Differentiation Demodulation without Companding

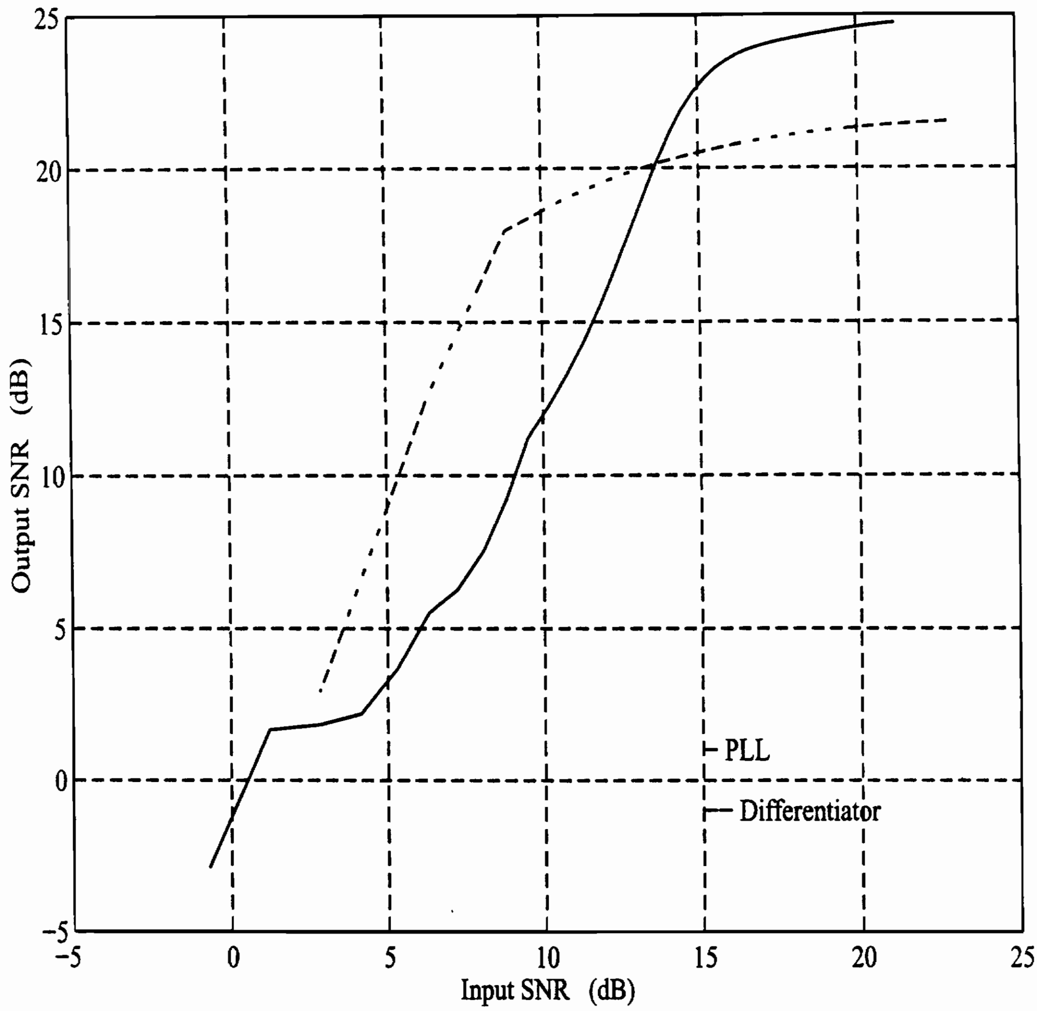

Figure 6.9: Output SNR versus Input SNR for PLL and Differentiation Demodulation with Companding

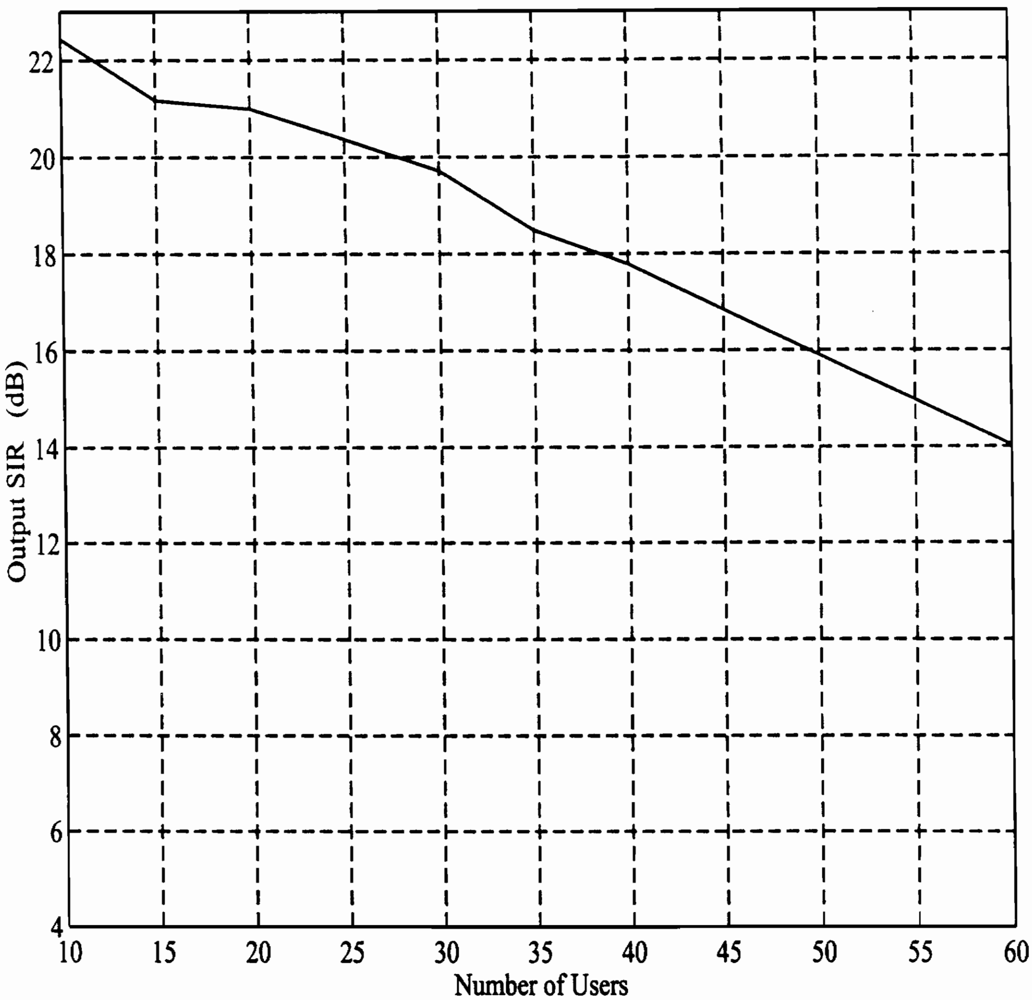

Figure 6.10: Output SIR versus the Number of Users, PN Code in Forward Link, 25 kHz IF Bandwidth

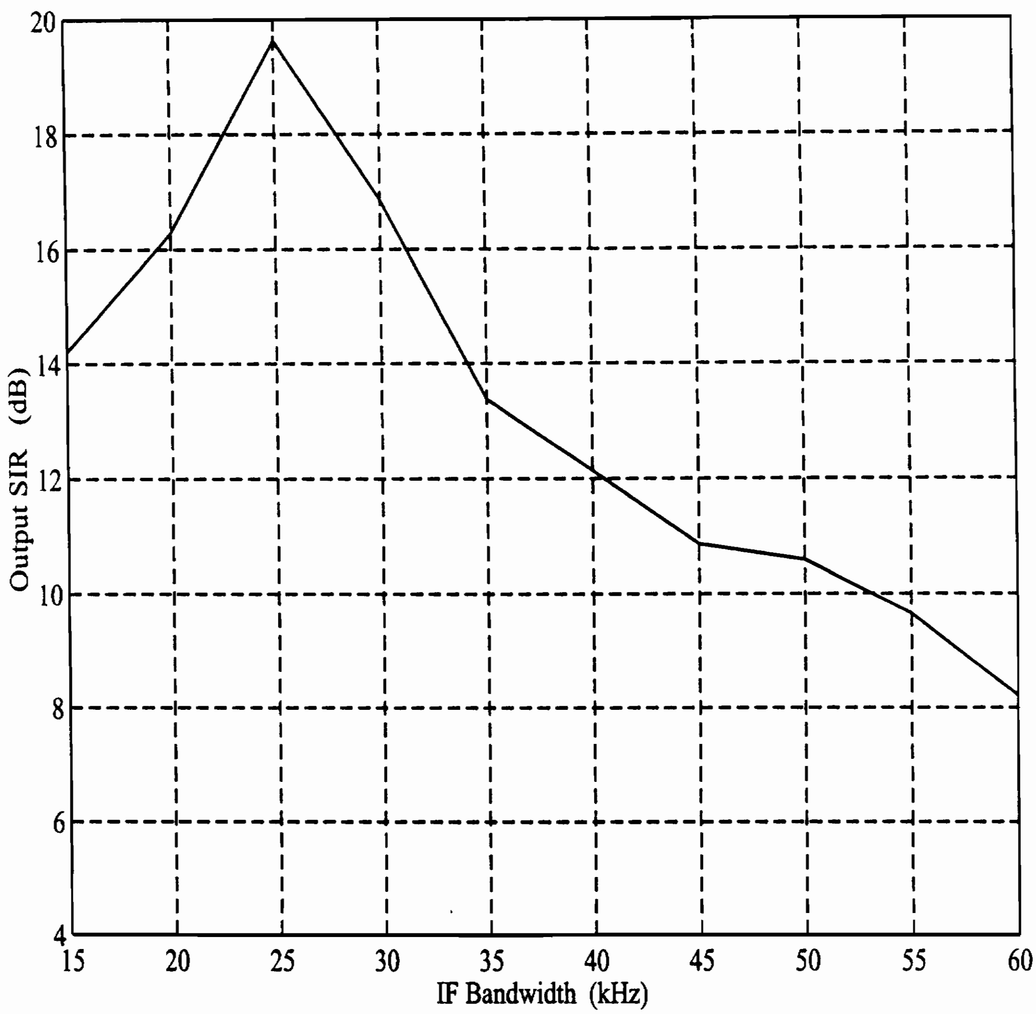

Figure 6.11: Output SIR versus the IF Bandwidth for PN Code in Forward Link with 24 Users

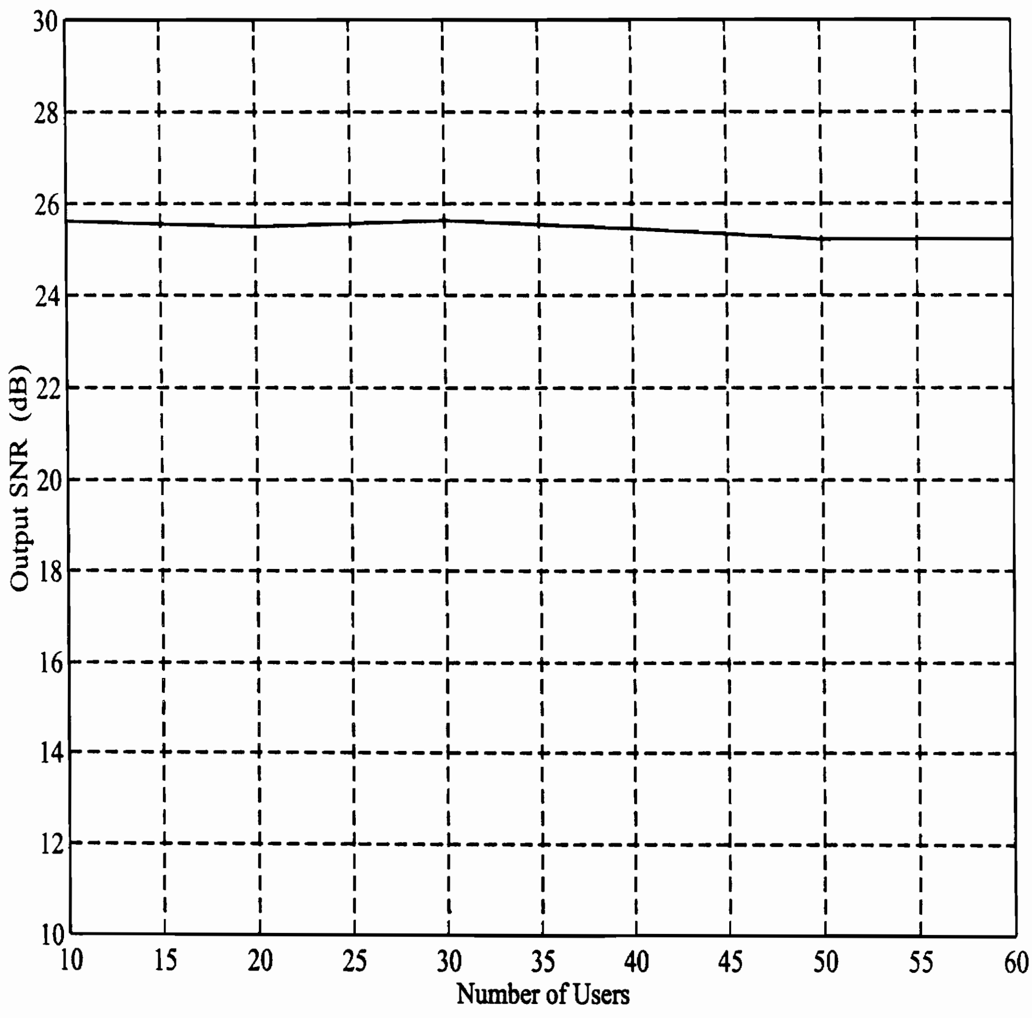

Figure 6.12: Output SIR versus the Number of Users for Walsh Code in Forward Link with 25 kHz IF Bandwidth

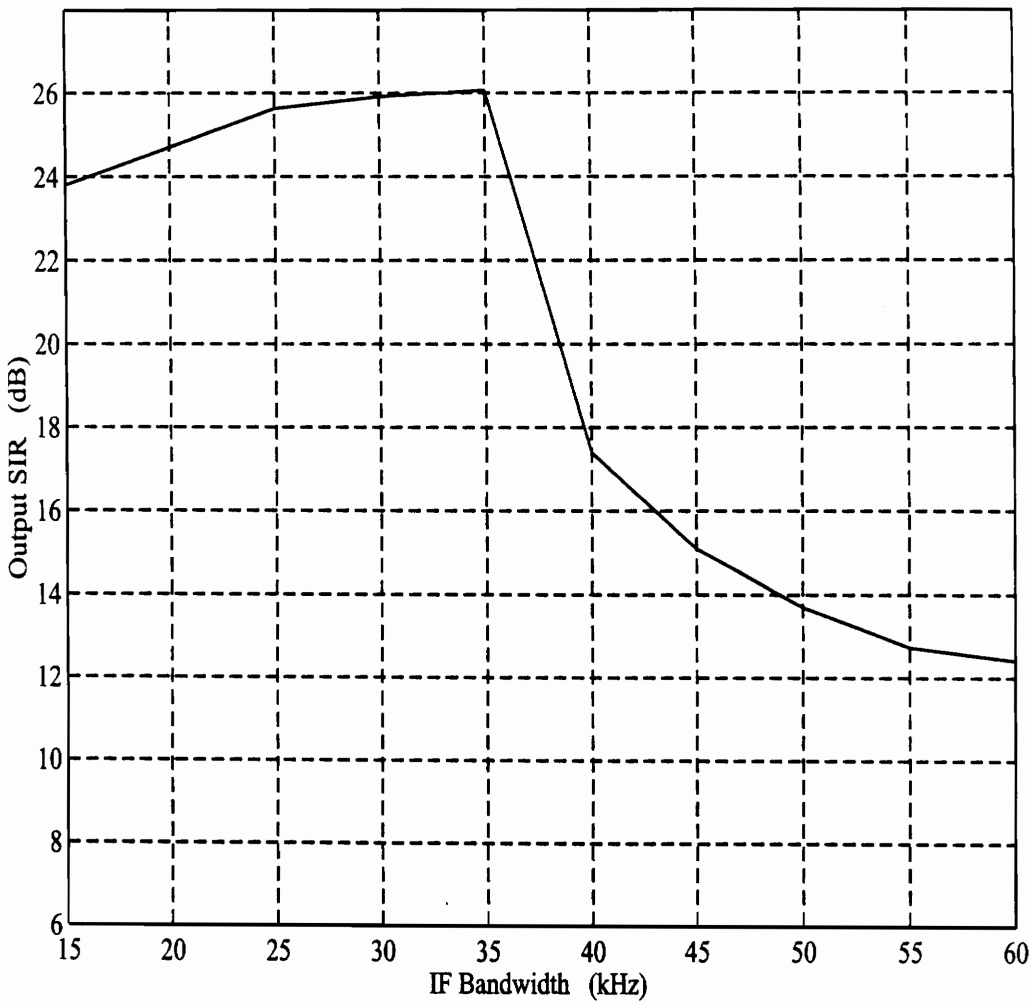

Figure 6.13: Output SIR versus the IF Bandwidth for Walsh Code in Forward Link with 24 Users

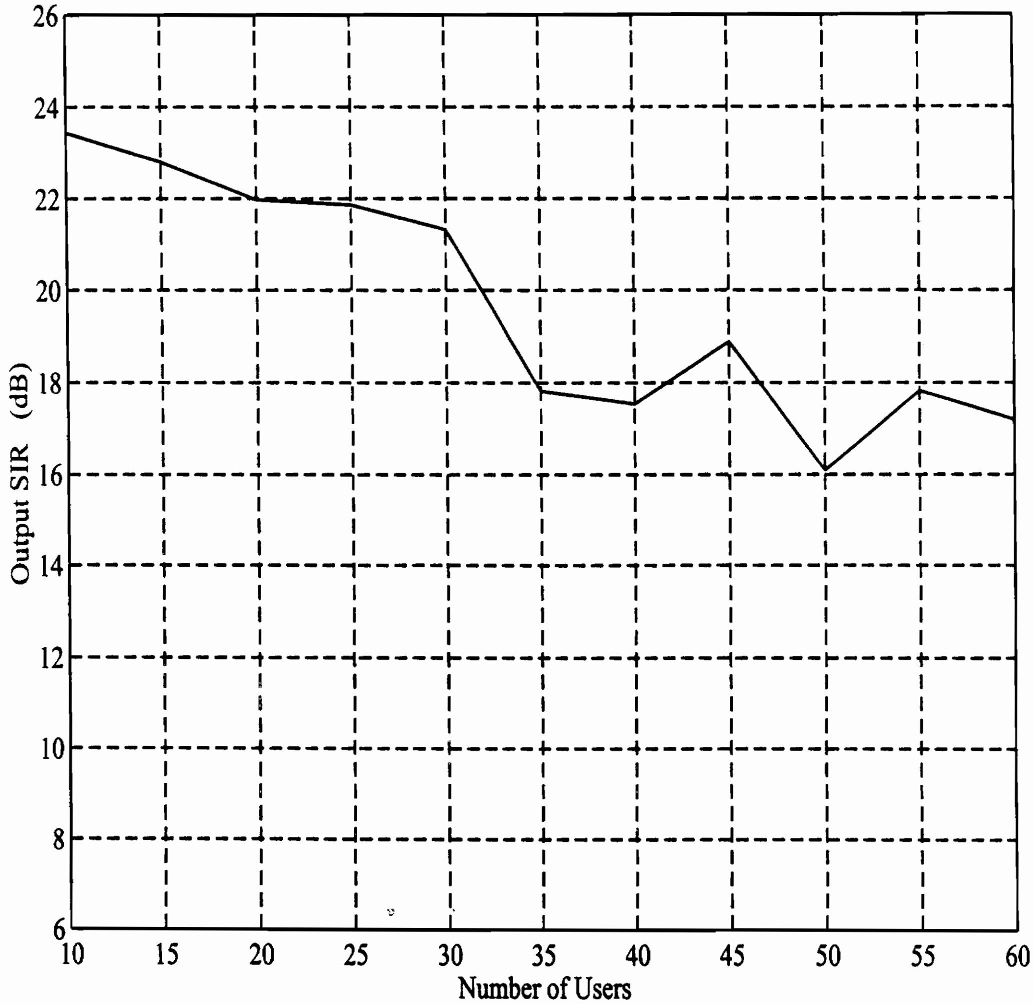

Figure 6.14: Output SIR versus the Number of Users with PN Code in Reverse Link for 25 kHz IF Bandwidth

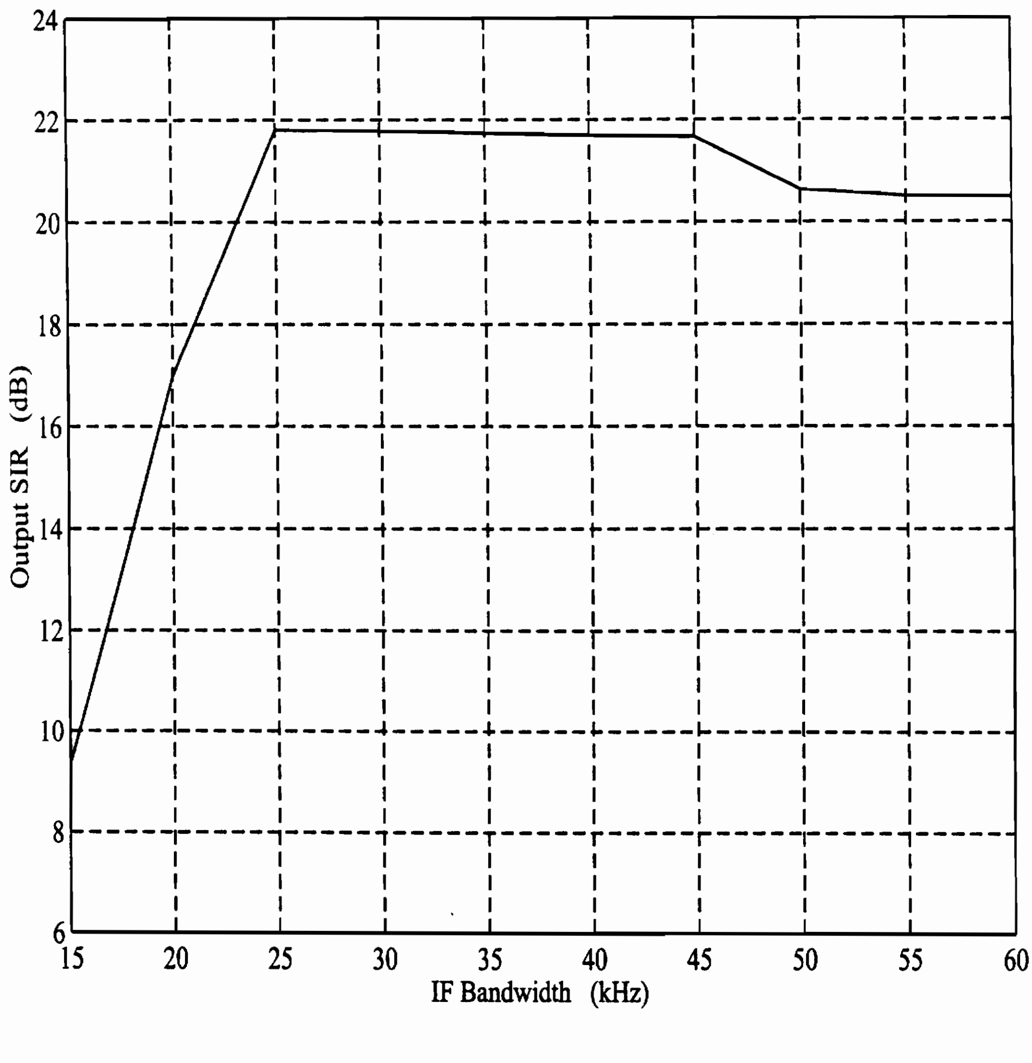

Figure 6.15: Output SIR versus the IF Bandwidth with PN Code in Reverse Link for 24 Users

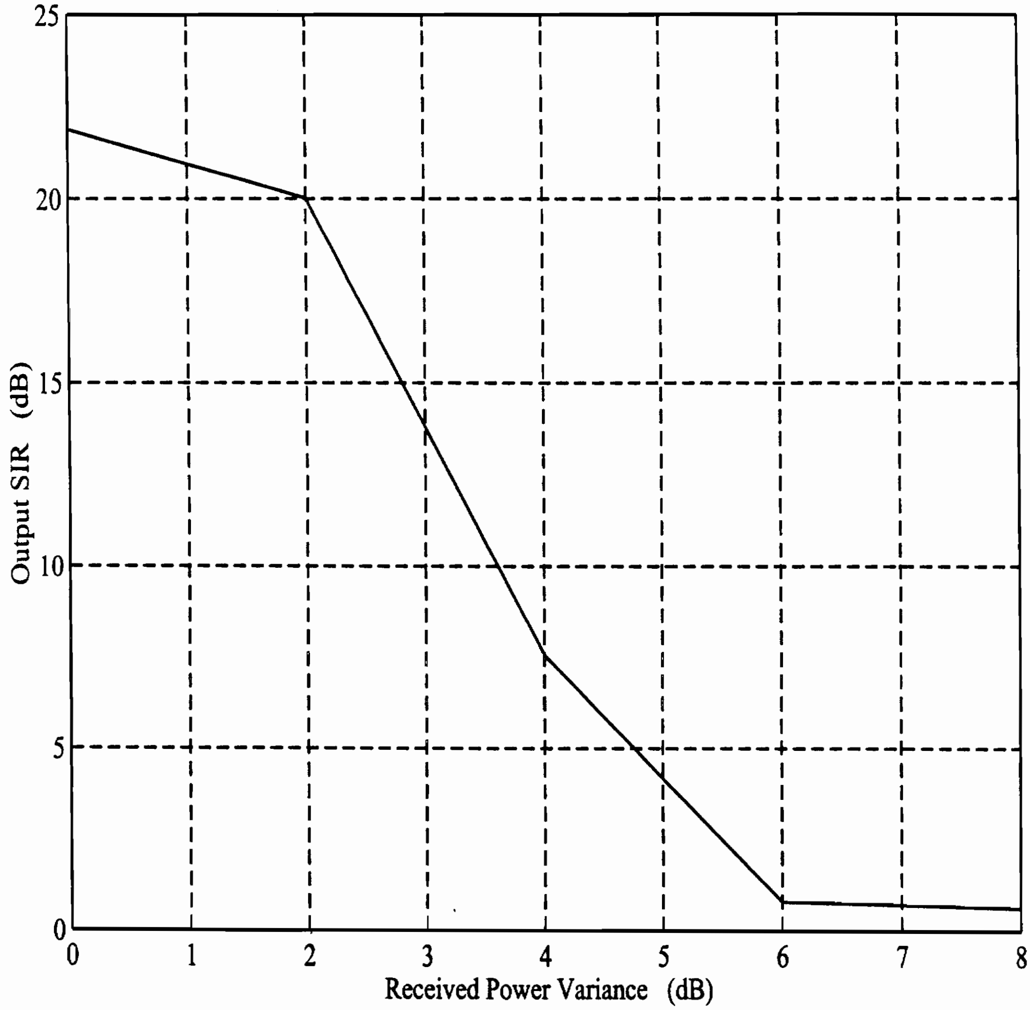

Figure 6.16: System Performance Under Imperfect Power Control for 24 Users with 25 kHz IF Bandwidth

Chapter 7

Conclusion

7.1 Summary

In this thesis, a unique hybrid FM/CDMA system for a WLL application is described and investigated. Input and output signal to interference ratios are selected as objective criteria to judge the system performance. Our main concern is two fold: improve the system capacity and the voice quality. These two qualities are interrelated and form an important tradeoff for a CDMA system design. The system performance was analyzed through a theoretical derivation of the input and output SIRs. Closed form expressions were obtained. Also, a software test-bed was developed to provide a realistic evaluation of system behavior.

In the theoretical analysis, the FM/CDMA system is able to obtain the upper bound or lower bound depending on the relative values of the processing gain and the frame length of the spreading sequence. The maximum difference of output SIR between these two cases is 3 dB. Based on the tentative parameters, the system is operating close to the lower bound, if uncorrelated codes are used to spread the FM signal. Contrary to conventional FM systems, the input SIR of an FM/CDMA system is not related to the IF bandwidth in the upper bound case because the power spectral density of multiple access interference is identical to that of FM signal. Increasing IF bandwidth includes no extra interference power as long as the CDMA frame length is less than twice of the processing gain. In the lower bound case, the interference is approximated as white Gaussian noise. The system behaves the same as a conventional FM system. Based on the theoretical analysis, a 30 kHZ IF bandwidth is preferred. The input SIR and the output SIR are 15.4 dB and 23.3 dB respectively for 24 users per cell.

An FM/CDMA simulator was developed in Matlab to allow variations of parameters to search for an optimal operating point. High output SNR, low threshold and low complexity are the main concern in selection of an FM demodulation scheme. Based on the experiments of a voice sample modulation/demodulation, the differentiator and the quadrature scheme exhibit almost identical characteristics. The PLL demodulator shows a 2 dB threshold extension for a 25 kHZ IF bandwidth occupancy. However, the PLL implementation is a higher cost solution. The arctangent demodulator performs slightly worse than the first two, due to the interaction of the signal and the channel noise.

The effect of companding provides SNR gain at a lower level of input SNR. However, saturation occurs due to the nonlinear operation of companding and the output SNR drops below that of non-companding modulation. Threshold is not affected anyway.

The forward link and the reverse link system performance is examined on the test-bed. In the forward link, the PN sequence and the Walsh sequence are applied separately to spread and despread the FM signal. For the PN sequence, the output SIR decreases almost linearly to the increase of the number of users, but finds a peak at 25 kHZ IF bandwidth. For Walsh sequence, the output SIR changes little as the number of users increases, but stays high between 25 to 35 kHZ of IF bandwidth. In the reverse link, only random PN sequences are used to spread/despread the FM signal. Asynchronous reception enhances the output SIR by 1-2 dB if the number of users is a variable parameter. Variation of IF bandwidth from 25 kHZ to 40 kHZ slightly changes the maximal output SIR.

Tight power control is absolutely necessary for a good voice quality. The variance of the received signal power should be less than 2 dB if the system is loaded with 24 users.

7.2 Future Work

So far the theoretical analysis and the software simulation are based on a signal cell model. In a multiple cell layout, the interference from adjacent cells can still further degrade the system performance. The effect of multipath should also be extensively investigated.

The theoretical work assumes that FM/CDMA system operates above the threshold. In the lower bound case, the system threshold is borrowed from conventional FM system. In the upper bound case, however, the MAI features a discrete spectrum. Within the bandwidth of interest, the MAI power spectral density is the summation of all the individual FM power spectral density. What is the FM threshold for a non-Gaussian noise channel? How does it affect the dynamic range of operating region? These issues need further investigation.

The system performance under different spreading code is of another interest. The selection of M-sequence or Gold sequence contributes differently to the power spectral density of MAI, especially within the FM bandwidth and it eventually affects the system performance.

One final important issue remaining is the performance of actual hardware. Extensive field trials on the Virginia Tech campus are being planned to investigate the performance of the hybrid FM/CDMA WLL system later this year. Although the optimization of a WLL network relies on the demography of the service area, the basic features of FM/CDMA WLL system can still be verified, and these trials offer an opportunity to compare the theory and the simulation to the field trial results.

REFERENCES

[Bra68] P. T. Brady, "A Statistical Analysis of On-Off Pattern in 16 Conversations," *The Bell Systems Technical Journal*, Vol. 47, pp. 73-91, 1968

[Cal95] V. Classens, "Transmitting Effectively in Local Loop," *Telecommunications*, Feburary 1995

[Cou93] L. W. Couch II, "Digital and Analog Communication Systems," *MacMillan*, New York, 1993

[Cox86] D. Cox, "Research Towards a Wireless Local Loop,," *Bellcore Exchange*, Vol. 2, pp. 2-7, Novermber 1986

[CTI91] Cellular Telecommunication Industry Association, "Next Generation Cellular: Results of Field Trials," *CTIA*, December 4-5 1991

[Eng93] T. Eng and L. B. Milstein, "Comparison of Hybrid FDMA/CDMA Systems in Frequency Selective Rayleigh Fading," *IEEE Journ. Select. Area Comm.*, Vol. 12, No. 5, pp. 1244-1253, June 1994

[Fun93] V. Fung and T. S. Rappaport, "Bit error Simulation for $\pi/4$ DQPSK Mobile Radio Communication Using Two-Ray and Measurement-Based Impulse Response Models," *IEEE Journ. Select. Area Comm.*, Vol. 11, No. 3, pp. 393-405, April 1993

[Gar79] F. M. Gardner, "Phaselock Techniques", *John Wiley and Sons*, New Jersey, 1976

[Gil90] K. S. Gilhousen, I. M. Jacobs, R. Padovani and L. A. Weaver, "Increased Capacity Using CDMA for Mobile Satellite Communications," *IEEE Journ. Selec. Area Comm.*, Vol. 8, No. 4, pp.503-514, May 1990

[Gil91] K. S. Gilhousen, I. M. Jacobs, R. Padovani, A. J. Viterbi, and C. E. Wheatley "On the capacity of Cellular CDMA System," *IEEE Trans. Veh. Tech. Conf.*, Vol. 40, No. 2, pp. 303-312, May 1991

[Haj96] R. Hajbandeh, "An Overview of the Fixed Wireless Local Loop Products and Their Development Status," *Proc. of Wireless Personal Communications*, Vol. 6, No.3, pp. 317-325, June, 1996

[Hat90] M. Hata, "Empirical Formula for Propagation Loss in Land Mobile Radio Services," *IEEE Trans. Veh. Tech. Conf.*, Vol. 29, No.3, pp. 317-325, August, 1980

[Hau94] R. Huagen, B. Olsen and B. Eskedal, "Radio in Local Loop in Rural and Suburban Environment," *Proc. of IEEE Conf. on Personal Wireless Communications*, pp. 12-16, 1994

[Jer92] M. C. Jeruchim, P. Balaban and K. S. Shanmugan, "Simulation of Communication System", *Plenum Press*, New York, 1992

[Kat91] S. Kato, M. Morikura and S. Kubota, "Implementation of Coded Modems," *IEEE Comm. Mag.*, Vol. 31, No.12, pp. 88-97, December 1991

[Kav87] M. Kavehrad and P. J. McLane, "Spread Spectrum Indoor Digital Radio," *IEEE Comm. Mag.*, Vol. 25, No.6, pp.32-40, June 1987

[Kei95] B. Keiser, "Digital Telephony and Network Integration," *Van Nostrand Reinhol*, New York, 1995

[Kon96] S. Kondo and L. B. Milstein, "Performance of Multicarrier DS CDMA System", *IEEE Trans. on Comm.*, Vol. 42, No. 2, pp.238-246, February 1996

[Lee89] W. C. Y. Lee, "Mobile Cellular Telecommunications Systems," *McGraw-Hill*, New York, 1989

[Lee91] W. C. Y. Lee, "Overview of Cellular CDMA," *IEEE Trans. on Veh. Tech. Conf.*, Vol. 40, No. 2, pp.291-302, May 1991

[Lib95] J. C. Jr. Liberti, "Analysis of Code Division Multiple Access Mobile Radio Systems with Adaptive Antennas," *Ph. D Dissertation*, Virginia Tech, Blacksburg, 1995

[Mac79] V. H. MacDonald, "The Cellular Concept", *The Bell Systems Technical Journal*, Vol. 58, pp. 15-43, 1979

[Mei96] R. P. Meinzer Jr., "PCS Development: Turning Obstacles into Opportunities," *Telecommunications*, pp. 64-65, January, 1996

[Mey96] J. Meyers, "The Next Big Challenge," *Telephony*, p. 6, May 13, 1996

[Mil92] L. B. Milstein, etc., "On the Feasibility of a CDMA Overlay for Personal Communications Networks," *IEEE Journ. Select. Areas Comm.*, Vol.10, No. 4, May 1992

[Mod92] A. R. Modarressi and R. A. Skoog, "An Overview of Signal System No. 7," *Proceedings of the IEEE*, Vol. 80, No. 4, pp.590-606, April 1992

[Mor89] R. K. Jr. Morrow, "Bit-to-bit Error dependence in Slotted DS/SSMA Packet System with Random Signature Sequences," *IEEE Trans. on Comm.*, Vol. 37, No. 10, pp.238-246, October 1989

[Mou92] M. Mouly, and M. B. Pautet, "The GSM system for Mobile Communications," *Addison-Wesley*, New York, 1992

[Mul91] R. J. Mulder, "DECT-A Unviersal Cordless Access System," *Philips Telecommunications Review*, Vol. 49, No. 3, pp.68-73, September 1991

[Non94] D. L. Noneaker and M. B. Pursley, "Selection of Spreading Sequences for DS Spread Spectrum Communications over a Doubly Selective Fading Channel," *IEEE Trans. on Comm.*, Vol. 42, No. 12, pp. 3171-3177, December 1994

[Non96] D. L. Noneaker and M. B. Pursley, "The Effect of Sequence Selection on DS Spread Spectrum with Selective Fading and RAKE Reception," *IEEE Trans. on Comm.*, Vol. 44, No. 2, pp.229-237, February 1996

[Och89] H. Ochsner, "DECT-Digital European Cordless Telecommunications," *IEEE Veh. Tech. Conf.*, Vol. 39, pp.718-721, 1989

[Oku68] T. Okumara, E. Ohimori and K. Fukuda, "Field Strength andIts Variability in VHF and UHF Land Mobile Service," *Review Electrical Communication Laboratory*, Vol. 16, No. 9-10, pp.825-873, September-October 1968

[Olm61] J. M. H. Olmsted, "Advanced Calculus," *Appleton-Century-Crofts*, New York, 1961

[Owe93] F. Owens, C. Geoffrey, "DECT standard in Local Loop Applications," *Proc. of 4th Europ. Conf. on Radio Relay Systems*, IEE Conference Publication, No. 386, pp. 103-107, 1993

[Pad94] R. Padovani, B. Butler and R. Boesel, "CDMA Digital Cellular: Field Test Results," *IEEE Veh. Tech. Conf.*, pp11-14, 1994

[Pal96] N. Palmer, "The Wireless Local Loop: a Matter of Simple Economics," *Telephony*, pp. 60-66, June 3, 1996

[Pan65] P. F. Panter, "Modulation, Noise, and Spectral Analysis," *McGraw-Hill*, New York, 1965

[Per77] M. B. Pursley, D. V. Sarwate and W. E. Stark, "Performance Evaluation for Phase Coded Spread-Spectrum Multiple-Acccess Communication-Part I: System Analysis," *IEEE Trans. on Comm.*, Vol. COM-25, pp. 795-799, October 1977

[Per79] M. B. Pursley and H. F. Reefs, "Numerical Evaluation of Correlation Parameters for Optimal Phases of Binary Shift-Register Sequences," *IEEE Trans. on Comm.*, Vol. COM-27, pp. 1597-1604, October 1979

[Pra69] V. K. Prabhu and H. E. Rowe, "Spectral Density Bounds of a PM Wave," *The Bell Systems Technical Journal*, Vol. 48, pp. 769-811, March 1969

[Qua92] Qualcomm, Inc, "An Overview of the Application of Code Division Multiple Access (CDMA) to Digital Systems and Personal Cellular Networks," May 1992

[Ram94] B. Ramamurthy and C. Mathiazhagan, "DECT Based WLL System," *Proc. of IEEE Conf. on Personal Wireless Communications*, pp. 55-59, 1994

[Rap96] T. S. Rappaport, "Wireless Communications: Principle and Practice," *Prentice Hall*, New Jersey, 1996

[Ric63] S. O. Rice, "Time-Series Analysis," *John Wiley and Sons*, New Jersey, 1963

[Row65] H. E. Rowe, "Signal and Noise in Communication Systems," *D. Van Nostrand*, New Jersey 1965

[Sal91] A. Salmasi and K. S. Gilhousen, "On the System Design Aspect of CDMA Applied to Digital Cellular and Personal Communications Networks," *IEEE Veh. Tech. Conf.*, pp. 57-62, 1991

[Sch82] R. A. Scholtz, "The Origins of Spread Spectrum Communications," *IEEE Trans. on Comm.*, Vol. COM-30, No. 5, pp. 822-854, May 1982

[Sig95] SigTek, Inc, "TELELINK CDMA System Description Document," *SigTek*, May 12 1995

[Sim94] K. Simon, J. Omura, R. Scholtz and B. Levitt, "Spread spectrum communications handbook," *McGraw-Hill*, New York, 1994

[Sou96] E. A. Sourour and M. Nakagawa, "Performance of Orthogonal Multicarrier CDMA in a Multipath Fading Channel," *IEEE Trans. on Comm.*, Vol. 44, No. 3, pp.356-367, March 1996

[Sta94] H. Stark and J. W. Woods, "Probability, Random Processes and Estimation Theory for Engineers," *Prentice-Hall*, New Jersey 1994

[Tau86] H. Taub and D. L. Schilling, "Principles of Communication Systems," *McGraw-Hill*, New York 1986

[Vas96] Y. Vasavada, "Performance Evaluation of a Frequency Modulated Spread-Spectrum System," *M. S. Thesis*, Virginia Tech, Blacksburg, 1996

[Vit92] A. J. Viterbi and R. Padovani, "Implications of Mobile Cellular CDMA," *IEEE Comm. Mag.*, pp.38-41, December 1992

[Vit96] A. J. Viterbi, "CDMA: Principles of Spread Spectrum Communications," *Addison-Wesley*, Massachusetts, 1996

[Woe92] B. D. Woerner and R. Comeron, "An Analysis of CDMA with Imperfect Power Control," *IEEE Trans. on Veh. Tech. Conf.*, May 1992

[You79] W. R. Young, "Advanced Mobile Phone Service: Introduction, Background, and Objectives," *The Bell Systems Technical Journal*, Vol. 58, pp. 1-14, January 1979

VITA

Tianshi Li was born in Harbin, China on October 1, 1963. He received his B.S. and M.S. degree in Beijing University, Beijing, China in 1987 and 1990 respectively. He entered Virginia Polytechnic Institute and State University in August 1994 as a Master student majoring in wireless communications and joined the Mobile and Portable Research Group (MPRG) in June 1995, focusing his research on CDMA communication system design. Before coming into U.S., he worked as an electrical engineer in Beijing Syntone, Inc. He will join Lucent Technologies as a member of technical stuff working in the area of Personal Communication Services (PCS).

Tianshi Li